Organoplatinum(II) Complexes with Hydrogen-Bonding Functionality and Their Potential Use as Molecular Receptors for Adenine

A Thesis Submitted for the Degree of Master of Science

Michael G. Crisp B.Sc (Hons.)

ADELAIDE
UNIVERSITY
AUSTRALIA

Department of Chemistry
January 2002

Errata

Table of Contents (pages viii and ix): The titles of complexes should commence with "*trans*" not "*Trans*".

Page 10, paragraph 1: Should read "Complexation plays…" not "Complexations play…".

Page 11, paragraph 1: Should read "…binding to the host…" not "…host binding…".

Page 20: The iodo ligand is used in this reaction as (**36**) is more reactive than the corresponding chloro complex (**35**) in the presence of silver ions.

Page 23, Table 1: "na" and "n/a" refer to the term "not applicable".

Page 29, paragraph 2, line 2: Picolinic acid complexes (**50**) - (**53**) contained more chemically-inequivalent protons than the other isomers owing to their low symmetry, thus leading to more complicated ^{1}H NMR spectra.

Page 29, paragraph 2, line –2: Should start "Complexes (**52**) and (**53**) were the only two complexes…".

Page 34: Entry for (**54**) H^3 should read "Obscured by $PMePh_2$" and not "Obscure d by $PMePh_2$". Entry for (**55**) H^5 should read "As for H^4" not "e".

Page 39: Preparation of the platinum(II)-iodo complex (**59**) is shown in Scheme 2.6.

Page 41, Table 9 and Page 52, Table 11: The IR spectra were recorded as Nujol mulls.

Page 60, paragraph 2: Should read "^{14}N" not "N^{114}"

Page 72, paragraph 1, line –3: should be "possess" not "posses".

Page 73: 2D NMR spectra were recorded at 600 MHz and not 300 MHz.

Declaration

This thesis contains no material which has been accepted for the award of any other degree or diploma in any university and, to the best of my knowledge, contains no material previously published or written by another person, except where due reference is made.

I consent for the thesis being made available for photocopying and loan if accepted for the award of this degree.

Michael G. Crisp
January 2002

Acknowledgements

Dr. Louis M. Rendina provided me with the opportunity to do this project. I would like to thank him for providing me with this opportunity, and for allowing me to develop my own project and helping me turn my ideas for this project into reality.

Thankyou to Dr. Edward Tiekink for his invaluable assistance with the crystallographic data.

Thanks to my fellow laboratory 10 members for their support, encouragement and friendship over the course of this project, Susan Woodhouse, David Gallasch, David Clarke, Jean Todd, Doug Smyth, Ben Ellis, and Daniela Caiazza.

I would like to thank Sarah who married me on the 30th of September 2001. Thankyou Sarah for being so supportive during the course of my work. You provided me with a great motivation to finish this project and always encourage me to follow my dreams.

I would like to thank my Mum and my Dad for their continued support in everything that I do. I would like to thank them for listening to my continual ranting about the ups and downs of my project.

Abstract

The preparation and characterisation of a novel series of organoplatinum(II) complexes with hydrogen-bonding functionality are described. The mononuclear platinum(II) complexes of the type *trans*-[Pt(σ-aryl)L(PPh_3)$_2$]OTf (L = nicotinic acid, picolinic acid, isonicotinic acid) and the dinuclear complexes of the type *trans*-[Pt(σ-aryl)(PPh_3)(μ-Y)Pt(σ-aryl)(PPh_3)$_2$](OTf)$_2$ (Y = 4,4'-bipyridyl, 4,7-phenanthroline, 4,4'-dipyrazolylmethane, 1,1'-phenyl-4,4'-dipyrazolylmethane) were investigated. The complexes were primarily characterised by multinuclear (^{31}P, ^{1}H) 1-D and 2-D NMR spectroscopy, IR spectroscopy and, in some cases, X-ray crystallography. These platinum(II) complexes, both mono-nuclear and di-nuclear, have the potential to act as hosts for nucleobase guests such as adenine, and this was investigated also. The mono-platinum complexes were found to interact with the guest 9-sec-pentyladenine in a variety of ways in $CDCl_3$ solution including, 1:1, 2:1 and in some cases 3:1 association ratios at both the Watson-Crick and the Hoogsteen site. The dinuclear platinum(II) molecular "tweezers" were found to bind simultaneously to two 9-sec-pentyladenine molecules in $CDCl_3$ solution.

Abbreviations

General:

°	degrees
°C	degrees Celsius
ΔG	change in free energy
1-D	one dimensional
2-D	two dimensional
Å	Angstrom
cm	centimetre
DNA	deoxyribonucleic acid
DPZM	4,4'-dipyrazolylmethane
g	gram
h	hour
K	Kelvin
MS	mass spectrometry
mL	millilitre
OTf, triflate	$CF_3SO_3^-$, trifluoromethanesulfonate
Ph	phenyl
THF	tetrahydrofuran

Nuclear magnetic resonance spectroscopy:

δ	nuclear magnetic resonance chemical shift in ppm
^{1}H NMR	proton nuclear magnetic resonance
^{31}P{^{1}H} NMR	proton decoupled ^{31}P nuclear magnetic resonance
d	doublet
dd	doublet of doublets
Hz	Hertz
I	nuclear spin quantum number
m	multiplet

MHz	megahertz
$^{n}J_{ij}$	n bond coupling constant between nuclei i and j
NMR	nuclear magnetic resonance
ppm	parts per million
s	singlet
t	triplet

Table of Contents

Declaration i

Acknowledgements ii

Abstract iii

Abbreviations iv

Table of Contents vii

Chapter 1 Introduction 1

1.1 Self Assembly 1

1.2 DNA/RNA Nucleobases 10

1.3 Platinum Complexes with Hydrogen-Bonding Functionality 14

1.4 Molecular Tweezers Containing Platinum(II) 16

Chapter 2 Preparation and Characterization of Mononuclear Platinum(II) Complexes with Hydrogen-Bonding Functionality 19

2.1 Synthesis and Characterisation of Iodoplatinum(II) Precursor Complexes 19

2.2 Synthesis and Characterisation of Mononuclear Platinum(II) Complexes with Hydrogen-Bonding Functionality 27

2.3 pKa Determinations for Complexes (**43**), (**46**), (**47**), (**48**), and (**51**) 44

Chapter 3 Preparation and Characterisation of Dinuclear Organoplatinum(II) Complexes with Hydrogen-Bonding Functionality 47

Chapter 4 Molecular Recognition of Adenine by Platinum(II) Complexes with Hydrogen-Bonding Functionality 56

4.1 Association Studies of Mononuclear Platinum(II) Complexes with 9-sec-pentyladenine 65

4.2 Association Studies of Dinuclear

Platinum(II) Complexes (**67**) and (**68**) with 9-sec-pentyladenine 71

Chapter 5 Conclusion 74

Chapter 6 Experimental 75

trans-iodophenyl-bis(triphenylphosphine)platinum(II) (**37**) 76

trans-iodo-bis(methyldiphenylphosphine)phenylplatinum(II) (**38**) 76

trans-iodophenylbis(triethylphosphine)platinum(II) (**39**) 76

trans-iodophenyl-bis(tricyclohexylphosphine)platinum(II) (**40**) 76

Trans-(nicotinic acid)phenyl
bis(triphenylphosphine)platinum(II) triflate (**42**) 77

Trans-(nicotinic acid)phenyl
bis(methyldiphenylphosphine)platinum(II) triflate (**43**) 77

Trans-(nicotinic acid)phenylbis(triethylphosphine)platinum(II) triflate (**44**) 77

Trans-(nicotinic acid)phenyl
bis(tricyclohexylphosphine)platinum(II) triflate (**45**) 78

Trans-(isonicotinic acid)phenyl
bis(triphenylphosphine)platinum(II) triflate (**46**) 78

Trans-(isonicotinic acid)phenyl
bis(methyldiphenylphosphine)platinum(II) triflate (**47**) 78

Trans-(isonicotinic acid)phenyl
bis(triethylphosphine)platinum(II) triflate (**48**) 79

Trans-(isonicotinic acid)phenyl
bis(tricyclohexylphosphine)platinum(II) triflate (**49**) **79**

Trans-(picolinic acid)phenyl
bis(triphenylphosphine)platinum(II) triflate (**50**) **79**

Trans-(picolinic acid)phenyl
bis(methyldiphenylphosphine)platinum(II) triflate (**51**) **79**

Trans-(picolinic acid)phenyl
bis(triethylphosphine)platinum(II) triflate (**52**) **80**

Trans-(picolinic acid)phenyl
bis(tricyclohexylphosphine)platinum(II) triflate (**53**) **80**

Trans-(isonicotinamide)phenyl
bis(methyldiphenylphosphine)platinum(II) triflate (**54**) **80**

Trans-(nicotinamide)phenyl
bis(methyldiphenylphosphine)platinum(II) triflate (**55**) **81**

Trans-iodo(N-methylbenzamide)bis(triphenylphosphine)platinum(II) (**59**) **81**

Trans-μ-4,4'-bipyridinebis[(N-methylbenzamide)
bis(triphenylphosphine)platinum(II)] bis(triflate) (**65**) **81**

Trans-μ-4,7-phenanthrolinebis[N-methylbenzamide]
bis(triphenylphosphine)platinum(II)] bis(triflate) (**66**) **82**

Trans-μ-4,4'-dipyrazolylmethanebis[(N-methylbenzamide)
bis(triphenylphosphine)platinum(II)] bis(triflate) (**67**) **82**

Trans-μ-1,1'-phenyl-4,4'-dipyrazolylmethanebis[(N-methylbenzamide)

bis(triphenylphosphine)platinum(II)] bis(triflate) (**68**) 82

Preparation of Samples for Job Plots 83

Determination of pKa values 84

References 85

Chapter 1. Introduction

The hydrogen bond has long been known to play a pivotal role in the areas of molecular recognition and supramolecular chemistry. Many natural and synthetic supramolecular systems owe their organisation to the presence of hydrogen-bonding functionalities. Hydrogen-bonding can control the organization of molecules in the solid state, and it has been used extensively in crystal engineering[1,2] and supramolecular synthesis[3-5]. In contrast, only more recently have major advances been made in the use of the coordinate-covalent bond for the assembly of discrete molecular arrays[6].

A large volume of information is at our disposal that can be used in the design of supramolecular systems containing transition metals. The coordination numbers and geometries of most transition metals are well established. This information can be drawn upon to determine what size a metal-based supramolecular complex will be, or what angles are involved[7]. There are numerous papers describing the various combinations of metal atoms with different organic "building blocks" to form a variety of discrete supramolecular structures[8-10]. Combining the hydrogen-bonding and coordinate-covalent motifs greatly expands the utility of metal complexes as molecular receptors. The hydrogen-bonding surface of carboxylic acids, and derivatives of carboxylic acids, are often used in the design of such receptors. In particular it has been used for the molecular recognition of nucleobases such as adenine, which is an important target in studies of molecular recognition.

1.1 Self-Assembly

Self-assembly has rapidly become a convenient means for obtaining large macrocycles and molecular polygons of predetermined shape, size and functionality[11-13]. Contemporary supramolecular chemistry has its roots in classical covalent macrocycles such as crown ethers, cyclophanes, cyclodextrins, calixarerenes, cryptands, and spherands to name a few. The field is dominated by the biomimetic motif of weak forces such as hydrogen-bonding, hydrophilic hydrophobic, π-π stacking, electrostatic and van der Waals. Separate to these forces is the spontaneous self-assembly of precursor building blocks using the coordination motif. This motif uses the transition metals, multidentate ligands and coordinate-covalent bonding to drive and direct the self-assembly process[10]. Self-assembly provides a means for the construction of

discrete, structurally well-defined complexes. Self-assembly can occur by covalent[9], non-covalent[12] and hydrogen-bonding motifs[6].

There are a number of examples in the literature of molecular polygons synthesised via self-assembly. These include; triangles[14,15], squares[8,12,14-24], rectangles[25], pentagons[15], hexagons[6,8,15,20] and parallelograms[15]. All of these molecular polygons require two or more basic units, sometimes referred to as "tectons" (building blocks). For example, the tectons for a molecular triangle are, three 180° units and three 60° units. A molecular square requires either four 90° corners, or four 90° corners joined by four 180° sides. A molecular hexagon can be constructed from six 120° units joined by six 180° linkers, or by six 120° units all joined to each other[15]. Examples of such molecular polygon construction are represented schematically in Figure 1.

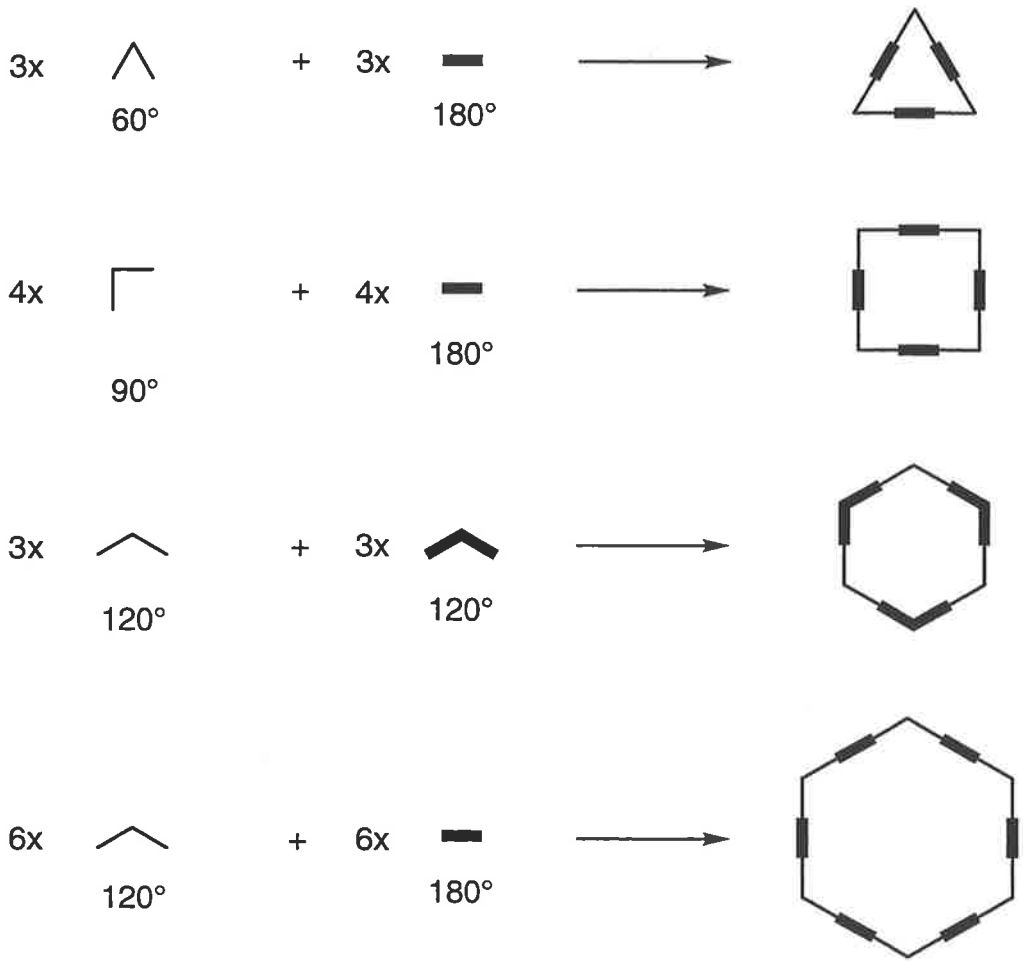

Figure 1. The schematic representation of some of the discrete molecular aggregates that may be formed spontaneously from the self-assembly of linear and angular subunits.

There exists a vast variety of suitable building blocks that can be used to construct molecular polygons. The form, shape and distribution of the building blocks must be strictly controlled in order to successfully construct a discrete molecular polygon. Complexes of transition metals have been widely utilised as suitable components for the construction of molecular polygons. Commonly-used metal centres for such chemistry include; platinum [17,26,27], palladium [17,26,27], titanium, cadmium [18], chromium [20], molybdenum [20], and tungsten[20] to name a few. Transition metals have well documented geometric and coordination properties. It is quite easy to determine the geometry of a metal complex, and thus exploit this knowledge for the construction of macrocycles. For example, it is well documented that complexes of platinum(II) adopt a four-coordinate, square planar geometry. A large number of organic ligands have been utilised for linking metal centres together to form macrocycles. Many of these joining ligands, or linkers, take advantage of N-donor atoms that can displace labile ligands at the metal centre, such as triflato ligands. The linker is chosen for its ability to coordinate to the metal centre and also for the angle that its geometry will confer upon the resulting macrocycle. An example of a useful 180° N-donor ligand is the bridging bidentate 4,4'-bipyridine and a common example of a 120° linker is 4,4'-bipyridyl ketone.

Controls on the nature of the bonding within molecular polygon systems must be implemented. The chemical bonding between the units must be thermodynamically stable, yet kinetically labile so that the entire macrocycle can self-rearrange if there is a flaw. This self-correction property is similar to that present in many naturally-occurring systems. By utilising building blocks that assemble into a desired conformation one is merely mimicking processes that have been present in Nature for many years.

Classically, large molecular polygons were constructed in a stepwise fashion using traditional covalent chemistry, requiring a multitude of reaction steps. For small organic compounds this is probably quite acceptable. However, when a much larger macrocycle is required, conventional synthetic methods begin to fail. There are usually a large number of individual steps required, each resulting in an undesirable loss of yield. Self-assembly offers the chemist a number of advantages over this conventional method. The other major disadvantage of traditional chemical synthesis is that covalent bonds are usually chemically inert, so that an error in the construction of a macrocycle would be irreversible and the product would have to be re-synthesised [14,15,28]. There are far fewer individual steps required for the synthesis when utilising self-assembly.

As mentioned earlier, molecular polygons containing transition metal centres have all utilised coordinate covalent bonding. Hydrogen-bonding motifs have also proven useful in the construction of discrete macrocyclic complexes. With the possibility of combining the coordinate-covalent motif with hydrogen-bonding in self-assembly one is presented with a number of new avenues for the synthesis of molecular polygons. One of the great advantages of such a process is that the polygons can be readily assembled in solution, and the cavity size of the macrocycle can be fine-tuned to suit the desired requirements[6,29,30].

Puddephatt and co-workers recently reported a new architecture of two interpenetrating chains of rings in an organometallic polyrotaxane containing three platinum centres. Their aim was to produce a polymer that was propagated through hydrogen-bonding, rather than through the more conventional method of covalent bonding[31]. Their work combined the techniques of organometallic chemistry, coordination chemistry, and self-assembly through hydrogen-bonding. The platinum(II) precursor was prepared by the facile oxidative addition of an alkyl halide, where the alkyl group contained the hydrogen-bonding function, to a dimethylplatinum(II) complex. The resulting platinum(II) complex was then treated with a tridentate N-donor ligand to form the basic building block for the polymer, (**1**). The polyrotaxane was then formed through hydrogen-bonded self-assembly. In the solid-state the complex forms two chains of rings that interpenetrate each other.

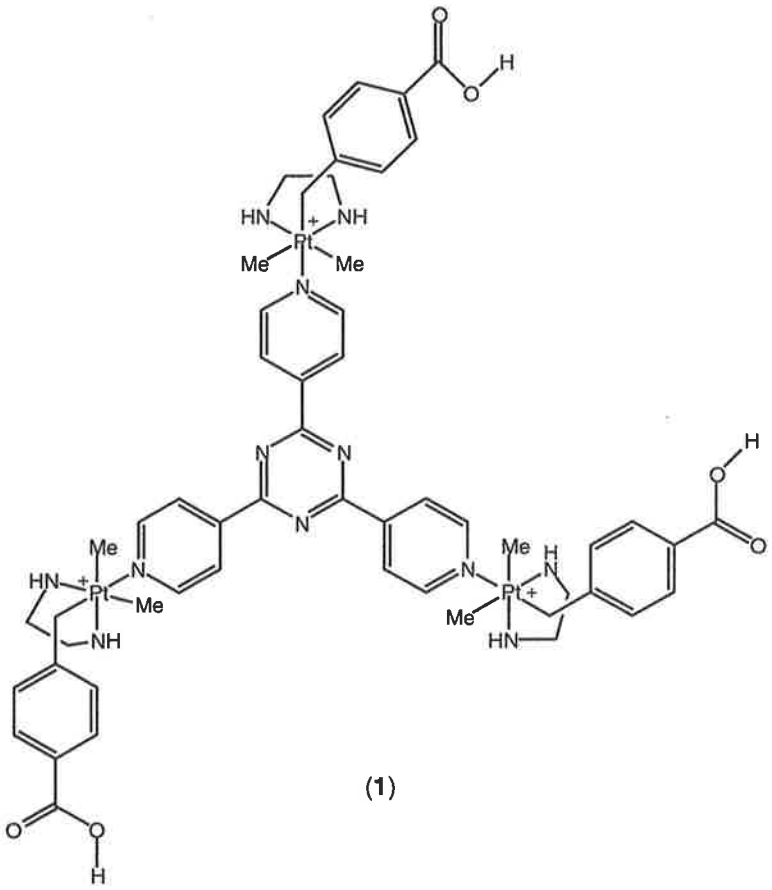

(1)

Recently, Stang and coworkers reported the synthesis of novel platinum(II), (**2**), and rhodium(III), (**3**), complexes with hydrogen-bonding functionalities. The X-ray structure of the platinum(II) complex lattice revealed a zig-zag crystal lattice formed by the head-to-head binding interaction of the complexes through hydrogen-bonding. The zig-zag chain also displayed cross-linking between chains to form a 2-D crystal lattice. The rhodium(III) complex formed two interwoven strands in the solid-state[32].

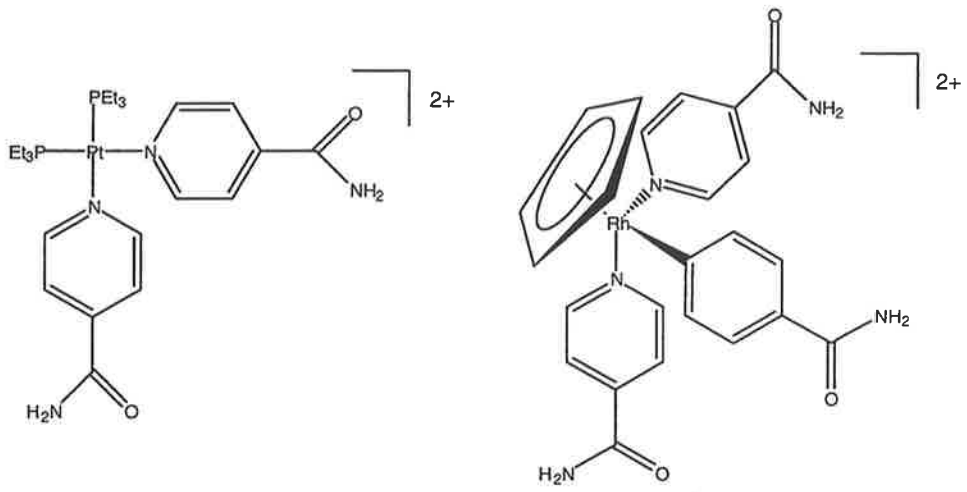

(2) (3)

The Rendina group has recently reported the synthesis of organoplatinum(II) macrocycles that combine both the coordinate-covalent motif, as well as the hydrogen-bonding motif. Recent efforts have seen the synthesis of platinum(II) tectons with hydrogen-bonding functionality. These building blocks then assemble into a discrete macrocyclic unit through hydrogen-bonding, this process is represented schematically in Figure 2. The result is a macrocycle that can readily reassemble itself, thus reducing the possibility of errors in its construction. The second advantage of this hydrogen-bonded macrocycle is that the cavity size is somewhat more flexible than if the macrocycle were constructed exclusively by coordinate-covalent bonding, thus allowing for the supramolecular complexation of a variety of guest molecules.

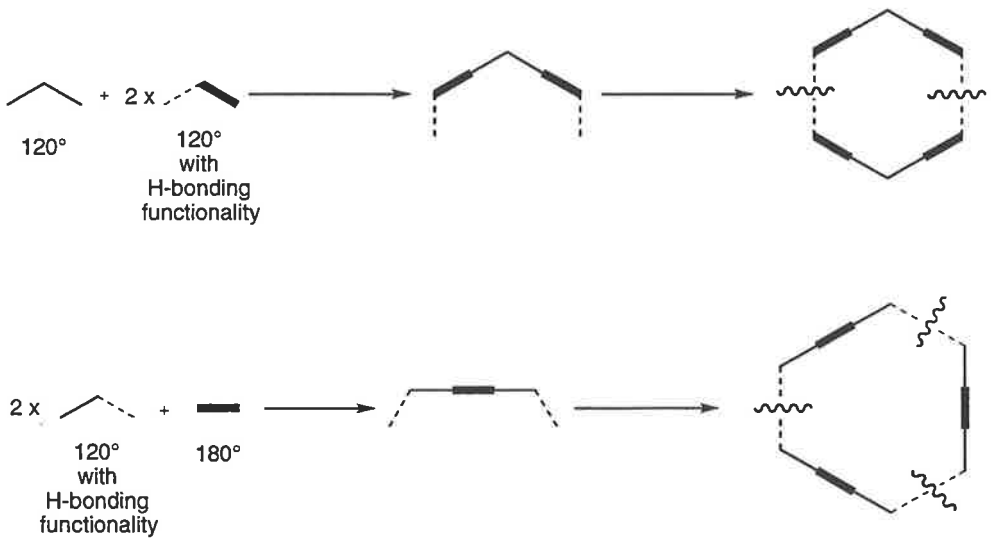

Figure 2. Schematic representation of the synthesis of self-assembling macrocycles through hydrogen-bonding.

Recent work by members of the Rendina group has yielded the synthesis of a number of novel mono- and di-organoplatinum(II) complexes with hydrogen-bonding functionality. Rendina and Gianneschi report the synthesis of a number of dinuclear organoplatinum(II) complexes of nicotinic acid (**4**), (**10**), (**11**), (**12**)[6]. They also report ^{1}H NMR titration studies for two of the complexes demonstrating the spontaneous self-association of the complexes into discrete, hydrogen-bonded aggregates of nanoscale dimensions in a non-aqueous solvent. Similar complexes have been reported for their ability to form macrocyclic aggregates in the solid-state, utilising x-ray crystallographic techniques[33-35]. Rendina and Gianneschi's work, on the other hand, demonstrates the ability of platinum(II) complexes with hydrogen-bonding functionality to form discrete macrocyclic entities in non-aqueous solution.

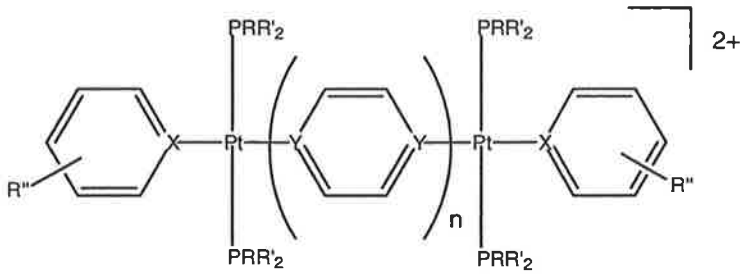

(**4**) R = R' = Ph, R" = 3-CO_2H, X = N, Y = C, n = 2
(**5**) R = Me, R' = Ph, R" = 3-CO_2H, X = N, Y = C, n = 1
(**6**) R = Me, R' = Ph, R" = 3-CO_2H, X = N, Y = C, n = 2
(**7**) R = Me, R' = Ph, R" = 3-CO_2H, X = N, Y = C, n = 3
(**8**) R = R' = Ph, R" = 3-CO_2H, X = C, Y = N, n = 2
(**9**) R = R' = Ph, R" = 4-CO_2H, X = C, Y = N, n = 2

Rendina and Crisp reported the preparation of a number of novel organoplatinum(II) complexes of methyldiphenylphosphine (**5**), (**6**), (**7**), (**13**)[29]. The hydrogen-bonding functionality of these complexes was conferred on the complex by the N-donor ligand nicotinic acid. These complexes are potentially useful tectons for the construction of self-assembled macrocycles in non-aqueous solvents. The $PMePh_2$ ligand enhanced the solubility of the corresponding complexes in organic solvents compared with the PPh_3 complexes reported previously[6]. The $PMePh_2$ ligand is also less bulky than the PPh_3 ligand[36], thus reducing the steric strain on the self-assembly process.

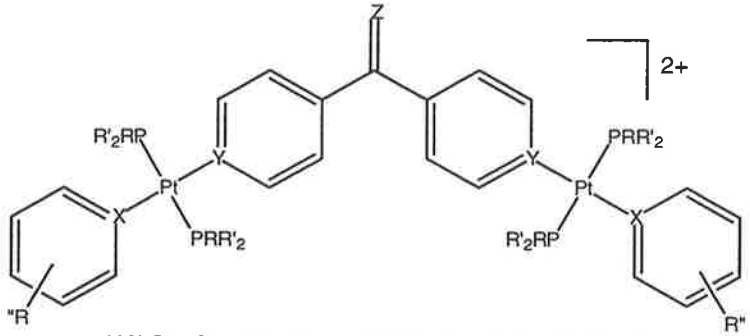

(**10**) R = R' = Ph, R" = 3-CO_2H, Y = C, X = N, Z = O
(**11**) R = R' = Ph, R" = 4-CO_2H, Y = C, X = N, Z = O
(**12**) R = R' = Ph, R" = 3-$CONH_2$, Y = C, X = N, Z = O
(**13**) R = Me, R' = Ph, R" = 3-CO_2H, Y = C, X = N, Z = O
(**14**) R = R' = Ph, R" = 3-CO_2H, Y = N, X = C, Z = CH_2
(**15**) R = R' = Ph, R" = 4-CO_2H, Y = N, X = C, Z = CH_2

The complexes (**4**) – (**15**) were synthesised by oxidative addition of an aryl iodide to a corresponding Pt(0) precursor complex, followed by the addition of the N-donor ligand with hydrogen-bonding functionality. Rendina and Gallasch also reported the synthesis of isomeric complexes (**8**), (**9**), (**14**), (**15**), (**16**), and (**17**)[30] isomeric to those reported previously, in which the hydrogen-bonding group was present on the aryl-iodide that was oxidatively added to the Pt(0) precursor. This proved to be quite challenging owing to the fact that platinum(0) complexes are known to oxidatively add across O-H bonds[37-39]. For this reason, a silyl-containing protecting group was utilised during the oxidative addition reaction and is was later removed, in a facile manner, to give the final product.

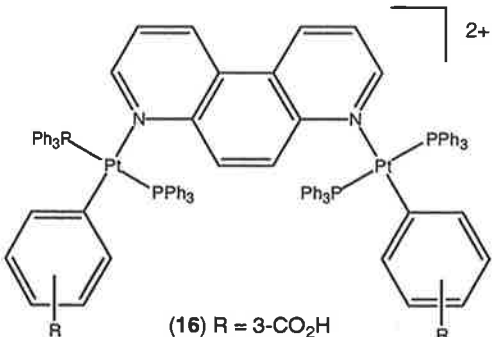

(**16**) R = 3-CO_2H
(**17**) R = 4-CO_2H

We were interested in the idea that complexes (**4**) – (**17**) may act as potential self-assembling molecular receptors in the presence of suitable guest molecules. Thus one of the major aims of this project was to investigate the synthesis of a number of novel mono- and diplatinum(II) complexes with hydrogen-bonding functionality, and to investigate their potential use as molecular receptors for a suitable guest molecule such as adenine. Cyclic and cage

compounds, such as crown ethers, have been shown to be useful for the binding of metal ions and guest compounds. Fujita reports examples of self-assembled palladium[28] and cadmium[18] macrocycles that demonstrate site-specific binding of electron-rich aromatic compounds. Fujita's palladium(II) complex (**18**) has a high affinity for electron-rich aromatic compounds with high shape specificity. The complex specifically binds polymethoxybenzenes (1300 – 2680 $L.mol^{-1}$) while other substrates are not bound so well. In the case of Fujita's molecular receptor, the molecular recognition of the electron-rich polymethoxybenzenes is ascribed to the electron-deficient cavity of the complex due to the presence of tetrafluorophenylene and the coordinated pyridyl groups[28].

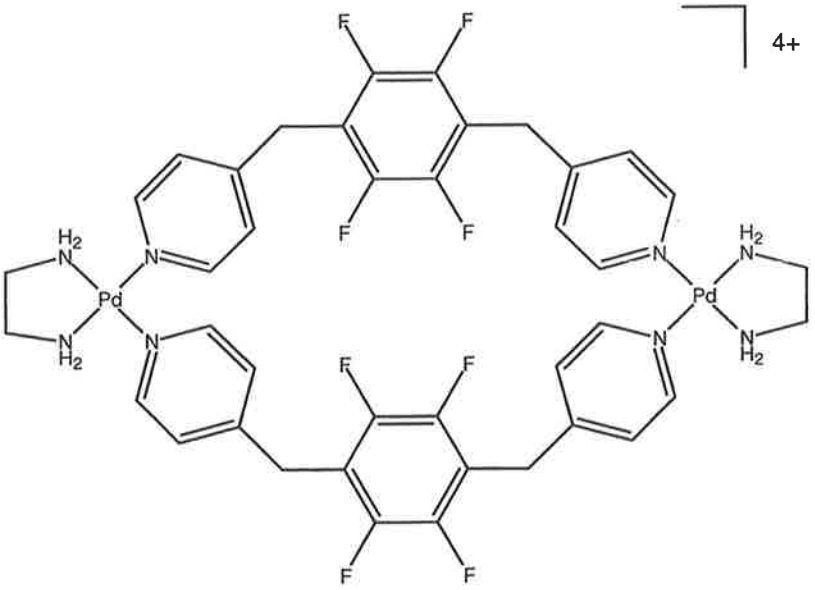

(**18**)

In summary there are a number of ways to synthesise compounds through self-assembly. These include using exclusively coordinate-covalent bonding, or a combination of coordinate covalent bonding and H-bonding. The products have high shape predictability due to the inherent geometries of the subunits used to assemble them. The compounds are usually the focus of solid-state characterisation of both polymers and discrete macrocycles with less work reported on self-assembly in solution. The utility of such self-assembled molecules for molecular recognition is described further in the following section.

1.2 DNA/RNA nucleobases

With molecular recognition being the foundation for a vast array of biological processes, it is not surprising that there is great interest in the study of host-guest chemistry and synthetic receptors[40]. Complexations play important roles in enzyme-substrate interactions, replication of nucleic acids, biosynthesis of proteins, membrane transport, antigen-antibody recognition, and many other examples are known in the literature[41]. Watson-Crick base pairing is a classic example of molecular recognition. The four DNA nucleobases that are involved in hydrogen-bonded base pairing are, adenine (A), guanine (G), cytosine (C) and thymine (T), as shown in Figure 3 [42].

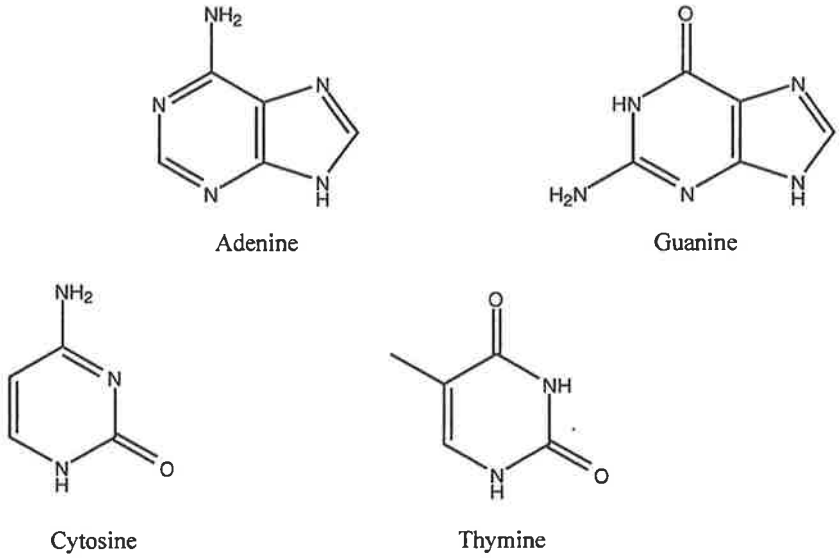

Figure 3. DNA/RNA nucleobases

Base pairing interactions are so fundamental that they are the very elements that hold double-helical DNA intact. Base pairing involves hydrogen-bonding interactions between pairs of nucleobases that are best suited to hydrogen-bond formation. Therefore, adenine pairs with thymine forming two hydrogen bonds, while guanine pairs with cytosine forming three hydrogen bonds, Figure 4.

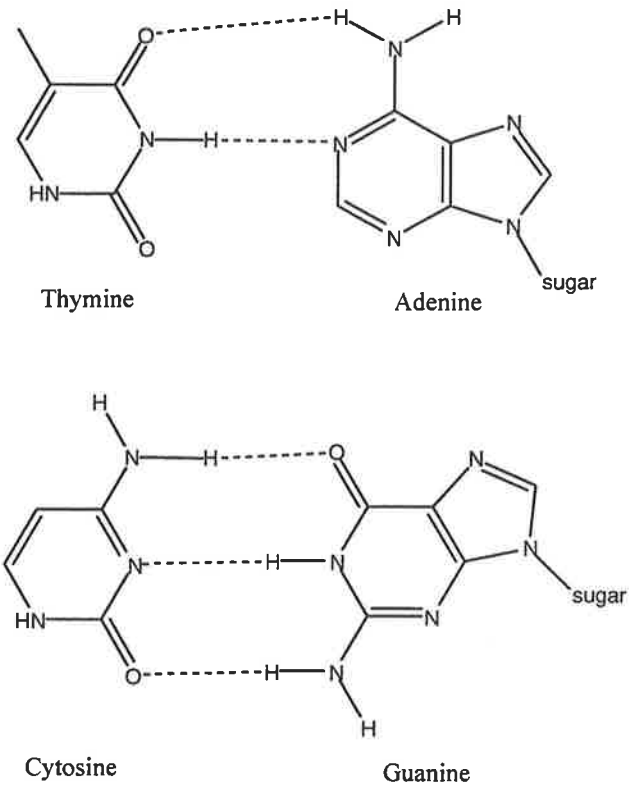

Figure 4. Watson-Crick base pairing

Adenine possesses two major sites for host binding through hydrogen-bonding, and can make a total of four hydrogen bonds. The sites that participate in hydrogen-bonding on adenine are; the Watson-Crick site (WC) at the N_6 and N_1 atoms, and the Hoogsteen (HG) site at the N_6 and N_7 atoms. Both the Watson-Crick and Hoogsteen sites are involved in 1:1 binding interactions. However there also exists the possibility of 2:1 binding which can occur at both sites simultaneously[40,43], Figure 5. Various modes of molecular recognition have been shown to occur between adenine and simple carboxylic acids. Previous work has shown that aromatic carboxylic acids preferentially bind Hoogsteen sites whereas aliphatic carboxylic acids bind preferentially at the Watson-Crick site[44,45]. It has been shown that the association constants can be determined for 1:1 modes of binding, but that for higher modes of binding, for example 2:1, it is much more difficult to determine each of the association constants[44].

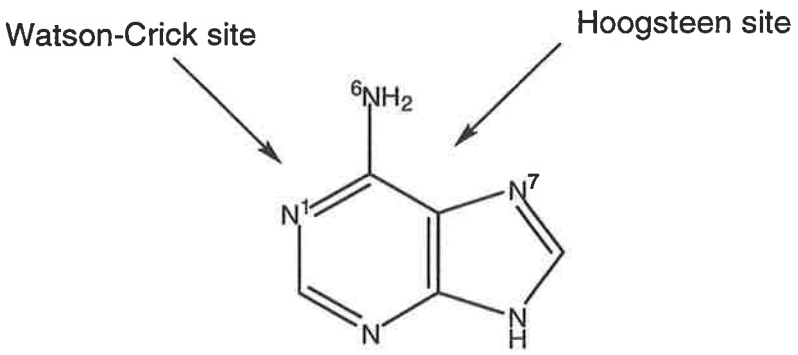

Figure 5. Watson Crick and Hoogsteen binding sites on adenine

Molecular recognition requires complementarity between several binding sites on both the receptor and the substrate. Hydrogen-bonding has previously been utilised in creating molecular receptors for adenine, and these will be discussed further. The main general feature of such receptors is inwardly pointing hydrogen-bonding functionalities, such as a carboxylic acids and their derivatives. As well as utilising hydrogen-bonding as a form of nucleobase interaction, some groups have reported π-stacking as an important interaction with DNA nucleobases. In some cases molecular receptors containing both hydrogen-bonding and π-stacking units have been synthesised, such as those reported by Goswami and co-workers (**19**) and (**20**)[43], and by Rebek and co-workers[40]. Goswami and co-workers found that the selectivity of the receptor could be varied by altering the size of the hydrogen-bonding region, and that the orientation of the aromatic-aromatic interaction could be changed by altering the electronic properties of the π-stacking region[43].

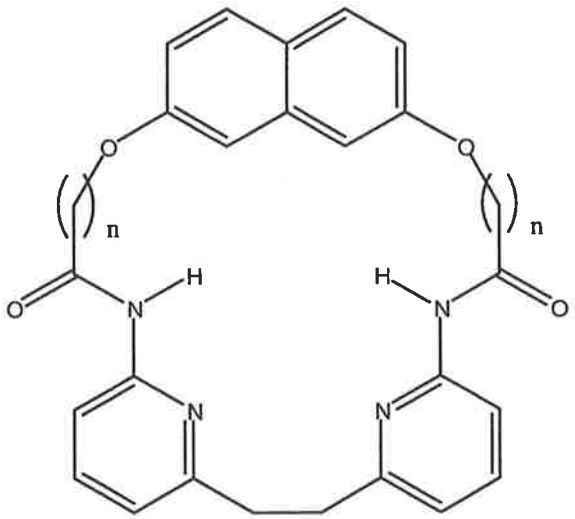

(**19**) n = 2
(**20**) n = 3

There are a number of reported synthetic receptors that utilise hydrogen-bonding as a means of nucleobase complexation. These receptors can be split into two groups with respect to their means of guest complexations. The first group are exclusively hydrogen-bonding molecules, where the sole means of complexation is a planar array of hydrogen-bonding functionalities. The second group has fewer hydrogen-bonding functionalities but incorporates at least one π-stacking interaction. We have so far seen examples of macrocyclic receptors that discriminate their guest molecule by such attributes as size, electronic properties, hydrogen-bonding groups and π-stacking interactions. It is also possible to have a molecular receptor that is non-macrocyclic. Such receptors are given the name "molecular tweezers". These are molecules that are constructed having two binding sites linked by a spacer unit. The more rigid the spacer the better, as there is less conformational flexibility, and therefore decreases the intricacy of the molecule[46]. In this case the tweezer is formed by converging hydrogen-bonding groups or, in some cases, converging aromatics surfaces to form π-stacking interactions. Of course, there are also tweezers that take advantage of both the hydrogen-bonding functionalities of the molecule as well as its π-stacking abilities. An example of a non-macrocyclic receptor, or molecular tweezer, was synthesised by Zimmerman and co-workers[47], in which the binding site for adenine was created between two converging aromatic faces and a single carboxylic acid, (**21**).

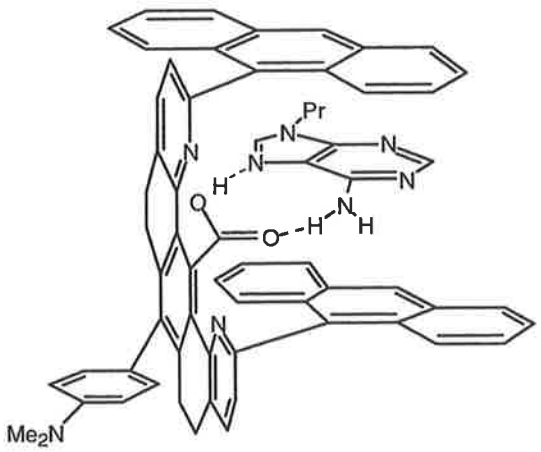

(**21**)

Zimmerman and co-workers reported that by synthesising a molecular tweezer, as opposed to a macrocyclic receptor, they could retain the complexing power of the macrocycle but bind large molecules such as adenine[47].

Another example of a molecular tweezer is reported by Adrian and Wilcox[48] in which the molecular tweezer (**22**), which has two carboxylic acids intersecting at 120°, is able to associate with substrates including adenine.

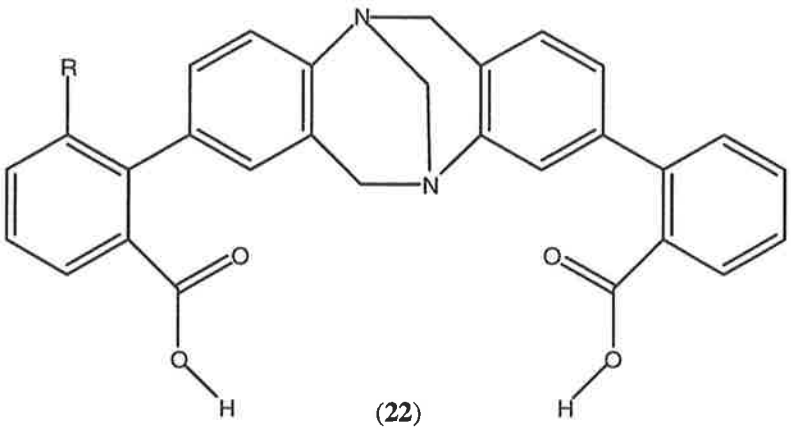

(**22**)

Similar in design to the tweezers designed and synthesised by Adrian are the tweezers reported by Yu (**23**) - (**26**)[49]. These receptors all take advantage of the inwardly pointing hydrogen-bonding groups of the 2,6-diaminoacyl pyridine groups. Of course, the key feature that makes the receptor adaptable is the ability to change its size by changing the nature of the spacer, R, to suit the size of the guest molecule.

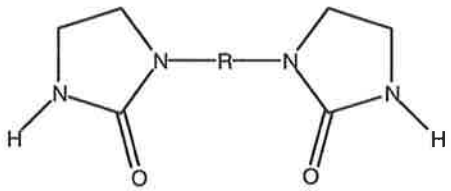

(**23**) R = Ph
(**24**) R = -$(CH_2)_5$-
(**25**) R = -$(CH_2)_6$-
(**26**) R = CH_2-Ph-CH_2

1.3 Platinum Complexes with Hydrogen-Bonding Functionality

The majority of molecular receptors that are reported in the literature are neutral, organic based molecules. This thesis reports the development of a new class of cationic mono- and di-organoplatinum(II) complexes that could potentially utilise hydrogen-bonding functionalities for the recognition of nucleobases, such as adenine. Figures 6 and 7 show the general structures for the complexes that were investigated in this work. The hydrogen-bonding functionality is

conferred on the platinum complex by the coordination of an aromatic N-donor ligand that possesses a hydrogen-bonding group. There are a number of hydrogen-bonding groups that can be used for the synthesis of such complexes. These include carboxylic acids, in the 2-, 3-, and 4-position of a pyridyl ring. Also useful are the analogous primary and secondary amides. The phosphine ligands were chosen for a variety of reasons. One can use alkyl phosphines such as PEt_3, or aryl phosphines such as PPh_3. The phosphines that were used in this project included PEt_3, $PMePh_2$, PPh_3 and PCy_3. The utilisation of phosphine ligands in the synthesis of the complexes assisted us in their characterisation as they allowed us to use $^{31}P\{^1H\}$ NMR spectroscopy. Furthermore, with the construction of a number of model mono-platinum(II) complexes (Figure 6.), certain properties of the complexes can be changed by altering the nature of the phosphine ligand. One can alter the steric bulk of the complex quite readily by varying the types of phosphine ligands used in the synthesis of the target complexes. A phosphine with a large cone angle, such as tricyclohexylphosphine (170°)[50], will lead to greater steric bulk than a phosphine such as triethylphosphine (137°)[51] which has a much smaller cone angle. The different alkyl and aryl substituents on the phosphine ligands may lead to other effects as well, e.g. enhancing the solubility of the complex in organic solvents, an important factor with charged species such as the ones prepared in this work.

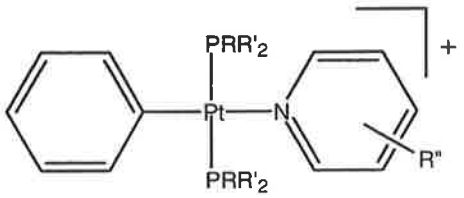

R = Me, Et, Ph, Cy
R' = Et, Ph, Cy
R" = 2-, 3-, 4-pyridine carboxylic acids or amides

Figure 6. General structure of cationic, mononuclear organoplatinum(II) complexes with hydrogen-bonding functionality

Figure 7 shows the general structure of the dinuclear organoplatinum(II) complexes with hydrogen-bonding functionality. The major difference between the mono- and the diplatinum(II) complexes is that the latter have two platinum(II) centres linked by a symmetrical N-donor ligand, and the H-bonding functionality resides on a σ-aryl ligand. The bridging N-donor ligand can be chosen to confer a variety of angles and shapes on the complex. The bridging ligand of

Figure 7 can be altered to change the angle at which the hydrogen-bonding functionalities converge and thus change the dimensions of the resulting molecular tweezer.

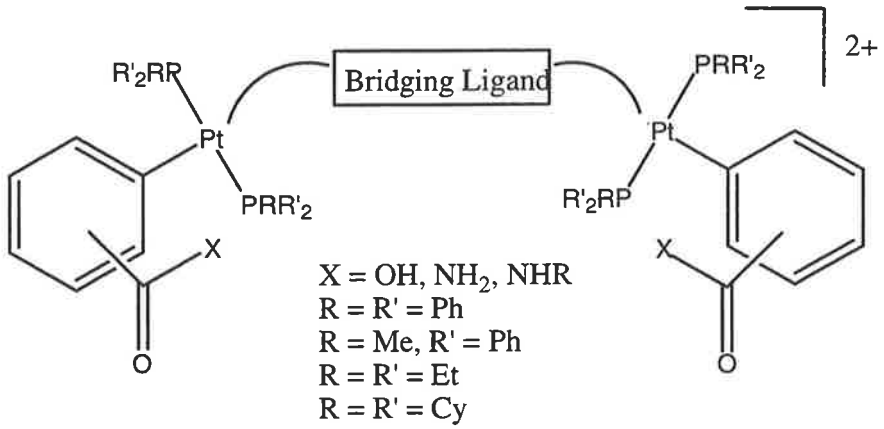

Figure 7. General structure of cationic, dinuclear organoplatinum(II) complexes with hydrogen-bonding functionality

1.4 Molecular Tweezers Containing Platinum(II)

Figure 8 shows a schematic representation of the assembly of a platinum(II) molecular tweezer. The first step is the self-assembly of the molecular tweezer from two basic units. The two units are, the bridging bidentate N-donor ligand and the platinum(II) complex with hydrogen-bonding functionality. When two of the platinum(II) precursor complexes combine with the N-donor ligand they form the platinum(II) molecular tweezer. The platinum(II) tweezer can then combine with a guest molecule.

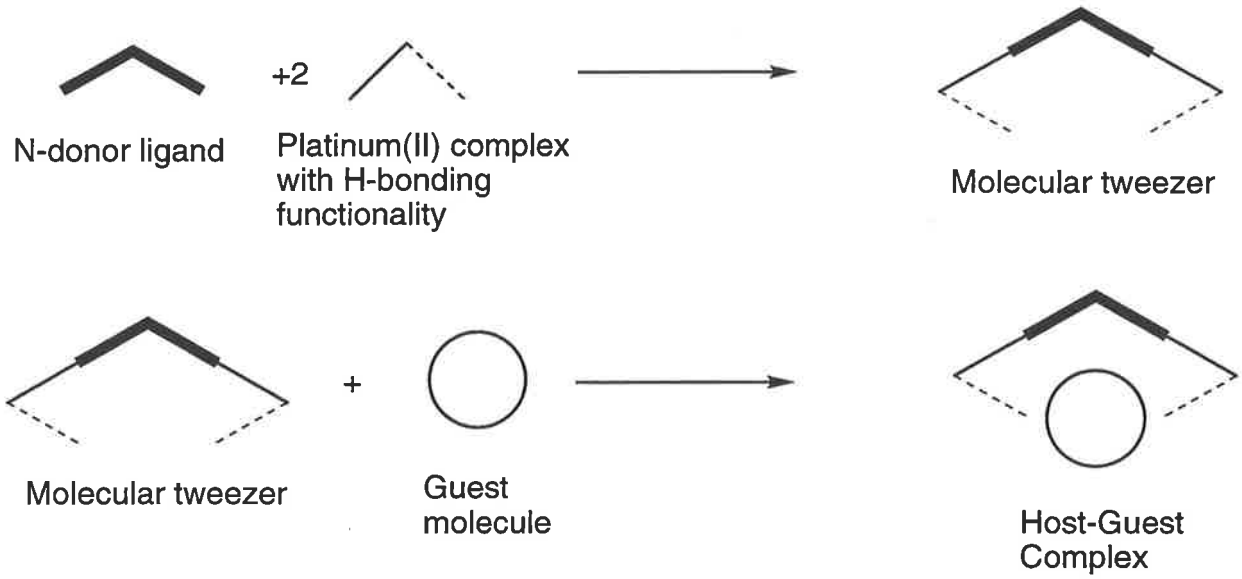

Figure 8. Schematic representation of the general construction of a self-assembling molecular receptor with hydrogen-bonding functionality

The ultimate goal of this work was to show that a dinuclear organoplatinum(II) complex with hydrogen-bonding functionality could be synthesised that would strongly bind simultaneously to both sides of adenine in a non-covalent manner, (**27**). This species would represent the first example of an organometallic molecular tweezer for a nucleobase. There are four literature reports of organometallic complexes that can act as metalloreceptors for DNA bases. One of these is the work by Loeb[52]. where the synthesis of an organopalladium complex is reported and shown to be a suitable receptor for the DNA nucleobases adenine and guanine (**28**). Loeb reported that the palladium complexes provided three forms of interaction with the DNA nucleobases through first sphere and second sphere interactions. The first interaction is the first sphere σ donation from an aromatic N atom to the palladium centre, the other two interactions are second sphere hydrogen-bonds between the NH_2 group and the polyether O atoms, and the π stacking between the electron-poor aromatic rings[52,53].

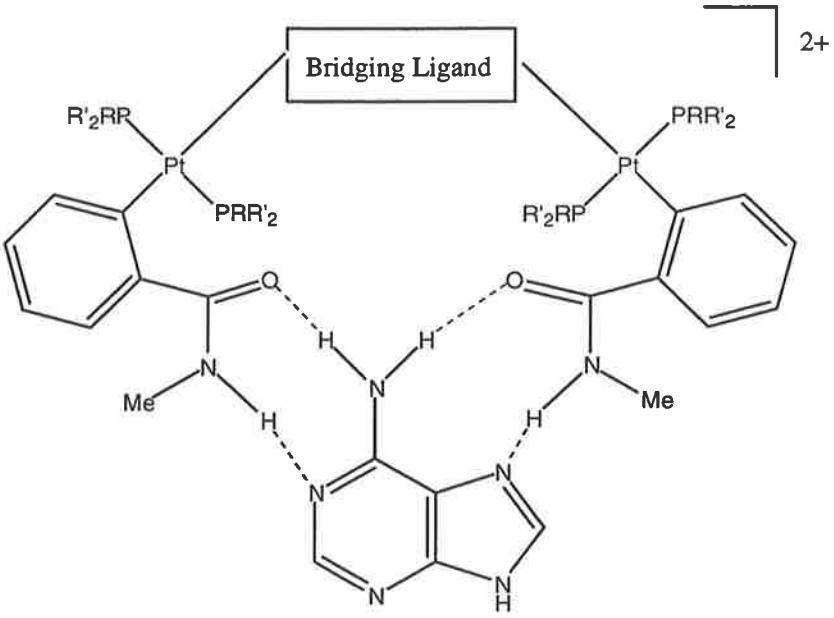

R = Me, Et, Ph, Cy
R' = Et, Ph, Cy

(**27**)

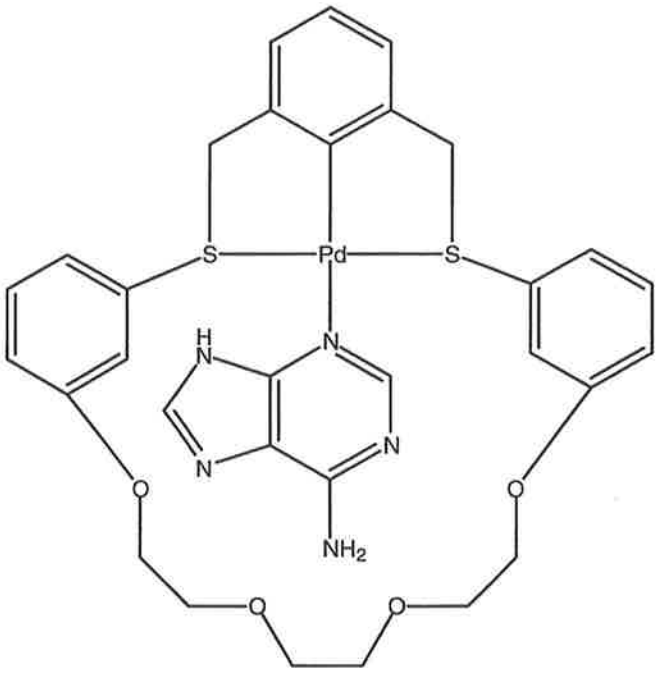

(**28**)

2. Preparation and Characterisation of mononuclear Organoplatinum(II) Complexes with Hydrogen-bonding Functionality

This chapter describes the synthesis and characterisation of several novel monoplatinum(II) complexes with hydrogen-bonding functionality. Section 2.1 describes the preparation of the iodoplatinum(II) complexes that are the precursors to the target monoplatinum(II) complexes with hydrogen-bonding functionality. Section 2.2 describes the reactions of the iodoplatinum(II) complexes with suitable aromatic ligands containing hydrogen-bonding functionalities. Section 2.3 reports the determination of pKa values for selected monoplatinum(II) complexes.

2.1 Synthesis and Characterisation of Iodoplatinum(II) Precursor Complexes

One of the key steps in the synthesis of the target mononuclear platinum(II) complexes with hydrogen-bonding functionality was to prepare precursor iodoplatinum(II) complexes. The most common method for the insertion of platinum into an aryl-halide bond is by an oxidative addition reaction employing the appropriate platinum(0) precursor with an aryl-halide[6,21,22,26,29], typically an aryl-iodide. This was attempted by heating iodobenzene and $Pt(PPh_3)_4$ in toluene solution as shown in Scheme 2.1. The oxidative addition method proved unsuitable in the preparation of the target complexes for two reasons. First, the platinum(0) complexes were difficult to prepare in high yield and purity, and a different platinum(0) precursor was required for each phosphine ligand used in our study[50,54]. Second, the oxidative addition reactions that were carried out resulted in products containing significant amounts of impurities. Therefore, we investigated the use of platinum-alkene precursor complexes as an alternative to the use of platinum(0) precursors. The platinum(II)-olefins were stabilised sufficiently to undergo Grignard-type reactions, while the olefin could be displaced by a suitable range of phosphine ligands[55,56]. Scheme 2.2 summarizes the synthetic route to the iodoplatinum(II) precursor complexes.

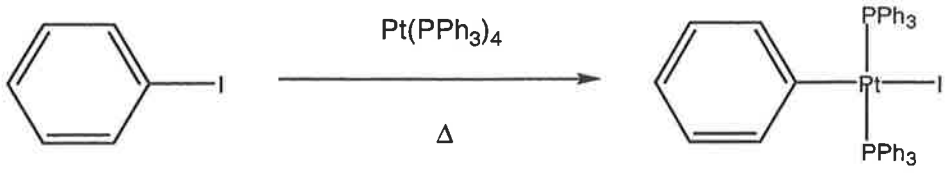

(29) (30)

Scheme 2.1

$Pt(cod)Cl_2$ (**32**) was prepared in good yield by the method reported by Clark and Manzer[55]. Metathetical replacement of the chloro ligand with iodide resulted in the formation of the corresponding diiodo complex (**33**) in quantitative yield. The Grignard reagent, phenylmagnesium bromide, was employed to afford the corresponding diphenylplatinum(II) complex (**34**). This reaction resulted in the formation of the expected product (**34**), and it could not be stopped at the mono-substitution stage[55]. One of the σ-phenyl ligands was selectively removed by using one molar equivalent of HCl formed *in situ* by reacting acetyl chloride with CH_3OH in CH_2Cl_2 solution[55], to give (**35**) in good yield. Once again it was a simple matter of reacting the resulting chloro species with NaI to form the corresponding iodophenylplatinum(II) complex (**36**).

All of these reactions were found to be high yielding (60-85%). Although there were a number of steps involved in using this scheme, the result was a less difficult, higher yielding preparation of the target complexes. The final result of this five-step synthesis was the highly pure and useful precursor (**36**). The 1,5-cyclooctadiene ligand could be displaced readily with ligands such as tertiary phosphines particularly as it is labilised by the strongly *trans*-labilising iodo and phenyl ligands[57].

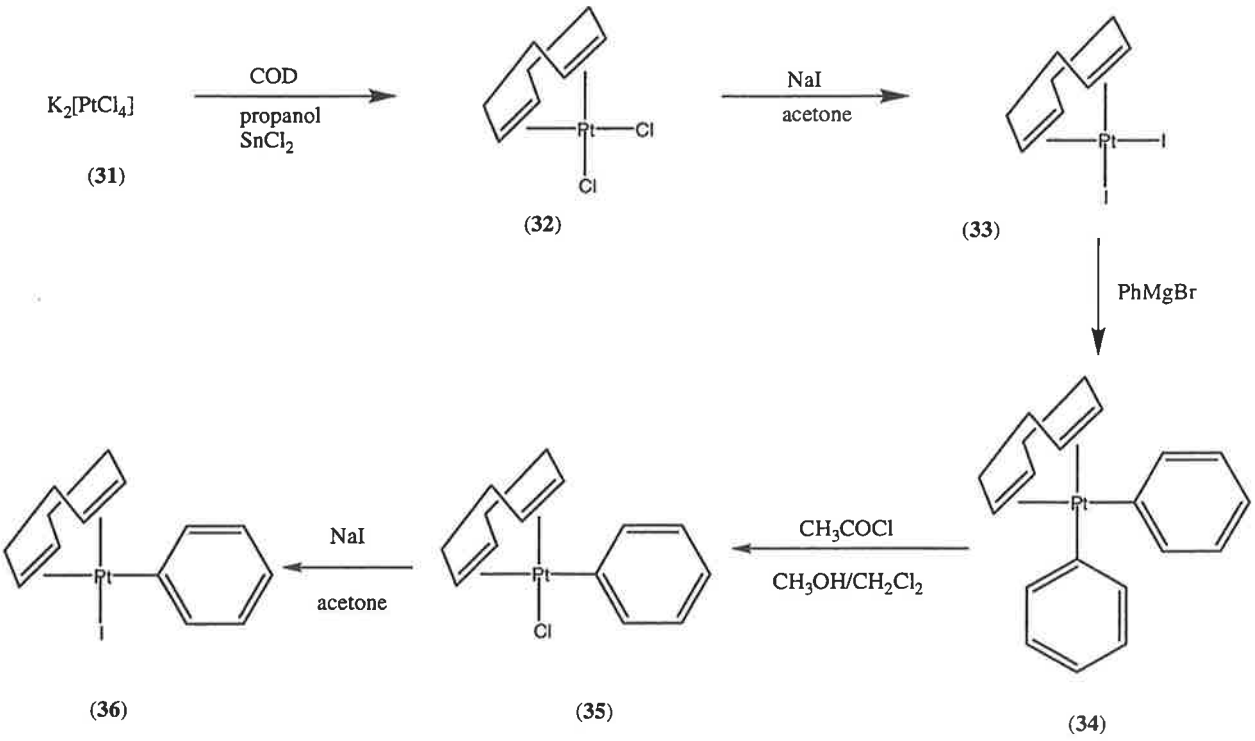

Scheme 2.2

Complex (**36**) was successfully reacted with four different tertiary phosphine ligands, PPh_3, PEt_3, and $PMePh_2$, and PCy_3 to form the corresponding *trans*-bis(phosphine)iodoplatinum(II) complexes (**37**), (**38**), (**39**) and (**40**), respectively. As the reactions were conducted at temperatures of up to 90 °C, it was possible to form exclusively the thermodynamically-favoured, *trans*-substituted platinum(II) complexes (**37**) - (**40**) as air-stable, colourless solids.

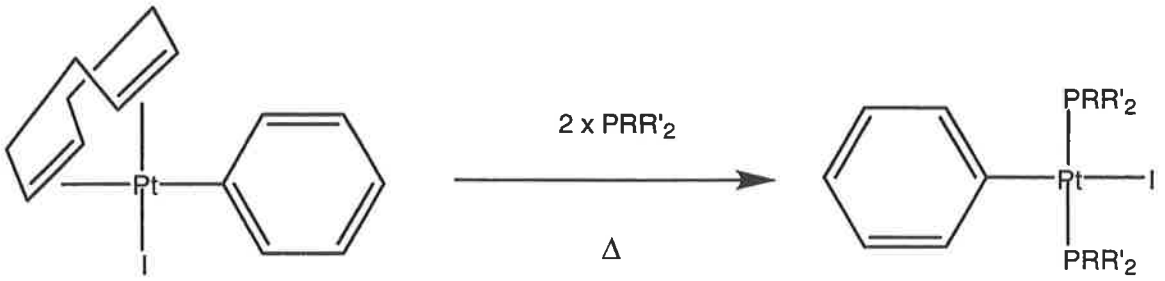

(**37**) R = R' = Ph
(**38**) R = Me, R' = Ph
(**39**) R = R' = Et
(**40**) R = R' = Cy

Scheme 2.3

Table 1 summarises some of the key spectroscopic data for the iodoplatinum(II) complexes (**37**) - (**40**). The ^{1}H NMR spectra of the complexes show the expected downfield doublet due to the *ortho* proton of the σ-aryl group at between δ 6.65 - 7.52. This signal shows distinctive three-bond ($^{3}J_{HPt}$) spin-spin coupling to ^{195}Pt (I = 1/2; natural abundance = 33.8%) of 29 - 36 Hz in the form of a pair of doublet satellites centred about the major signal. The *ortho* proton always appears downfield of the *meta* and *para* protons due to its proximity to the Pt-C bond. The *meta* and *para* protons appear as multiplets as a result of non-first order coupling to the other protons; these signals always appear upfield to the *ortho*-protons.

Table 1. ^{1}H- and $^{31}P\{^{1}H\}$ NMR[a] Data for the iodoplatinum(II) Complexes (37) - (40).

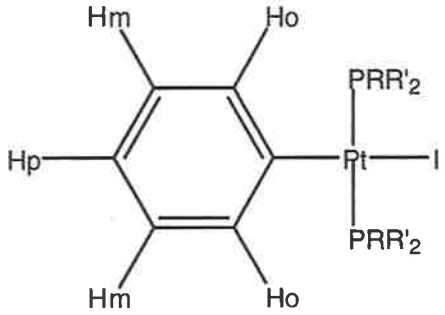

(**37**) R = R' = Ph
(**38**) R = Me, R' = Ph
(**39**) R = R' = Et
(**40**) R = R' = Cy

Complex	δ(^{1}H)					δ (^{31}P)[b]
	H_{ortho}	H_{meta}	H_{para}	PRR'_2	PCH_3	
37	6.65, 2H, d, ($^{3}J_{HH}$ = 7.8 Hz, $^{3}J_{PtH}$ = 29 Hz)	6.10, 2H, m	6.24, 1H, m	7.57-7.20, 30H, m	na	22.0 (3087)
38	6.81, 2H, d, ($^{3}J_{HH}$ = 7.8 Hz, $^{3}J_{PtH}$ = 30 Hz)	6.46, 3H, m	6.46, 3H, m	7.56-7.13, 20H, m	1.85, 6H, m	4.7 (2935)
39	7.28, 2H, d, ($^{3}J_{HH}$ = 7.2 Hz, $^{3}J_{PtH}$ = 36 Hz)	6.92, 2H, m	6.81, 1H, m	1.86-1.00, 30H, m	na	9.4 (2739)
40	7.52, 2H, d, ($^{3}J_{HH}$ = 6.6 Hz, $^{3}J_{PtH}$ = 32 Hz)	6.84, 3H, m	6.84, 3H, m	1.91-0.98, 60H, m	na	13.0 (2745)

[a]Chemical shifts in ppm measured in $CDCl_3$; quoted multiplicities do not include ^{195}Pt satellites. [b] $^{1}J_{PtP}$ coupling constants (Hz) in parentheses.

Each signal in the $^{31}P\{^{1}H\}$ NMR spectrum appears as a sharp singlet flanked by ^{195}Pt satellites in a 1:4:1 ratio. This is consistent with *trans* substitution around the platinum(II) centre. The Pt-P spin-spin coupling ($^{1}J_{PPt}$) ranges from 2739 – 3087 Hz, which is also consistent with the *trans* arrangement of the phosphine ligands in a platinum(II) complex[26].As expected, the aryl-substituted PPh_3 (δ 22.0) appears downfield with respect to the alkyl-substituted phosphine ligands PEt_3 (δ 9.4), PCy_3 (δ 13.0), and $PMePh_2$ (δ 4.7), the data are consistent with those of related complexes reported in the literature[26].

Utilising phosphine ligands in these complexes benefited us in several ways. First, the presence of phosphine ligands enabled us to monitor the reactions and analyse the products using $^{31}P\{^{1}H\}$ NMR spectroscopy, which is a sensitive probe for *cis-trans* isomerisation in Pt(II)-phosphine complexes, enabling us to quickly and easily determine the final stereochemistry of the platinum complex. Second, the various phosphines greatly altered the solubility of the product in various solvents, with alkyl phosphines such as PEt_3 being highly soluble in chlorinated organic solvents, and partially soluble in diethyl ether, while the aryl phosphines such as PPh_3 were much less soluble in the same solvents[26]. Third, different phosphine ligands also conferred different crystallising properties on the complexes by changing their packing efficiency. Finally, phosphines such as PEt_3 or PPh_3 have small cone angles, 137° and 145°[50] respectively, compared with phosphines such as PCy_3 (170°)[50] which have relatively large cone angles. Large cone angles result in greater steric congestion than small cone angles. This may confer interesting properties upon the target complexes once the iodo ligand is substituted with a ligand possessing H-bonding functionality, e.g. intermolecular H-bonding characteristics.

In general, complexes (**37**) – (**40**) are generally air-stable solids, but it was found that in solution (**39**) was quite reactive toward dioxygen and water. On dissolving (**39**) in n-hexane at room temperature, colourless crystals were found to form overnight. The crystals were of X-ray quality, and the molecular structure of the complex was determined as shown in Figure 9. The crystal structure showed that the original complex had undergone loss of the σ-phenyl ligand and that the PEt_3 had been oxidised to form the corresponding diethyl phosphine-oxide and -hydroxide, the latter being hydrogen-bonded to free $OPEt_3$ in the solid state (Scheme 2.4). The by-products of the reaction were not identified and their fate remains undetermined. At this stage we are unable to propose a suitable mechanism for the oxidation process.

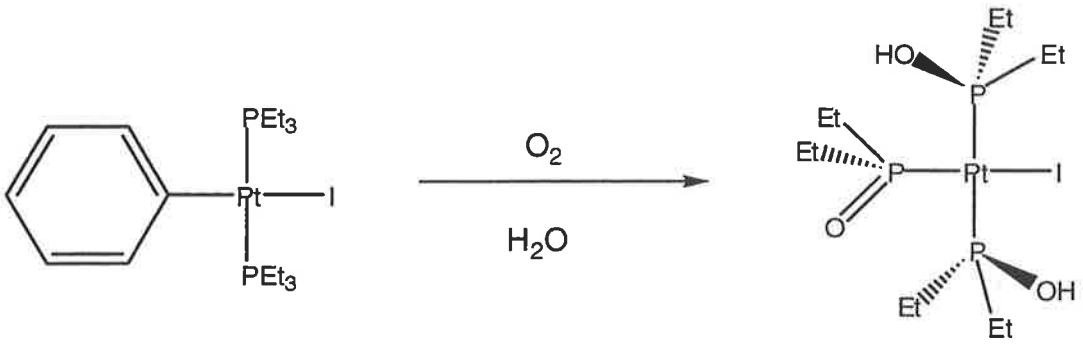

(39) **(41)**

Scheme 2.4

Figure 10 shows the molecular structure of (**41**) in which the platinum atom exists in the expected square planar geometry. The platinum atom lies 0.0069(3) Å above the IP_3 donor set. The $Et_2P(OH)$ ligands occupy mutually *trans* positions as do the anionic $[Et_2P\text{-}O]^-$ and I^- species. The d(Pt-P1, P2) of 2.325(2) Å and 2.319(2) Å are significantly longer than d(Pt-P3) of 2.250(2) Å confirming the assignment of hydroxy- and oxo-functions. The complex is stabilised by an intramolecular H-bond between O1-H1---O3 with d(H1---O3) = 1.50 Å, d(O1---O3) = 2.400(6) Å and angle at H1 of 156.0°. An intermolecular H-bonding interaction is found between O2-H2 and O4 of the $Et_3P{=}O$ molecule of the solvent so that d(H2---O4) is 1.57 Å, d(O2---O4) is 2.493(5) Å and angle at H2 is 162.5°[58].

Table 2. Data collection and handling

Crystal	colourless block
	size 0.16 x 0.32 x 0.36 mm
Wavelength	Mo K_α radiation (0.7107 Å)
μ	58.71 cm^{-1}
Diffractometer, scan mode:	Rigaku AFC7R, $\omega/2\theta$
$2\theta_{max}$	55°
$N(hkl)_{measured}$, $N(hkl)_{unique}$	7599, 7151
Criterion for I_{obs}, $N(hkl)_{gt}$	$I_{obs} > 3\ \sigma(I_{obs})$, 5055
$N(param)_{refined}$	251
Programs	TeXan, DIRDIF92, DIFABS

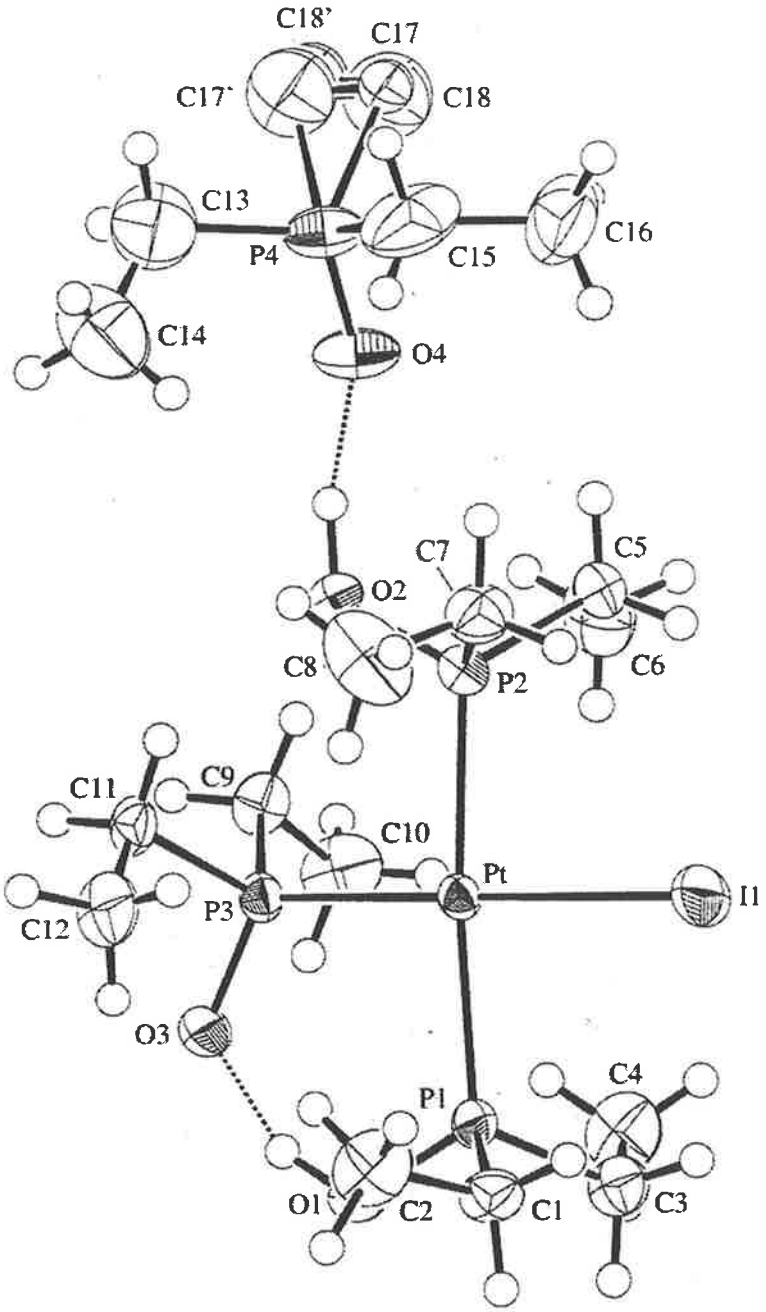

Figure 10. Molecular structure of (41)

2.2 Synthesis and Characterisation of Mononuclear Platinum(II) Complexes with Hydrogen-Bonding Functionality

Mononuclear platinum(II) complexes with hydrogen-bonding functionality were prepared from the platinum precursors (**37**) – (**40**) by substitution of the iodo ligand by a suitable N-donor ligand containing a hydrogen-bonding group. In this case, the N-donor groups that were chosen included 2-, 3-, and 4-pyridine carboxylic acids, also known as picolinic acid, nicotinic acid and isonicotinic acid, respectively. Each acid contained a pyridine ring that forms a strong coordinate-covalent bond with platinum(II), and each molecule also contained a free carboxylic acid group which conferred hydrogen-bonding functionality on the cationic complex.

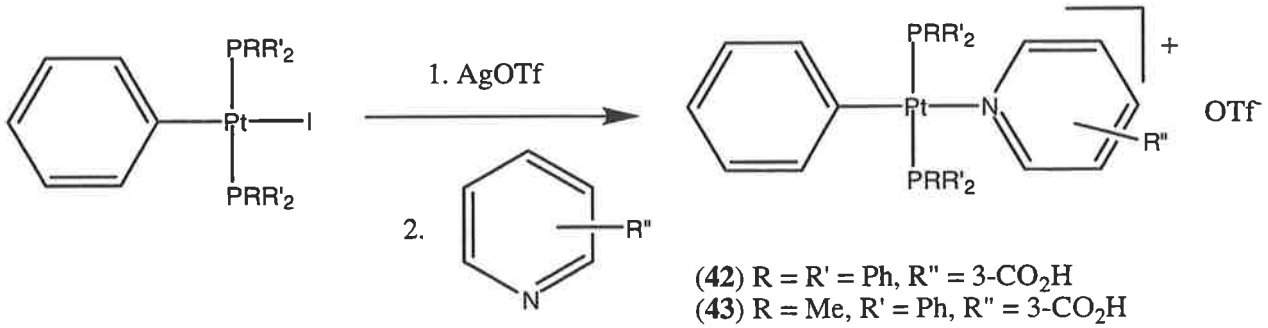

(**42**) R = R' = Ph, R" = 3-CO_2H
(**43**) R = Me, R' = Ph, R" = 3-CO_2H
(**44**) R = R' = Et, R" = 3-CO_2H
(**45**) R = R' = Cy, R" = 3-CO_2H
(**46**) R = R' = Ph, R" = 4-CO_2H
(**47**) R = Me, R' = Ph, R" = 4-CO_2H
(**48**) R = R' = Et, R" = 4-CO_2H
(**49**) R = R' = Cy, R" = 4-CO_2H
(**50**) R = R' = Ph, R" = 2-CO_2H
(**51**) R = Me, R' = Ph, R" = 2-CO_2H
(**52**) R = R' = Et, R" = 2-CO_2H
(**53**) R = R' = Cy, R" = 2-CO_2H
(**54**) R = Me, R' = Ph, R" = 4-$CONH_2$
(**55**) R = Me, R' = Ph, R" = 3-$CONH_2$

Scheme 2.5

The iodo ligand was not particularly labile when coordinated to a platinum(II) centre, and thus AgOTf (OTf = trifluoromethanesulfonate; triflate) was employed to remove the iodo ligand and replace it with the much more labile triflato ligand. It was then a matter of displacing the triflato ligand with the various N-donor ligands. Reactions involving AgOTf were highly water sensitive, as were the triflato complexes thus formed. For this reason, all reactions were carried out under anhydrous conditions using standard Schlenk techniques.

Tables 2.2, 2.3, and 2.4 summarise the ^{1}H- and $^{31}P\{^{1}H\}$ NMR data for the target Pt(II) complexes (**42**) - (**53**). Complex (**42**) shows multiplet signals at δ 6.74, 6.37, and 6.53 which correspond to the *ortho*, *meta* and *para* σ-aryl protons, respectively. The PPh_3 protons appear at δ 7.57 - 7.14. The signals for the pyridyl protons, H^2, H^4, H^5, and H^6 appear at δ 8.57, 8.20, 6.82, and 7.84, respectively. As expected, the two protons adjacent to the electronegative nitrogen atom, H^2 and H^6, are shifted downfield compared to the other aromatic protons. The $^{31}P\{^{1}H\}$ NMR spectrum of (**42**) appears as a singlet at δ 20.8, flanked by ^{195}Pt satellite signals ($^{1}J_{PtP}$ = 3045 Hz). This is the expected shift of organoplatinum(II) complexes containing mutually *trans* PPh_3 ligands. Complex (**43**) has a very similar ^{1}H NMR spectrum to that of (**42**), the main difference being the presence of the $PMePh_2$ methyl proton multiplet at δ 1.62.This multiplet signal constitutes the X part of an $AMM'X_3X'_3$ spin system (where A = ^{195}Pt, M = ^{31}P, and X = ^{1}H). At this stage we are unable to extract reasonable coupling data from the spectra, but related spin systems have been reported elsewhere[59,60], and a theoretical analysis of spin systems of the type $MM'X_nX'_n$ (where n = 3 and 6) has been described previously by Harris[61]. The $^{31}P\{^{1}H\}$ NMR spectrum appeared again as a singlet, but in this instance the signal had been shifted dramatically upfield to δ 9.4, when compared to (**42**). The $^{31}P\{^{1}H\}$ NMR spectrum of complex (**44**) appeared as a sharp singlet at δ 13.9 flanked by ^{195}Pt satellites ($^{1}J_{PtP}$ = 2698 Hz). The interpretation of the ^{1}H NMR spectrum of (**44**) was facilitated by the fact that there were no aromatic protons due to the phosphine ligand, as was the case for (**42**) and (**43**). The ethyl protons appear upfield at δ 1.23 – 0.96. The signal due to H^2 appeared as a downfield shifted singlet at δ 9.19, while H^6 exists as downfield shifted doublet at δ 8.88 ($^{3}J_{HH}$ = 5.4 Hz) due to three bond coupling to H^5. H^2 and H^6 were shifted downfield due to their proximity to the electronegative nitrogen atom of the nicotinic acid ligand. H^4 and H^5 appeared as a doublet and a multiplet, at δ 8.54 and δ 8.00 ($^{3}J_{HH}$ = 7.8 Hz and 5.7 Hz), respectively. The signals due to the σ-aryl protons, H_{ortho}, H_{meta} and H_{para}, were attributed to δ 7.28, δ 7.03 and δ 6.93, respectively. Each of these signals appeared as a complex multiplet. The hydroxyl proton appeared as a very broad singlet at δ 5.89, which disappeared upon the addition of one drop of D_2O to the NMR-tube.

As expected, complexes (**46**) - (**49**), containing the isonicotinic acid ligand, have the simplest ^{1}H NMR spectra due to the high symmetry present in the complexes. Complex (**48**) had the characteristic signals at δ 7.32, 6.87, and 7.05, assigned to the *ortho*, *meta* and *para* σ-aryl protons, respectively. As anticipated, the aromatic region of the spectrum was significantly

simplified without the presence of the PPh_3 proton signals. This aided in the assignment of the other aromatic protons that are sometimes masked by the PPh_3 protons. The two signals at δ 8.17 and 8.27 were attributed to the $H^{2/6}$ and $H^{3/5}$ protons of the isonicotinic acid ligand. The $^{31}P\{^1H\}$ NMR spectrum showed a singlet at δ 13.4, with ^{195}Pt satellites ($^1J_{PtP}$ = 2697 Hz), as expected for the *trans* geometry of the complex. Complexes (**46**) and (**47**) had similar ^1H and $^{31}P\{^1H\}$ NMR spectra to that of (**48**).

The ^1H NMR spectra of the picolinic acid complexes (**50**) - (**53**) were more complicated as they contained several chemically-inequivalent protons, thus giving rise to a greater number of signals then their isomers. Complex (**50**) showed a signal at δ 6.63 which was assigned to the *ortho* proton while the *meta* and *para* protons appeared as overlapping signals at δ 6.33. H^3 appeared at δ 8.69, while H^6, H^5 and H^4 appeared as signals at δ 8.03, 8.28 and 7.75 respectively. The $^{31}P\{^1H\}$ NMR spectrum of (**50**) appeared as a sharp singlet at δ 23.0 ($^1J_{PtP}$ = 3212 Hz). Complex (**51**) displayed a signal at δ 6.55 which was assigned to the *ortho* σ-aryl protons, while the signal at δ 6.87 was assigned to the *meta* and *para* σ-aryl protons, which were overlapping. The $^{31}P\{^1H\}$ NMR spectrum of (**51**) displayed a sharp singlet at δ 6.5 with ^{195}Pt satellites ($^1J_{PtP}$ = 3089 Hz). Complex (**52**) gave rise to signals at δ 6.63, 6.97 and 6.91 which were assigned to the *ortho*, *meta*, and *para* protons respectively. The signals due to the protons H^3, H^6, H^5, and H^4 where assigned to δ 6.33, 8.79, 8.04 and 7.64, respectively. The $^{31}P\{^1H\}$ NMR spectrum of (**52**) appeared as a singlet at δ 11.1 flanked by ^{195}Pt satellites ($^1J_{PtP}$ = 2840 Hz). Complex (**53**) gave rise to a signal at δ 7.01 attributed to the *meta* proton, and a signal at δ 6.96 attributed to the *para* proton. The signals at δ6.33, 8.25, 7.98 and 7.61 were assigned to the H^3, H^6, H^5, and H^4 protons respectively. The $^{31}P\{^1H\}$ NMR spectrum of (**53**) appeared as a sharp singlet at δ 17.2 ($^1J_{PtP}$ = 3067 Hz). Unfortunately, complexes (**52**) and (**53**) were the only two complexes that could not be prepared in an analytically pure manner, despite repeated recrystallisations.

Obviously, a carboxylic acid is not the only functional group capable of hydrogen-bonding interactions. With the successful synthesis of a number of platinum(II) complexes containing carboxylic acids, two platinum(II) complexes containing an amide functionality were also synthesised. In the same manner as described for complexes (**42**) - (**53**), the iodo ligand was removed from the iodo precursor (**38**) with AgOTf and the more labile triflato ligand was displaced with the N-donor ligands, isonicotinamide and nicotinamide, to afford (**54**) and (**55**), respectively.

The ^{1}H NMR spectrum of complex (**54**) showed a signal at δ 7.16 that was assigned to the *ortho* σ-aryl protons. In a similar manner to that of complex (**51**), the signals for the *meta* and *para* σ-aryl protons were overlapping at δ 6.84. The $^{31}P\{^{1}H\}$ NMR signals appeared as a δ 9.8 singlet, flanked by ^{195}Pt satellites ($^{1}J_{PtP}$ = 2888 Hz) which is similar to complex (**47**) (δ 9.4, $^{1}J_{PtP}$ = 2914 Hz), suggesting that the nature of the hydrogen-bonding group has little effect on the electronic environment of the Pt-P bond. The spectroscopic features of (**55**) were more difficult to analyse than for (**54**). The fact that the amide was in the 3- position rather than the 4- position destroyed the symmetry of the complex and therefore results in a more complicated spectrum. H^{2} appeared as a downfield shifted singlet at δ 8.62, while the signals due to H^{4}, H^{5}, and H^{6} appeared as an overlapping multiplet signal at δ 7.98. Similarly the *ortho, meta* and *para* σ-aryl protons appeared as an overlapping multiplet at δ 6.98 - δ 6.67. The signal due to the NH_2 protons of the amide appeared as a broad singlet at δ 5.57. As with the other complexes that possess the $PMePh_2$ ligand, there was a signal due to the methyl group of the phosphine ligand at δ 1.69. The $^{31}P\{^{1}H\}$ NMR signal appeared as a δ 10.0 singlet, flanked by ^{195}Pt satellites ($^{1}J_{PtP}$ = 2927 Hz).

Table 3. ^{1}H- and $^{31}P\{^{1}H\}$ NMR Data for the nicotinic acid Complexes (42) - (45)[a].

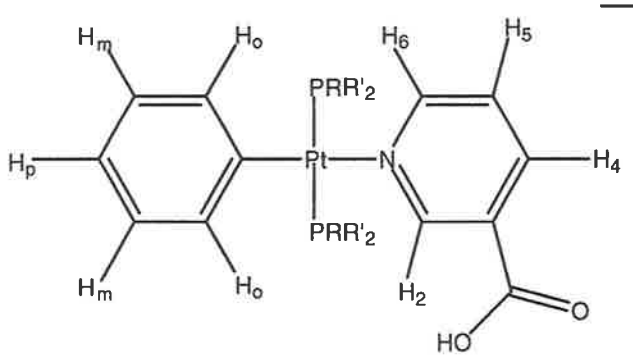

(**42**) R = R' = Ph
(**43**) R = Me, R' = Ph
(**44**) R = R' = Et
(**45**) R = R' = Cy

Complex	δ (^{1}H)								δ (^{31}P)[b]
	H_{ortho}	H_{meta}	H_{para}	H^2	H^6	H^5	H^4	PRR'_2	
42	6.74, 2H, d, ($^{3}J_{HH}$ = 7.5 Hz)	6.37, 2H, m	6.53, 1H, m	8.57, 1H, s	8.20, 1H, d, ($^{3}J_{HH}$ = 5.7 Hz)	6.82, 1H, m	7.84, 1H, d, ($^{3}J_{HH}$ = 7.8 Hz)	7.57-7.14, 30H, m	20.8 (3045)
43	c	6.89, 3H, m	6.89, 3H, m	8.37, 1H, s	8.19, 1H, d, ($^{3}J_{HH}$ = 4.8 Hz)	c	7.88, 1H, d, ($^{3}J_{HH}$ = 8.1 Hz)	7.52-7.16, 20H, m	9.4 (2870)
44	7.28, 2H, d, ($^{3}J_{HH}$ = 7.2 Hz)	7.03, 2H, m	6.93, 2H, m	9.19, 1H, s	8.88, 1H, d, ($^{3}J_{HH}$ = 5.4 Hz)	8.00, 1H, m	8.54, 1H, d, ($^{3}J_{HH}$ = 7.8 Hz)	1.23 – 0.96, 30H, m	13.9 (2698)
45	7.40, 2H, m	6.83, 2H, m	7.01, 1H, m	9.30, 1H, s	8.94, 1H, d, ($^{3}J_{HH}$ = 6.9 Hz)	7.77, 1H, m	8.68, 1H, d, ($^{3}J_{HH}$ = 7.8 Hz)	1.91-0.86, 60H, m	13.4 (2724)

[a]Chemical shifts in ppm measured in $CDCl_3$; quoted multiplicities do not include ^{195}Pt satellites. [b] $^{1}J_{PtP}$ coupling constants (Hz) in parentheses.
[c]Obscured by $PMePh_2$ protons.

Table 4. ^{1}H- and $^{31}P\{^{1}H\}$ NMR Data for the isonicotinic acid Complexes (46) - (49)[a].

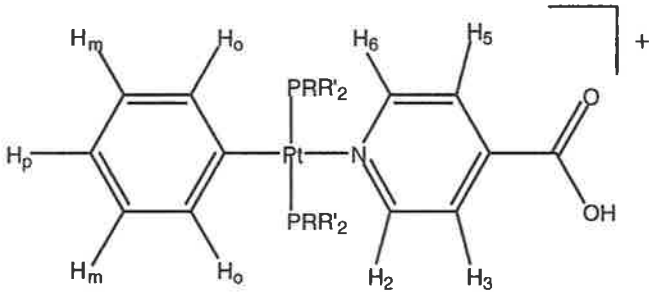

(46) R = R' = Ph
(47) R = Me, R' = Ph
(48) R = R' = Et
(49) R = R' = Cy

Complex	δ(^{1}H)							δ (^{31}P)[b]
	H_{ortho}	H_{meta}	H_{para}	$H^{2/6}$	$H^{3/5}$	PRR'_2	$PMePh_2$	
46	6.75, 2H, d, ($^{3}J_{HH}$ = 6.9 Hz, $^{3}J_{PtH}$ = 24 Hz)	6.31, 2H, m	6.51, 1H, m	8.35, 2H, d, ($^{3}J_{HH}$ = 8.1 Hz)	7.20, 2H, m	7.43-7.27, 30H, m	na	22.1 (3054)
47	7.24, 2H, d, ($^{3}J_{HH}$ = 7.2 Hz)	6.79, 3H, m	6.79, 3H, m	8.17, 2H, d, ($^{3}J_{HH}$ = 6.6 Hz)	c	7.45-7.23, 20H, m	1.64, 3H, m	9.4 (2914)
48	7.32, 2H, d, ($^{3}J_{HH}$ = 8.1 Hz, $^{3}J_{PtH}$ = 29 Hz)	6.87, 2H, m	7.05, 1H, m	8.89, 2H, d, ($^{3}J_{HH}$ = 6.3 Hz)	8.27, 2H, d, ($^{3}J_{HH}$ = 6.6 Hz)	1.73-1.02, 30H, m	na	13.4 (2697)
49	7.50, 2H, d, ($^{3}J_{HH}$ = 6.6 Hz, $^{3}J_{HH}$ = 32 Hz)	6.84, 3H, m	6.84, 3H, m	8.83, 2H, d, ($^{3}J_{HH}$ = 6.3 Hz)	8.42, 2H, d, ($^{3}J_{HH}$ = 6.6 Hz)	1.87-0.83, 60H, m	na	17.5 (2792)

[a]Chemical shifts in ppm measured in $CDCl_3$; quoted multiplicities do not include ^{195}Pt satellites. [b] $^{1}J_{PtP}$ coupling constants (Hz) in parentheses.
[c]Obscured by $PMePh_2$.

Table 5. ^{1}H- and $^{31}P\{^{1}H\}$ NMR Data for the picolinic acid Complexes (50) - (53)[a].

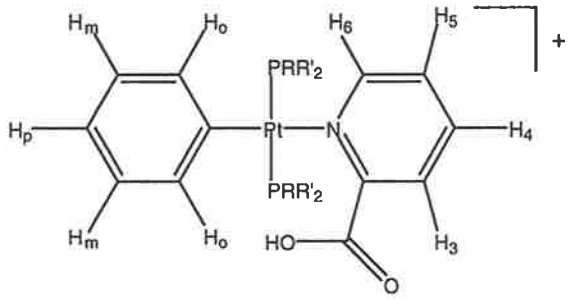

(**50**) R = R' = Ph
(**51**) R = Me, R' = Ph
(**52**) R = R' = Et
(**53**) R = R' = Cy

Complex	δ(^{1}H)							δ (^{31}P)[b]
	H_{ortho}	H_{meta}	H_{para}	H^3	H^6	H^5	H^4	
50	δ 6.63, 2H, d, ($^{3}J_{HH}$ = 7.5 Hz)	δ 6.33, 2H, m	δ 6.33, 1H, m	δ 8.69, 1H, m	δ 8.03, 1H, d, ($^{3}J_{HH}$ = 7.8 Hz)	δ 8.28, 1H, td, ($^{3}J_{HH}$ = 6.0 Hz, $^{4}J_{HH}$ = 1.4 Hz)	δ 7.75, 1H, m	23.0 (3212)
51	δ 6.55, 2H, m	δ 6.87, 2H, m	δ 6.87, 1H, m	δ 7.60, 1H, m	δ 8.68, 1H, d, ($^{3}J_{HH}$ = 4.5 Hz)	δ 7.99, 1H, td, ($^{3}J_{HH}$ = 7.4 Hz, $^{4}J_{HH}$ = 1.8 Hz)	δ 8.25, 1H, dt, ($^{3}J_{HH}$ = 7.5 Hz, $^{4}J_{HH}$ = 1.2 Hz)	6.5 (3089)
52	δ 6.63, 2H, d, ($^{3}J_{HH}$ = 7.5 Hz)	δ 6.97, 2H, m	δ 6.91, 1H, m	δ 6.33, 1H, m	δ 8.79, 1H, d, ($^{3}J_{HH}$ = 4.5 Hz)	δ 8.04, 1H, td, ($^{3}J_{HH}$ = 7.2 Hz, $^{4}J_{HH}$ = 1.5 Hz)	δ 7.64, 1H, m	11.1 (2840)
53		δ 7.01, 2H, m	δ 6.96, 1H, m	δ 6.33, 1H, m	δ 8.25, 1H, d, ($^{3}J_{HH}$ = 7.8 Hz)	δ 7.98, 1H, td, ($^{3}J_{HH}$ = 8.1 Hz, $^{4}J_{HH}$ = 1.8 Hz)	δ 7.61, 1H, m	17.2 (3067)

[a]Chemical shifts in ppm measured in $CDCl_3$; quoted multiplicities do not include ^{195}Pt satellites. [b] $^{1}J_{PtP}$ coupling constants (Hz) in parentheses.

Table 6. ^{1}H- and $^{31}P\{^{1}H\}$ NMR Data for the nicotinamide complexes (54) and (55)[a].

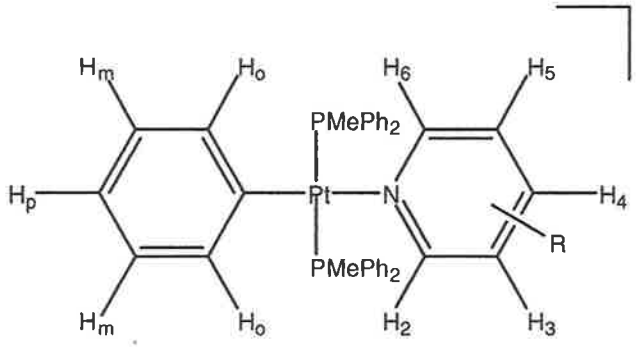

(54) R = 4-$CONH_2$
(55) R = 3-$CONH_2$

Complex	δ (^{1}H)											δ (^{31}P)[b]
	H_{ortho}	H_{meta}	H_{para}	H^2	H^3	H^4	H^5	H^6	NH_2	PRR'_2	PCH_3	
54	7.16, 2H, d, ($^{3}J_{HH}$ = 7.8 Hz)	6.84, 3H, m	6.84, 3H, m	7.94, 2H, d, ($^{3}J_{HH}$ = 6.3 Hz)	Obscured by PMePh2	c	d	e	8.14, 5.66, 1H, s.	7.57-7.34, 20H, m	1.56, 6H, m	9.8 (2888)
55	6.98, 2H, m	6.82, 2H, m	6.67, 1H, m	8.62, 1H, s	c	7.99-7.96, 3H, m	e	As for H4	5.57, 2H, s	7.64 – 7.19, 20H, m	1.69, 6H, m	10.0 (2927)

[a]Chemical shifts in ppm measured in $CDCl_3$; quoted multiplicities do not include ^{195}Pt satellites. [b] $^{1}J_{PtP}$ coupling constants (Hz) in parentheses. [c]Not present in complex. [d]As for H^3. [e]As for H^2.

Crystals of complexes (**47**) and (**48**) that were suitable for X-ray analysis were grown from CH_2Cl_2/n-hexane solvent mixtures, utilising diffusion layering techniques. The molecular structures of (**47**) and (**48**) are shown in Figures 11 and 12, respectively. The asymmetric unit of each of (**47**) and (**48**) comprises a univalent complex cation, a triflate anion and a solvent dichloromethane molecule of crystallisation. In each complex, the platinum atom exists in the expected square planar geometry defined by a C, N, P_2 donor set indicating that the nicotinic acid is N-bound. The platinum atom lies 0.0102(1) Å and 0.0465(1) Å out of the respective coordination planes in (**47**) and (**48**). In (**48**), the platinum-bound phenyl and isonicotinic acid groups are effectively orthogonal to the square plane as seen in the magnitude of the dihedral angles of 88.6° and 89.4°, respectively. By contrast, in (**47**), the respective dihedral angles are 74.5° and 91.5° with the large deviation for the phenyl group been ascribed to the reduced steric hindrance imposed by the phosphine ligands.

Table 7. Selected bond distances (Å) around the Pt(II) centre for complexes (47) and (48)

Atom 1	Atom 2	Complex (47)	Complex (48)
Pt	N(1)	2.132(3)	2.120(3)
Pt	P(1)	2.303(1)	2.309(1)
Pt	P(2)	2.308(1)	2.310(1)
Pt	C(8)	2.002(4)	2.029(4)

Table 8. Selected bond angles (°) around the Pt(II) centre for complexes (47) and (48)

Atom 1	Atom 2	Atom 3	Complex (47)	Complex (48)
P(1)	Pt	P(2)	173.52(4)	174.33(4)
P(1)	Pt	N(1)	92.08(9)	92.3(1)
P(1)	Pt	C(8)	88.4(1)	87.5(1)
P(2)	Pt	N(1)	93.78(9)	93.4(1)
P(2)	Pt	C(8)	85.7(1)	86.9(1)
N(1)	Pt	C(8)	178.9(2)	178.8(2)

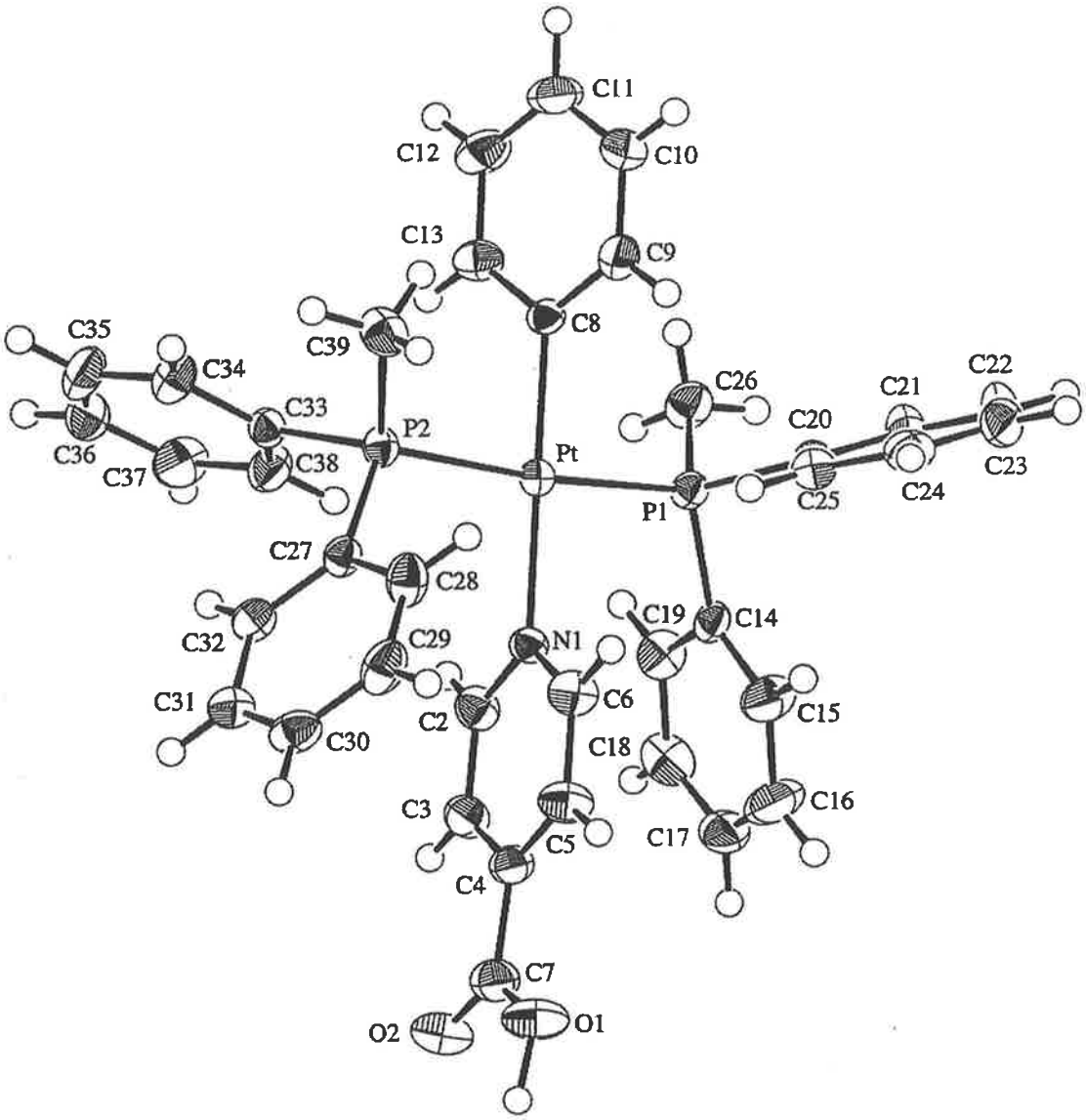

Figure 11. Molecular structure of (47).

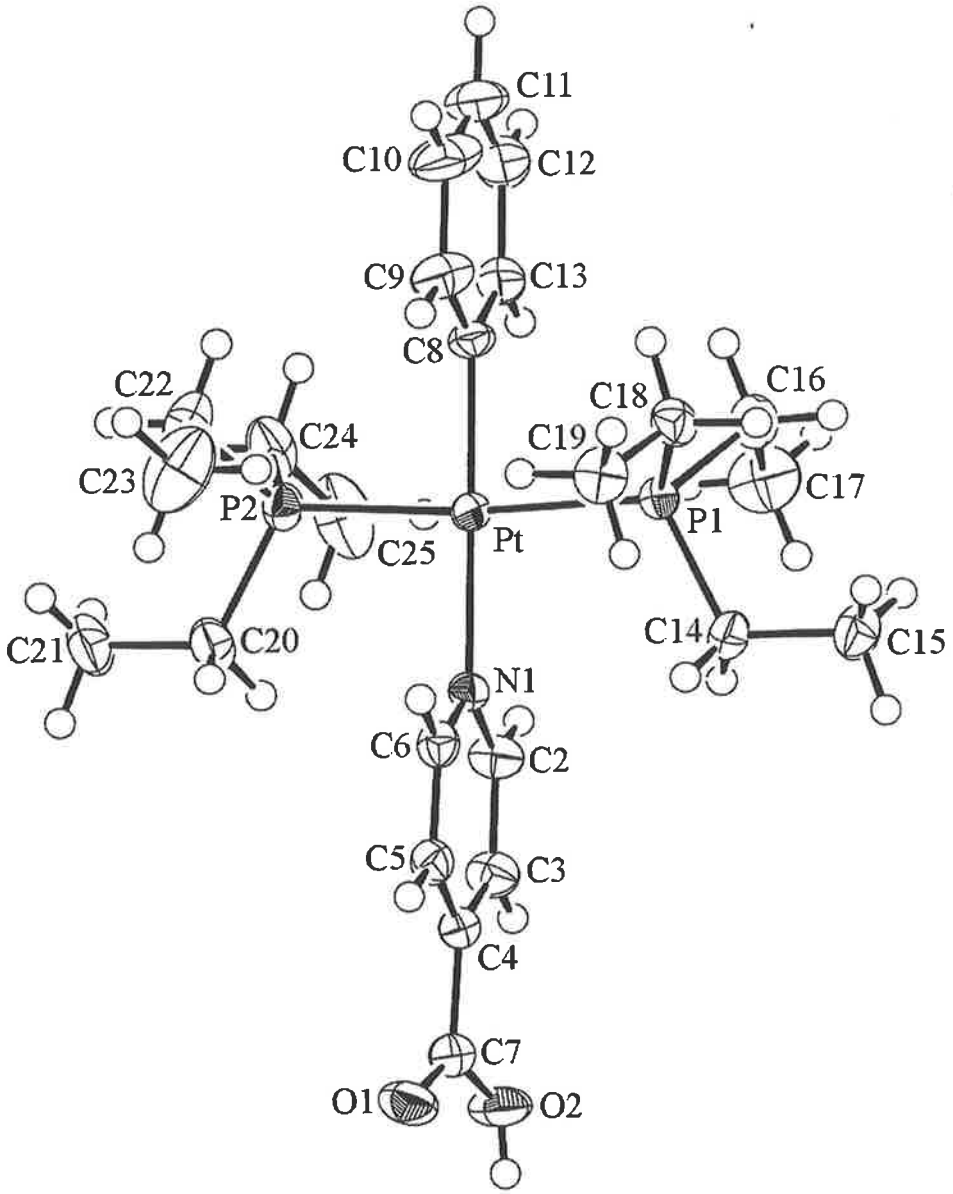

Figure 12. Molecular structure of (48)

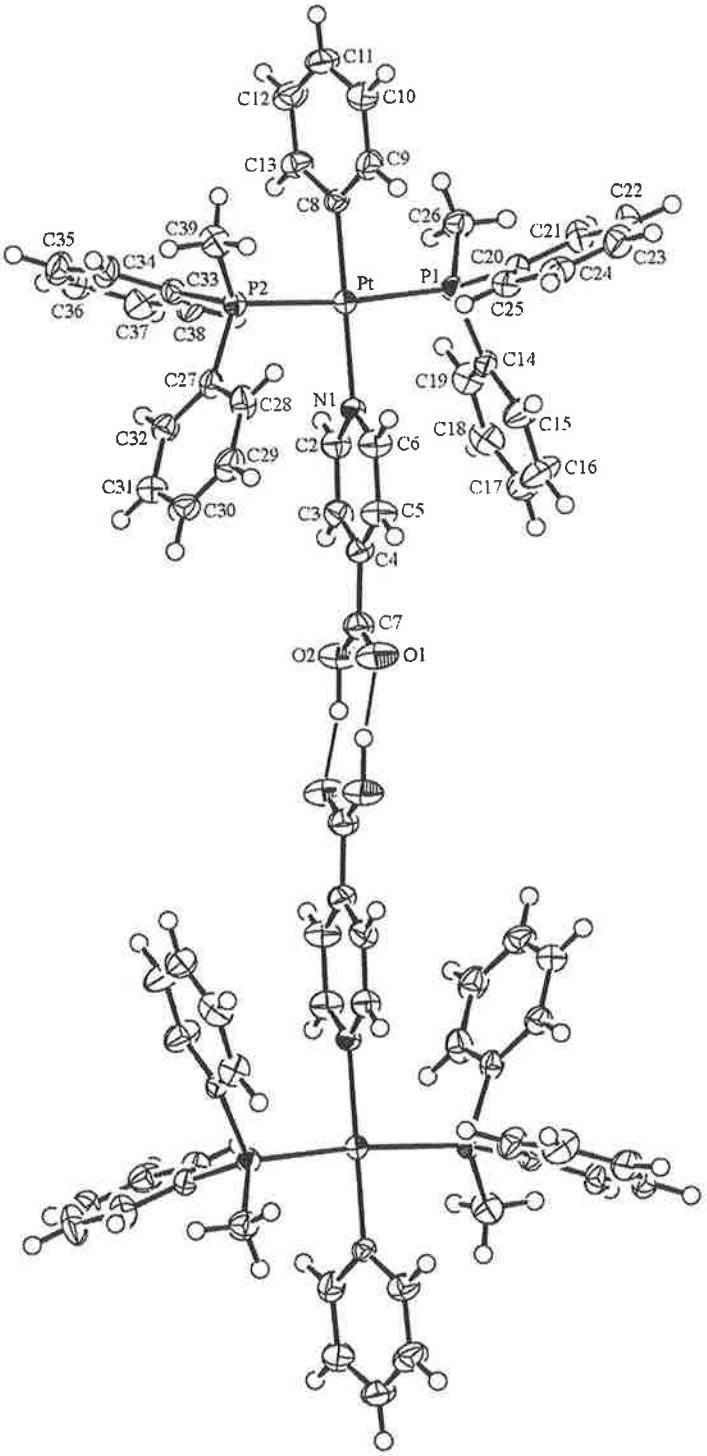

Figure 13. Molecular structure of hydrogen-bonded dimer of (47).

With complexes (**42**) – (**55**) it was the N-donor ligand that conferred the hydrogen-bonding functionality on the complex. It was also possible to prepare a platinum(II) complex in which the hydrogen-bonding functionality was not part of a N-donor ligand but rather a C-donor ligand. In an effort to control the manner in which intermolecular hydrogen-bonding occurred, we chose a methyl substituted amide group for this type of complex. Unfortunately, the method for the synthesis of complexes (**37**) – (**40**) could not be used here. The synthesis of the desired amide complex involved the use of a suitable aryl iodide that already possessed hydrogen-bonding functionality. In this case, 3-*N*-methylbenzamide was used. The carbon-iodine bond provided us with a means of facile oxidative addition to Pt(0) precursors, while the secondary amide group provided the means of introducing hydrogen-bonding functionality into the complex. Previous studies by the Rendina group have shown that oxidative addition of 3-iodobenzoic acid to Pt(0) leads to an intractable mixture of products[30]. This is due to the fact that several transition metal complexes of low oxidation state are known to react with the O-H bond of water[37,62-66], alcohols[37,65,67] and carboxylic acids[37-39]. Rendina and co-workers reported the utilisation of a silyl ester as a suitable protecting group for the carboxylic acid during the oxidative addition reaction to $Pt(PPh_3)_4$[30]. The silyl ester was found to be both sufficiently robust to withstand the reaction conditions while it could also be cleaved under mild conditions in order to preserve the platinum(II) coordination sphere[30]. Silyl group protection was not required in our work, possibly due to the significantly lower acidity of the amide compared to the carboxylic acid group.

The acid (**56**) was converted to the amide using methods obtained from literature procedures[68-76]. This involved the conversion of (**56**) to the acid chloride (**57**) by the use of $SOCl_2$. The resulting acid chloride (**57**) was then reacted with an excess of methylamine to form the N-methylamide (**58**). Its oxidative addition to $Pt(PPh_3)_4$ proceeded cleanly to form the platinum(II) complex (**59**) in good yield.

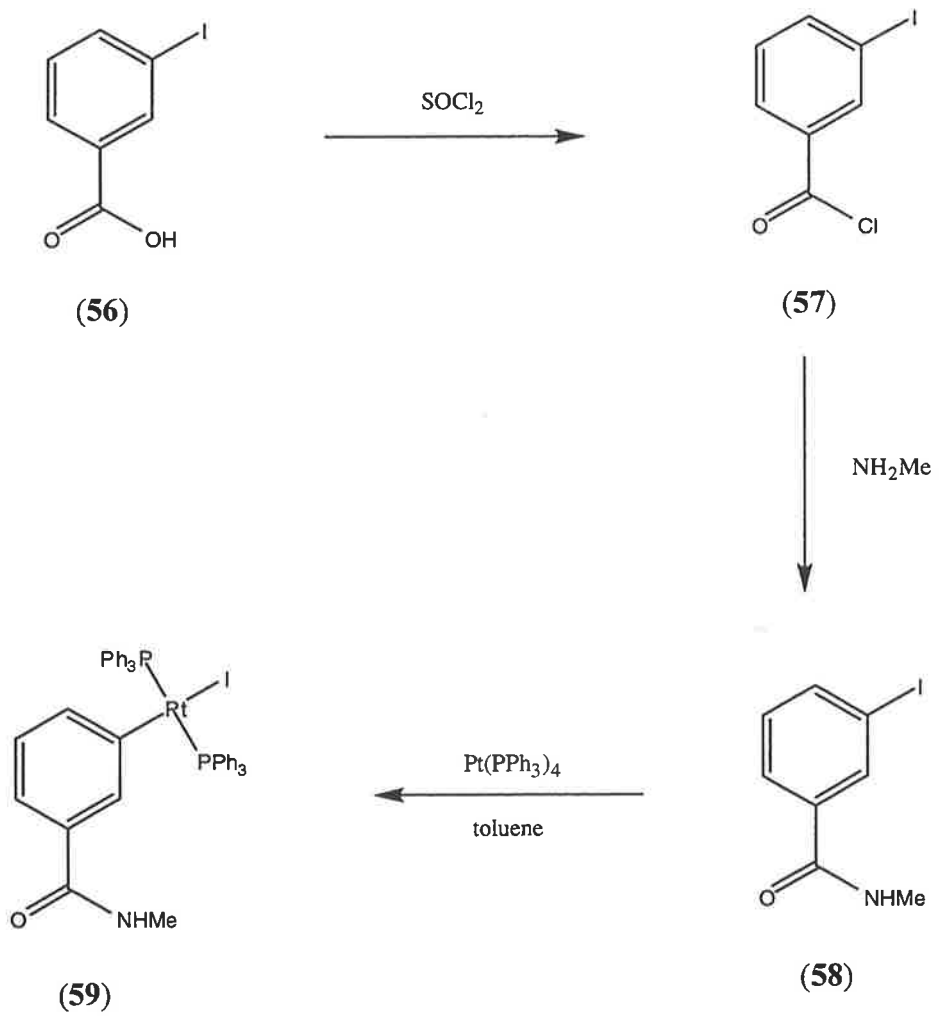

(56) (57) (58) (59)

Scheme 2.6

The ^{1}H NMR spectrum of complex (**59**) showed signals at δ 6.67, 6.72, 6.24, and 6.96 that are assigned to H^2, H^4, H^5 and H^6, respectively. The methyl protons of the NHMe group appear as a doublet at δ 2.76 ($^{3}J_{HH}$ = 4.8 Hz), and the NH proton appears as a broad multiplet at δ 4.98. The $^{31}P\{^{1}H\}$ NMR signal is a sharp singlet at δ 22.0, flanked by ^{195}Pt satellite signals ($^{1}J_{PtP}$ = 3029 Hz).

Complex (**59**) is a very useful compound. On its own, it is a mononuclear platinum(II) complex that has the potential to form intermolecular hydrogen-bonding interactions via the amide group. The other useful aspect of the complex is that it contains an iodo ligand. This ligand was readily removed with AgOTf to form the corresponding triflato complex, which was then reacted with number of N-donor ligands to form novel mono- and di-nuclear cationic platinum(II) complexes with two hydrogen-bonding functionalities. The results of this work are reported in Chapter 3.

Table 9 shows selected infrared stretching frequencies for complexes (**42**) – (**55**) and (**59**). The carboxylic acid ν(C=O) bands all occur around 1712 – 1736 cm^{-1}, and this is the expected region to find such signals[77]. The O-H stretching frequencies for (**42**) - (**53**) are all in the vicinity of 3000 cm^{-1}, which is also characteristic of $-CO_2H$ functionalities. The primary amides have ν(N-H) bands appearing in the region 1671 – 1697 cm^{-1}, which is characteristic of primary amides[77].

Table 9. Selected IR stretching frequencies (cm^{-1}) for complexes (42) – (55) and (59)

Complex	ν(C=O)	ν(O-H)	ν(N-H)
(**42**)	1720	2800-3200	a
(**43**)	1720	2800-3200	a
(**44**)	1725	2800-3200	a
(**45**)	1732	2800-3100	a
(**46**)	1726	2800-3100	a
(**47**)	1712	2500-3000	a
(**48**)	1731	2700-3100	a
(**49**)	1736	2700-3100	a
(**50**)	1720	2800-3100	a
(**51**)	1725	2700-3200	a
(**52**)	1725	2750-3000	a
(**53**)	1726	2750-3000	a
(**54**)	1671	a	1629
(**55**)	1697	a	1630
(**59**)	1680	a	1628

[a]Not present in this complex

2.3 pKa determination for complexes (**43**), (**44**), (**47**), (**48**), and (**51**).

In many cases, it is beneficial to know the acid dissociation constant for a Brønsted acid. This data can be used to rationalise behaviour of a particular compound in a certain environment. In particular, the acid dissociation constant can tell one whether the compound is in its ionised or un-ionised form at a pH of interest[78].

The qualitative factors which affect pKa values are mainly inductive, electrostatic and mesomeric effects, as well as contributions from hydrogen-bonding, conformational differences and steric factors[79]. NMR spectroscopy can be employed to determine the acid dissociation constant of a compound of interest, however, there are limitations on its usefulness. The compound has to possess a spin-active observable nucleus for NMR spectroscopy and its concentration has to be sufficient enough to observe a spectrum[80]. Potentiometric pH titration is by far the most convenient method for the determination of dissociation constants[78], and this is the method used in this work in order to determine the pKa values of selected complexes. All pKa values were measured in 1:1 ethanol-water mixtures[81,82] as the complexes were not, as expected, completely soluble in water alone. The aqueous ethanol solution of the complex was titrated against KOH solution in 1:1 ethanol-water mixture. The pH was recorded at various concentrations and the pKa calculated by a procedure reported by Albert and Serjeant[83].

The pKa values of complexes (**43**), (**46**), (**47**), (**48**), and (**51**) were determined, and the results are shown in Table 10.

Table 10. pKa values of complexes (43), (46), (47), (48), and (51)[a].

Complex	pKa
(43)	4.85 ± 0.10
(46)	3.26 ± 0.07
(47)	3.51 ± 0.08
(48)	3.21 ± 0.08
(51)	5.23 ± 0.09

[a]Measured in 1:1 H_2O/EtOH at 22 °C.

Table 10 summarises the pK_a values that were experimentally determined for the complexes (**43**), (**46**) – (**48**), and (**51**). In order to determine the significance of our pKa values, one needs to compare them to literature values. It was difficult to compare these values directly with those of pyridine carboxylic acids as the free acids have the internal base, the nitrogen atom, that can react with the proton. Complexes (**43**), (**46**) – (**48**), and (**51**) do not have the nitrogen atom free to react with the acidic proton as it is coordinated to the platinum atom.

In the literature, two pK values are reported, i.e. pK_1 and pK_2, which refer to the loss of two protons from the pyridine carboxylic acid, ie the carboxylic acid proton and the N-H proton respectively[82]. Literature values for the overall pK_a of the pyridine carboxylic acids in various ethanol/H_2O mixtures were calculated by Niazi[82] assuming that the equilibrium constant for the proton loss from the nitrogen atom of the pyridine carboxylic acid was the same as for the proton loss from the corresponding methyl ester. The pK_1 and pK_2 values for nicotinic acid and picolinic acid in 50% aqueous ethanol solution were calculated to be 1.77 ± 0.02, 4.60 ± 0.02, 1.54 ± 0.04 and 5.24 ± 0.02, respectively[82]. These values, as mentioned previously are not particularly relevant to the discussion of the pK_a of our complexes as the free nitrogen atom of the pyridine carboxylic acid is not present in our complexes.

It is more useful to compare the pK_a values of our complexes to the pK_a of aromatic acids such as benzoic acid in 50% aqueous ethanol solution. The pKa for benzoic acid in 50% ethanol solution is 5.67 ± 0.02[82]. It is clear that the platinum(II) complexes are significantly more acidic than benzoic acid in 50% aqueous ethanol solution. This enhanced acidity is attributed to the cationic charge of the complexes, i.e. the loss of the H^+ cation is favoured for the platinum(II) complexes. Although the pyridine carboxylic acid ligand does not exist as a zwitterion in our platinum(II) complexes, the resulting complexes upon loss of H^+ are zwitterions (Scheme 3.1). Attempts at isolating these species were unsuccessful.

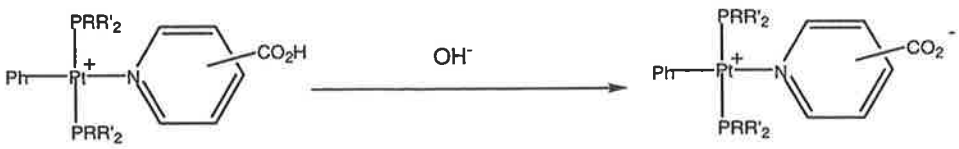

Scheme 3.1

The acidity of the complexes does not appear to be a function of the of the steric bulk of the phosphine ligands or their basicity. The acidities of the isonicotinic acid complexes (**46**) –

(**48**) are all comparable. Indeed, the pK_a of complexes (**46**) and (**48**) are the same within experimental error.

3. Preparation and Characterisation of Dinuclear Organoplatinum(II) Complexes with Hydrogen-Bonding Functionality

Following the successful synthesis of a number of monoplatinum(II) complexes with hydrogen-bonding functionality, the second aim of the work was to synthesise a series of symmetrical diplatinum(II) complexes possessing two hydrogen-bonding functionalities.

As with the mononuclear platinum(II) complexes (**42**) - (**55**), two components were required to assemble the final dinuclear platinum(II) complex. The first component that was required was a suitable bridging bidentate ligand. There are, of course several types of suitable bridging bidentate N-donor ligands that can coordinate to two platinum(II) centres. Four suitable bridging bidentate N-donor ligands were utilised in this work, thus providing us with the means to prepare dinuclear complexes. These N-donor ligands included; 4,4'-bipyridine (**60**), 4,7-phenanthroline (**61**), 4,4'-dipyrazolylmethane (**62**)[84], and 1,1'-diphenyl-4,4'-dipyrazolylmethane (**63**)[84].

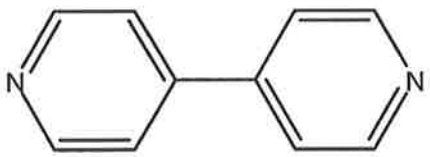

(**60**)

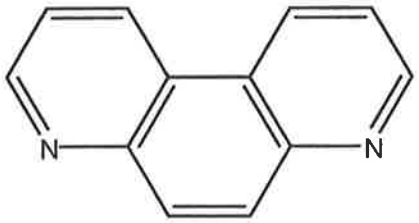

(**61**)

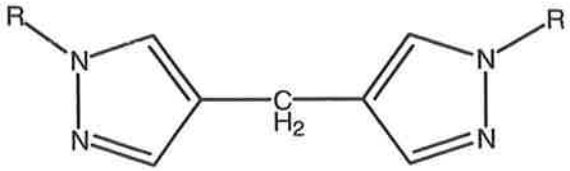

(**62**) R = H
(**63**) R = Ph

In the synthesis of the dinuclear platinum(II) complexes, we decided to utilise the synthetic method developed by Rendina and Gallasch[30], in which the hydrogen-bonding group was present on the σ-aryl ligand rather than on the N-donor ligand. Complex (**59**) was an ideal precursor platinum(II) complex for these syntheses. It incorporated the hydrogen-bonding functionality directly into the σ-aryl ligand. The hydrogen-bonding functionality in this case is the N-methylamide, which does not require any protection during the synthesis of the target complex, unlike the corresponding carboxylic acid ligand[30].

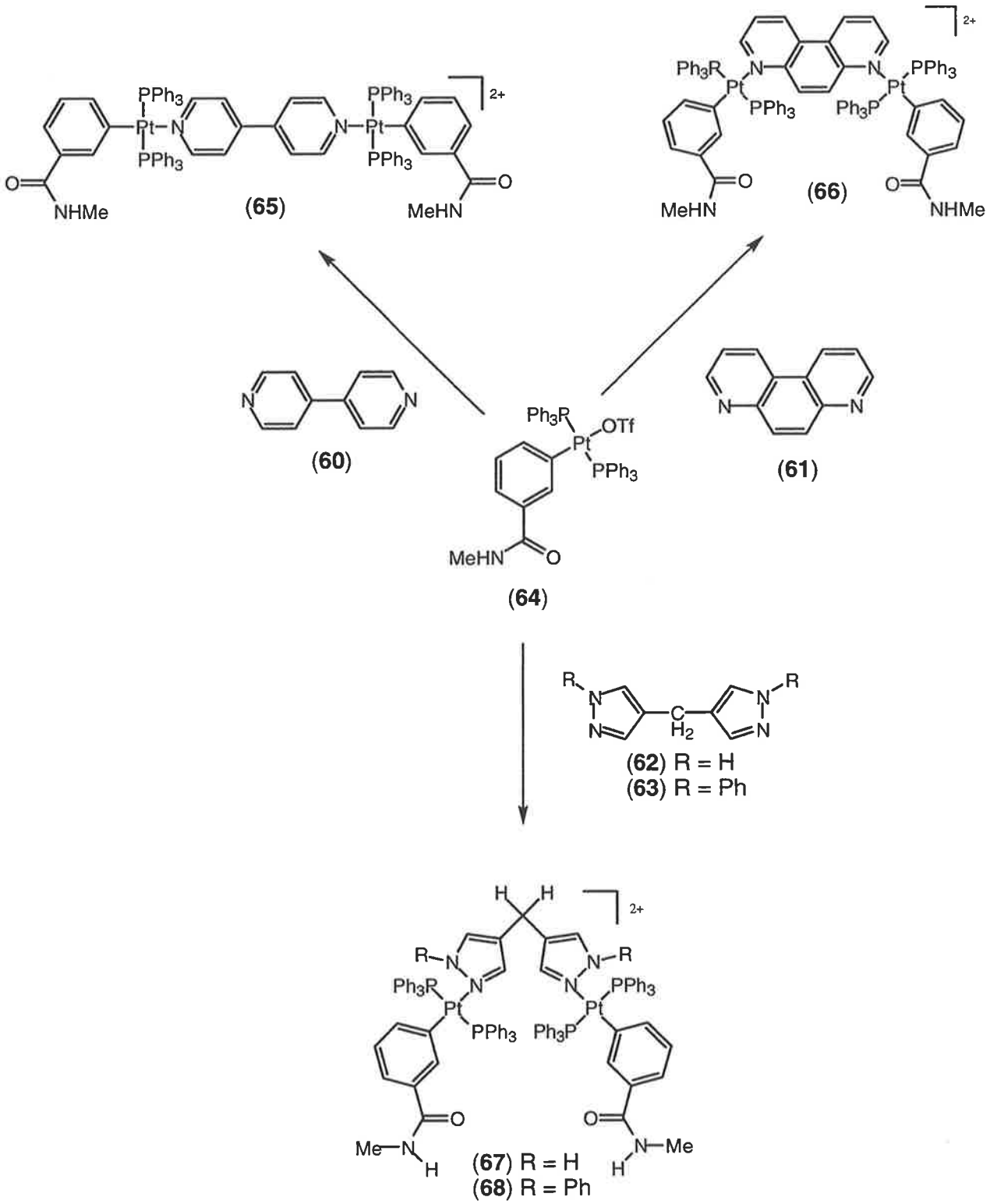

Scheme 3.2

Complex (**59**) was converted to complex (**64**) by using AgOTf to remove the inert iodo ligand and replace it with the more labile triflato ligand. Two equivalents of (**64**) were then added to one equivalent of 4,4'-bipyridine to form the dicationic diplatinum(II) complex (**65**). Complex

(**59**) was converted to complex (**64**) by treatment with AgOTf. Two equivalents of (**59**) were then added to one equivalent of 4,7-phenanthroline (**61**) to form the diplatinum(II) complex (**66**) in good yield. Complexes of the DPZM ligands (**62**) and (**63**) were prepared from the precursor platinum(II) complex (**59**). Hydrogen-bonding functionality was conferred on the complex by the precursor platinum(II) complex (**59**). The inert iodo ligand of (**59**) was replaced by the much more labile triflate ligand. The triflate ligand was then readily displaced by the N-donors (**62**) and (**63**).

The $^{31}P\{^{1}H\}$ NMR spectrum of complex (**65**) appeared as a sharp singlet at δ 20.9 flanked by platinum satellites ($^{1}J_{PtP}$ = 3008 Hz) consistent with the four chemically equivalent phosphines in the structure each pair possessing a mutually *trans* geometry. Complex (**65**) showed a doublet signal in the ^{1}H NMR spectrum at δ 7.03 ($^{3}J_{HH}$ = 7.5 Hz) attributed to the H^{6} proton of the methylbenzamide group. The signal due to the H^{4} proton appeared as a doublet at δ 6.81 ($^{3}J_{HH}$ = 7.5 Hz). The H^{5} proton gave rise to the triplet at δ 6.39 ($^{3}J_{HH}$ = 7.8 Hz). The *ortho* proton of the 4,4'-bipyridine group was masked by the PPh_3 signals at δ 7.34 – 7.19, while the *meta* hydrogen appeared as a singlet at δ 6.83.

The ^{1}H and $^{31}P\{^{1}H\}$ NMR spectra of (**65**) were measured in both $CDCl_3$ and CD_2Cl_2 solution. The reason for this was that the complex appeared to dissociate to afford free 4,7-phenanthroline at room temperature over a period of a few hours in $CDCl_3$, while it remained quite stable in CD_2Cl_2 solution. This effect has been observed in the MS of related complexes, and it is probably the result of the strong *trans* effect associated with the σ-aryl ligand although we are unsure of the reactivity. The $^{31}P\{^{1}H\}$ NMR spectrum of (**66**) appeared as a sharp singlet at δ 19.5 flanked by ^{195}Pt satellite signals ($^{1}J_{PtP}$ = 3003 Hz) in $CDCl_3$ solution, and as a sharp singlet at δ 19.5 flanked by ^{195}Pt satellite signals ($^{1}J_{PtP}$ = 2990 Hz) in CD_2Cl_2 solution. Overnight, complex (**66**) had decomposed in $CDCl_3$ to form a variety of unidentified products, as determined by $^{31}P\{^{1}H\}$ NMR spectroscopy. In contrast, the same complex dissolved in CD_2Cl_2 solution did not display this phenomenon. The ^{1}H NMR spectrum of complex (**66**) gave rise to a doublet at δ 9.40 ($^{3}J_{HH}$ = 9.3 Hz) attributed to $H^{1,10}$ of the 4,7-phenanthroline ligand. $H^{3,8}$ appeared as a doublet at δ 9.07 ($^{3}J_{HH}$ = 4.2 Hz). H^{15} appeared as a two proton triplet at δ 6.38 ($^{3}J_{HH}$ = 8.1 Hz). The N-H proton appeared as a very broad singlet at δ 5.96, while the signal due to the N-methyl

protons appeared as a doublet at δ 2.84 ($^3J_{HH}$ = 4.8 Hz). The signal due to $H^{5,6}$ appeared as a sharp singlet at δ 9.05. H^{14} appeared as doublet at δ 6.88 ($^3J_{HH}$ = 7.8 Hz.).

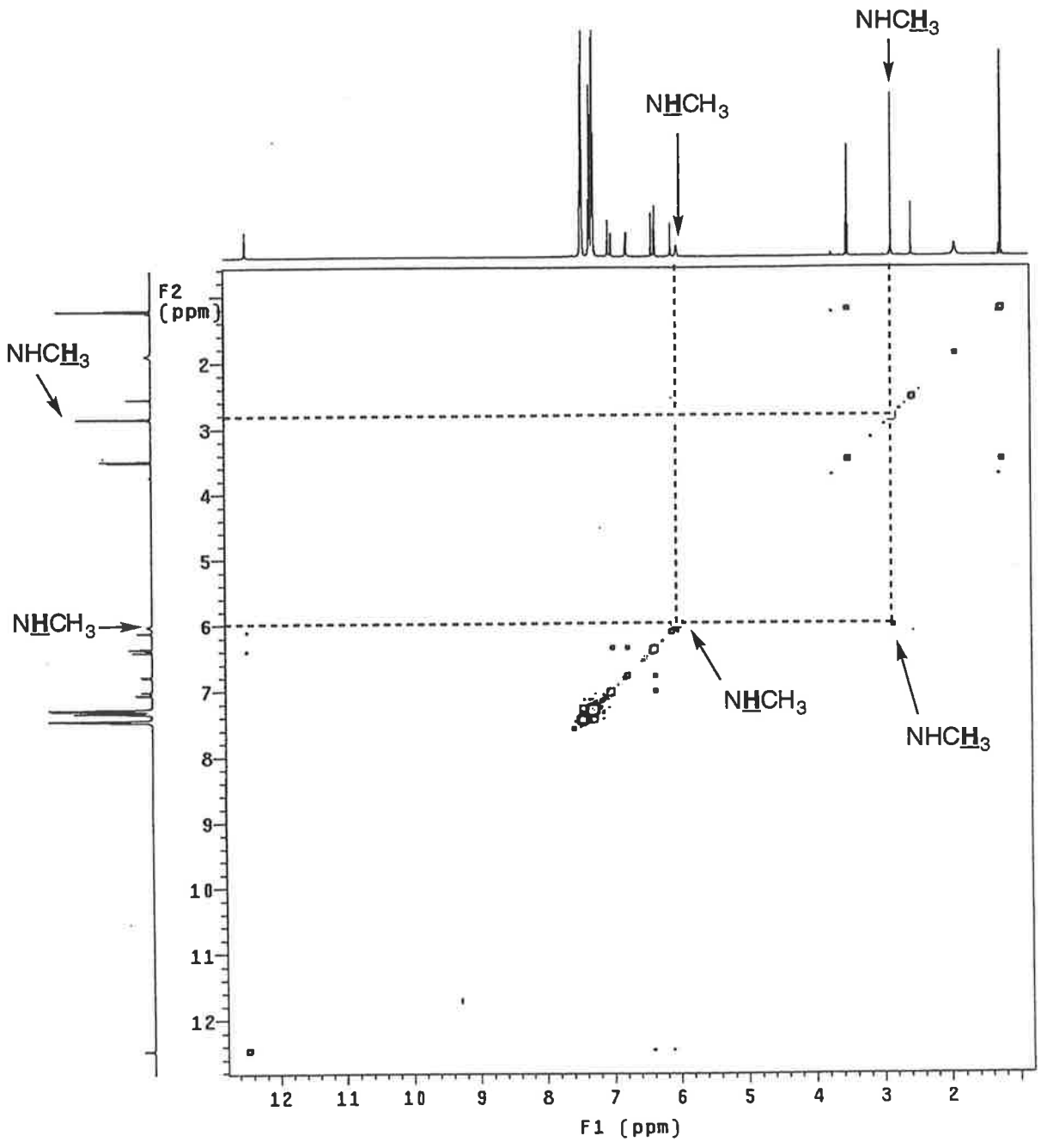

Figure 14. COSY NMR spectrum of (67) in $CDCl_3$ solution at 600 MHz.

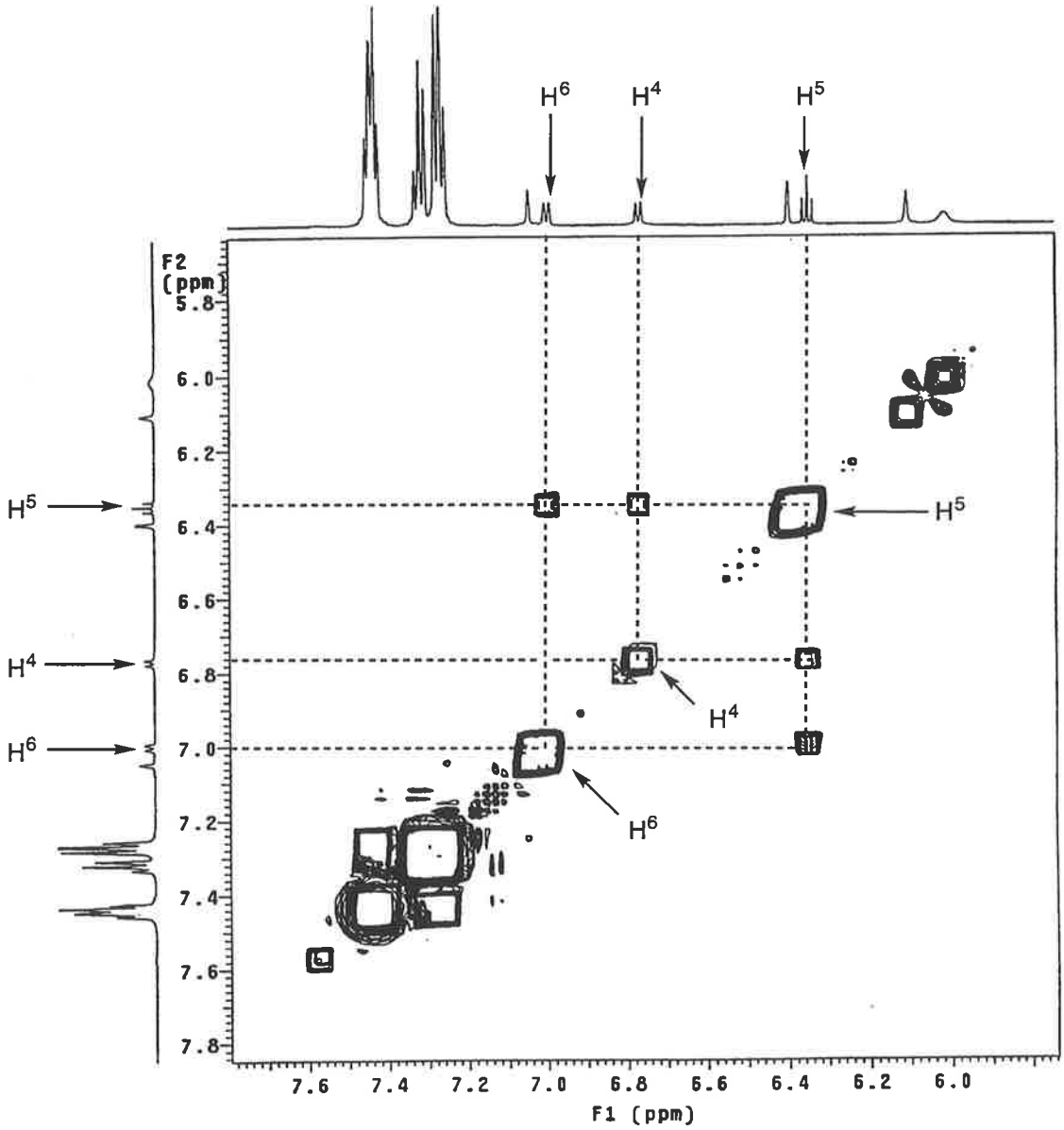

Figure 15. Expanded COSY NMR spectrum of (67) in $CDCl_3$ solution at 600 MHz.

Table 12 summarises some of the key spectroscopic features of the dinuclear complexes (**67**) and (**68**). The assignment of aromatic proton resonances was facilitated by 2D COSY (correlation spectroscopy) NMR experiments for (**67**), whereby distinct cross-peaks were observed for coupled protons of the ring systems (Figures 14 and 15). The spectrum of (**67**) showed that protons H^4 and H^6 appeared as doublets at δ 6.77 and δ 7.00, respectively. H^5 appeared as a two proton triplet ($^3J_{HH}$ = 7.2 Hz) at δ 6.35. The signal due to H^2 appeared as a sharp singlet at δ 6.10. The N-Me protons appeared as a doublet at δ 2.83 ($^3J_{HH}$ = 4.8 Hz). The NH proton appeared as a broad singlet at δ 6.01. The signal due to the $-CH_2-$ protons appeared as a sharp singlet at δ 2.53. The signal due to the N-H of the pyrazolyl group appeared as a singlet, shifted dramatically downfield at δ 12.45. The signals due to the PPh_3 protons appeared as multiplets between δ 7.45 and δ 7.25. The $^{31}P\{^1H\}$ NMR spectrum of (**67**) appeared as a sharp singlet at δ 20.8 flanked by ^{195}Pt satellites ($^1J_{PtP}$ = 3022 Hz).

The $^{31}P\{^1H\}$ NMR spectrum of complex (**68**) appeared as a sharp singlet at δ 18.2 flanked by ^{195}Pt satellites ($^1J_{PtP}$ = 3035 Hz). The ^1H NMR spectrum of complex (**68**) showed the PPh_3 protons as a 60H multiplet at δ 7.64 – 7.28. The CH_2 protons appeared as a two proton singlet at δ 3.11. The amide proton appeared as a two proton multiplet at δ 5.70 while the amide methyl group appeared as a six proton doublet at δ 2.84 ($^3J_{HH}$ = 4.5 Hz). Compared to the ^1H NMR spectrum of complex (**67**), complex (**68**) had many broad, unresolved signals, with the signals attributed to H^2, H^4, H^5, and H^6 all appearing as broad singlets at δ 6.69, 6.58, 6.25, and 6.94 respectively. This effect is most likely related to the dynamic phenomenon of analogous Pt(II)-species[30], whereby free rotation of the 1,1'-diphenyl-4,4'-dipyrazolylmethane ligand about the Pt-N bond is restricted. Considerable steric interactions between the N-Ph group and the bulky PPh_3 ligands would largely account for this phenomenon. There is most likely a nondegenerate intermolecular rearrangement between the *syn-syn, syn-anti(anti-syn)* and the *anti-anti* isomers of complex (**68**). This proposal is also supported by the fact that the related 4,4'-dipyrazolylmethane complex (**67**) does not exhibit this related dynamic NMR behaviour, suggesting that in this case there exists free rotation around the Pt-N bond for complex (**67**). VT ^1H-NMR experiments are required to confirm this hypothesis.

Table 11 shows selected IR stretching frequencies for complexes (**65**) - (**68**). The carboxyl group of the amide shows characteristic ν(C=O) bands between 1641 – 1655 cm^{-1}, and

ν(N-H) bands at 3400 cm^{-1}. The difference between the frequency of the ν(C=O) bands for the amides and the acids can be explained as follows. The more electronegative the group X in the system R-CO-X-, the higher is the frequency. This is the combined result of the σ framework, where the inductive effect operates, and the π system, where the lone pairs on X have an effect. Therefore, the inductive effect alone raises the frequency of the absorption, thus the O of the carboxylic acid, being more electronegative than the N of the amide results in the acid having a higher frequency. Also present in the IR spectra are the bands due to ν(aryl-H) between 1532 – 1556 cm^{-1}.

Table 11. Selected stretching frequencies (cm^{-1}) for complexes (65) – (68)

Complex	ν(C=O)	ν(N-H)	ν(aryl-H)
(65)	1655	3400	1532
(66)	1641	3400	1556
(67)	1643	3400	1556

Table 12 ^{1}H- and ^{31}P{^{1}H} NMR Data for complexes (67) and (68)[a].

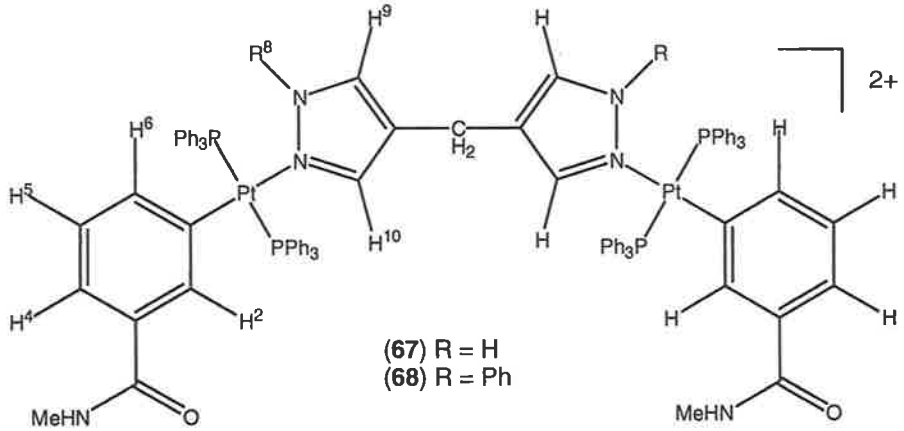

Complex	δ(^{1}H)											δ(^{31}P)[b]
	H^2	H^4	H^5	H^6	H^8	H^9	H^{10}	$-CH_2-$	NH	NMe	PPh_3	
67	6.40 2H, s	6.77, 2H, d, ($^3J_{HH}$ = 7.2 Hz)	6.35, 2H, t, ($^3J_{HH}$ = 7.2 Hz)	7.00, 2H, d, ($^3J_{HH}$ = 7.8 Hz)	12.45, 2H, s	6.10, 2H, s	7.04, 2H, s	2.53, 2H, s	6.01, 2H, m	2.83, 6H, d, ($^3J_{HH}$ = 4.8 Hz)	7.45-7.25, 60H, m	20.8 (3022)
68	6.69 2H, br.s	6.58, 2H, br.s	6.25, 2H br.s	6.94, 2H, br.s	n/a	c	c	3.11, 2H, s	5.70, 2H, m	2.84, 6H, d, ($^3J_{HH}$ = 4.5 Hz)	7.64-7.28, 60H, m	18.2 (3035)

[a]Chemical shifts in ppm measured in $CDCl_3$; quoted multiplicities do not include ^{195}Pt satellites. [b]J_{PtP} coupling constants (Hz) in parentheses.
[c]Signals obscured.

4. Molecular Recognition of Adenine by Platinum(II) Complexes with Hydrogen-Bonding Functionality

With the successful synthesis of a number of dinuclear platinum(II) complexes with hydrogen-bonding functionality, we now had a range of diplatinum(II) complexes with the ability to form intermolecular hydrogen bonds. Complexes (**65**) - (**68**) all possessed two hydrogen-bonding functionalities that conferred on them the ability to form either intramolecular hydrogen bonds via self-association, or to form hydrogen bonds with a suitable guest molecule, i.e. a host-guest interaction. The dominant factors that determined whether the complexes would actually recognise a particular guest by means of "molecular chelation" included the angle that the hydrogen-bonding units converged at and the distance between the two platinum centres. Molecular modelling studies suggested that the most suitable complexes for molecular recognition of adenine were (**67**) and (**68**).

In order to determine whether our hypothesis of adenine binding was feasible in terms of the size and shape of the platinum(II) complex, molecular modelling of the 4,4'-dipyrazolylmethane complex (**67**) with adenine was performed. Molecular mechanics modelling (SYBYL force field) was performed by means of the MacSpartan computer program. The results of this molecular modelling can be seen in Figure 16. The molecular modelling revealed that upon minimisation the dinuclear platinum(II) complex (**67**) did indeed have an energetically-favourable conformation for the binding of adenine. Complex (**67**) can potentially act as a molecular tweezer with adenine as a guest molecule incorporated into the space between the two converging arms of the complex. It can be seen that simultaneous Watson-Crick site and Hoogsteen site binding by the two amide groups, resulting in the formation of four strong hydrogen-bonds between the substrate and the receptor, is a feasible adduct in the gas phase.

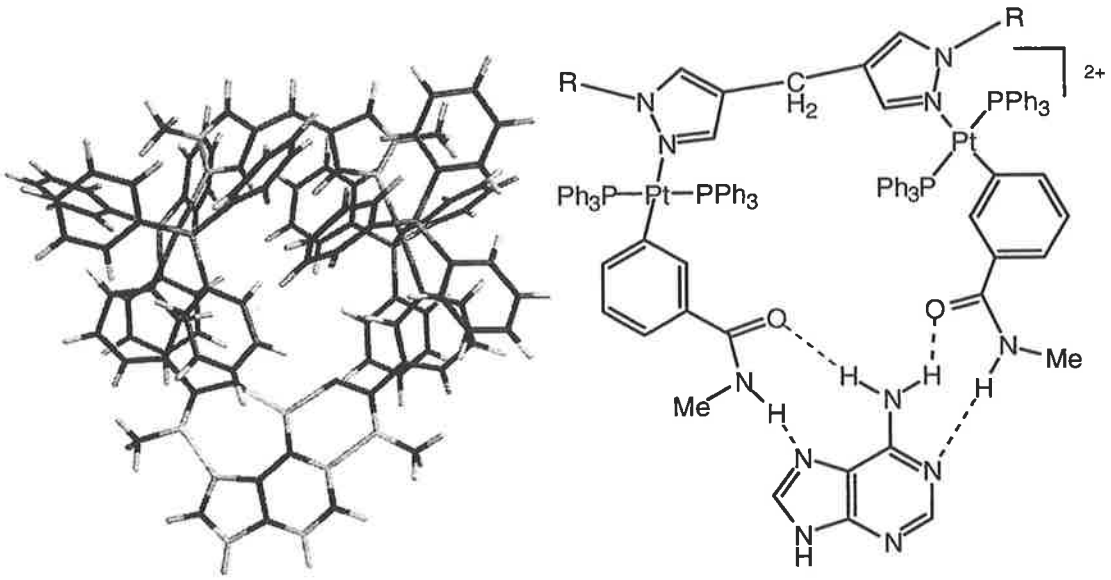

Figure 16.

The formation of a non-covalent complex between two or more chemical units is one of the most fundamental and important processes in supramolecular chemistry[41]. There has been much work done in the area of supramolecular association, whether it be self-association or host-guest association. There are various means by which these processes can be observed, including conductivity measurements[85], ultraviolet spectroscopy[86], vapour pressure osmometry[87] and, of course, NMR spectroscopy[41,88-90].

^{1}H NMR spectroscopy is one of the most useful tools a chemist possesses for the analysis of supramolecular processes such as complexation. ^{1}H NMR spectroscopy can provide microscopic information on the aggregate structure. In order for ^{1}H NMR spectroscopy to be utilised as a method of studying a particular system, there must be some form of complexation-induced shift (CIS) associated with the system. In other words, there must be a signal that shifts significantly between the free and complexed species. Such shifts are often observed when hydrogen-bonding is involved in the complexation process[41,90].

The stability constant of a complexation process is a measure of the selectivity or the specificity of the host molecule for a particular guest. In order to determine the stability constant for the equilibrium process a plausible binding model is required. To construct a binding model it is useful to know the stoichiometry of the reaction. There are several methods for the determination of the stoichiometry of a complexation reaction. One simple, yet extremely effective and powerful, method is Job's method of continuous variations[41].

Job's method of continuous variations is a commonly used procedure for determining the composition of host-guest complexes in solution[91,92]. Job's method of continuous variation allows one to determine the stoichiometry of a complexation. For example whether the host is binding the guest in a 1:1 ratio or a 2:1 ratio.

There has been much interest in the area of "molecular recognition". The molecular recognition of nucleobases such as adenine is of topical interest in this area of chemistry. The association between a host molecule and a nucleobase guest can be monitored readily using ^1H NMR spectroscopy. One usually monitors the NMR shift of the H^2 and H^8 protons on the adenine as a function of concentration. These are dramatically shifted by the effect of association on the hydrogen-bonding sites present in adenine. The data obtained from running ^1H NMR concentration/titration experiments can be manipulated and plotted to produce a Job plot in order to determine the stoichiometry of the association. The Job plot shows the dominant species present at equilibrium.

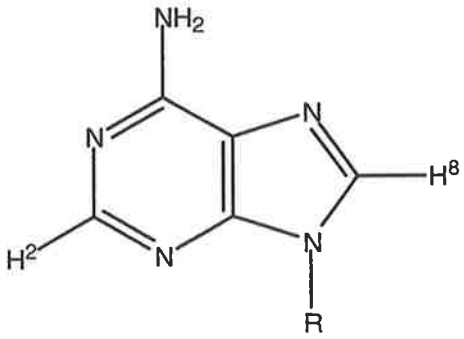

R = butyl, pentyl etc

Figure 17. The structure of adenine (R = H) and its derivatives

If one considers a complex formation equilibrium (R_mS_n) involving two species R and S, where R = receptor and S = substrate:

$$mR + nS \rightleftharpoons R_mS_n \qquad (1.1)$$

In the method of continuous variations, a series of solutions is prepared where the total molar concentration (M) is kept constant, i.e.

$$[R_0] + [S_0] = M \qquad (1.2)$$

while $[R_0]/[S_0]$ varies in small steps. It can be shown that the concentration of the product R_mS_n, $[R_mS_n]$, has a maximum for a R:S molar ratio equal to m/n. So if one plots $[R_mS_n]$ or any property that is a linear function of $[R_mS_n]$ against x, where x is the mole fraction:

$$x = [S_0]/[R_0] + [S_0] \qquad (1.3)$$

it results in a curve possessing a maximum at:

$$x = n/m + n = 1/(m/n + 1) \qquad (1.4)$$

and zero values for x = 0 and x = 1. For example, if one has a 1:1 complex formation, i.e. RS, a maximum would appear at x = 0.5 (m = n = 1) in the Job plot. In the case of a 1:2 complex formation, i.e. RS_2, a maximum appears at 0.67 (m = 1, n = 2). It is usual in an NMR study to plot $(\Delta/\Delta_0)*[R_0]$ versus the mole fraction (x) where $\Delta = \delta_{obs} - \delta_{free}$ and $\Delta_0 = \delta_{complex} - \delta_{free}$.

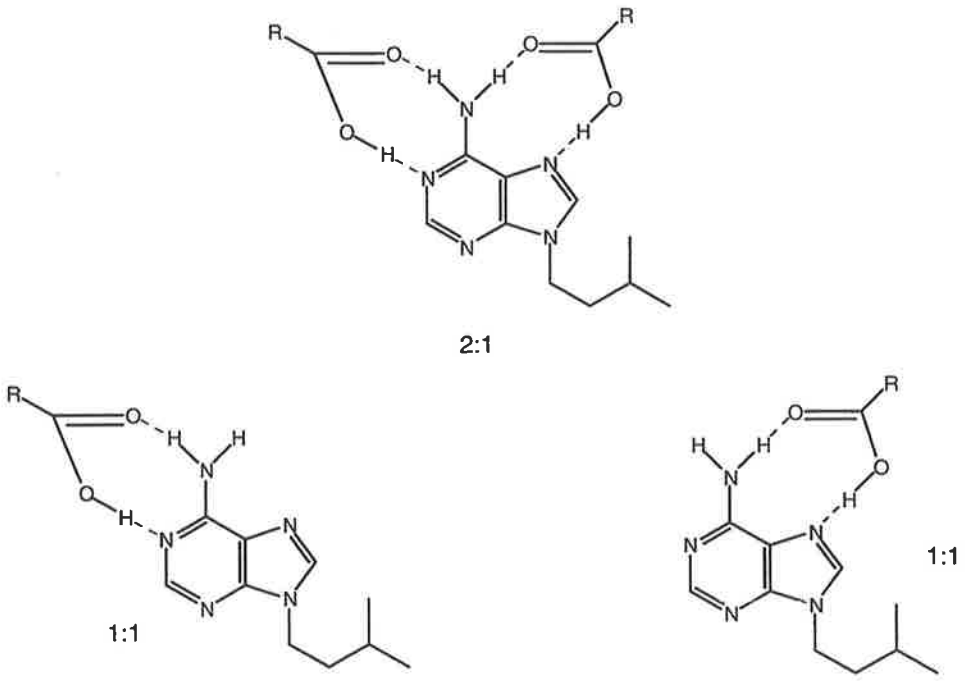

Figure 18. Examples of different modes of carboxylic receptor binding to 9-sec-pentyl adenine (substrate)

Once a binding model has been decided upon, one can determine the equilibrium association constant (K) for the system of interest. In this case, the systems that were found to bind in a 1:1 ratio were used. It is possible to determine K by graphing a Scatchard plot of the data[93]. First, one again considers the equilibrium (m = n = 1):

$$R + S \rightleftharpoons RS \qquad (1.5)$$

The equilibrium expression for this reaction can be expressed as:

$$K = [RS]/[R][S] \qquad (1.6)$$

Where [R], [S], and [RS] are the equilibrium concentrations of free R, S, and RS, respectively. Upon formation of RS, if there is a considerable chemical shift difference from R and there is rapid exchange between R and RS, then a mole fraction weighted shift can be written as follows:

$$\delta_{obs} = N_R\delta_R + N_{RS}\delta_{RS} \qquad (1.7)$$

where δ_{obs} is the chemical shift of a certain nucleus in either R or S in equilibrium solution. δ_R is the shift of free R, and δ_{RS} is the shift of pure complex. The N values are therefore the mole fractions of the complexes that are defined as:

$$N_R = [R]/[R] + [RS] \qquad (1.8)$$

and

$$N_{RS} = [RS]/[R] + [RS] \qquad (1.9)$$

Re-writing the expression for δ_{obs} in eq. (1.7) one obtains:

$$\delta_{obs} = \delta_R + [RS]/[R] + [RS]\ (\delta_{obs} - \delta_{obs}) \qquad (1.10)$$

Now if one allows the total concentration of R and S to be $[R^0]$ and $[S^0]$, then

$$[R^0] = [R] + [RS] \quad (1.11)$$

$$[S^0] = [S] + [RS] \quad (1.12)$$

and from equations 1.10 and 1.11 one obtains:

$$[RS] = [R^0](\delta_{obs} - \delta_R)/(\delta_{RS} - \delta_R) = [R^0](\Delta/\Delta_0) \quad (1.13)$$

Where $\Delta = \delta_R - \delta_{obs}$ and $\Delta_0 = \delta_R - \delta_{RS}$. Δ/Δ_0 is the saturation fraction, and is equal to N_{RS}. Now if one substitutes $[R] = [RS]/K[S]$ into the above equation the resulting expression is:

$$[R^0] = [RS]/K[S] + [RS] = [RS](1/K[S] + 1) \quad (1.14)$$

From equations 1.13 and 1.14 one obtains:

$$1/\Delta = 1/\Delta_0 K[S] + 1/\Delta_0 \quad (1.15)$$

If this is multiplied through by $\Delta\Delta_0 K$, and then rearranged to give the x-reciprocal plotting form, one obtains the Scatchard equation:

$$\Delta/[S] = -K\Delta + \Delta_0 K \quad (1.16)$$

So by plotting $\Delta/[S]$ against Δ one obtains a negative straight line plot with a slope equal to K and a y-intercept equal to $\Delta_0 K$.

One difficulty associated with this method is the value that is used for [S]. [S] is the equilibrium concentration of S in the *solution* and must be determined from the equation $[S] = [S^0] - (\Delta/\Delta_0)[R^0]$ and using an assumed value of Δ_0 calculated from chemical shift data[41,45,70,94,95].

In order to determine whether selected platinum(II) complexes prepared in this work had the ability to act as receptors for adenine we utilised the Job plot method. This involved making up a series of NMR solutions containing varying amounts of 9-sec-pentyladenine and the Pt(II) complex to be analysed, keeping the total molar concentration constant. The chemical shifts of the two adenine protons, H^2 and H^8 were recorded and then plotted against the mole fraction. Figure 19 displays an example of two 300 MHz ^1H NMR spectra of 9-sec-pentyladenine recorded

in the absence and presence of complex (**47**). The resonances appearing at δ 8.371 and δ 7.804 are due to protons H^2 and H^8, respectively. The proton due to the NH_2 is clearly seen at δ 6.607 as a broad singlet. It can be seen that the two singlets due to protons H^2 and H^8 are significantly shifted in the presence of the Pt(II) complex. The H^2 proton shifts 0.024 ppm upfield while the H^8 proton has shifts 0.103 ppm downfield. Furthermore, the NH_2 signal moves downfield by 0.584 ppm, indicating that it is directly involved in the association process.

The upfield shift of the H^2 proton is a phenomenon noticed by Lancelot in his pioneering work on nucleobase binding by simple carboxylic acids[45]. Lancelot failed to explain this observation, however Maitra suggests a possible reason in his work when he reported the same phenomenon[44]. Maitra suggests that the upfield shift of H^2 is the result of binding-promoted π-polarisation, inducing a negative charge on the adjacent N[144]. Not only is a chemical shift change observed for the resonances but a change in the relative heights of the two signals is also observed, with the H^2 proton signal gradually increasing in intensity, while the H^8 signal gradually decreases. The minor signals in spectrum (b) are attributed to the platinum(II) complex (**47**). As expected, these signals gradually increase in strength as the concentration of the platinum(II) complex is increased.

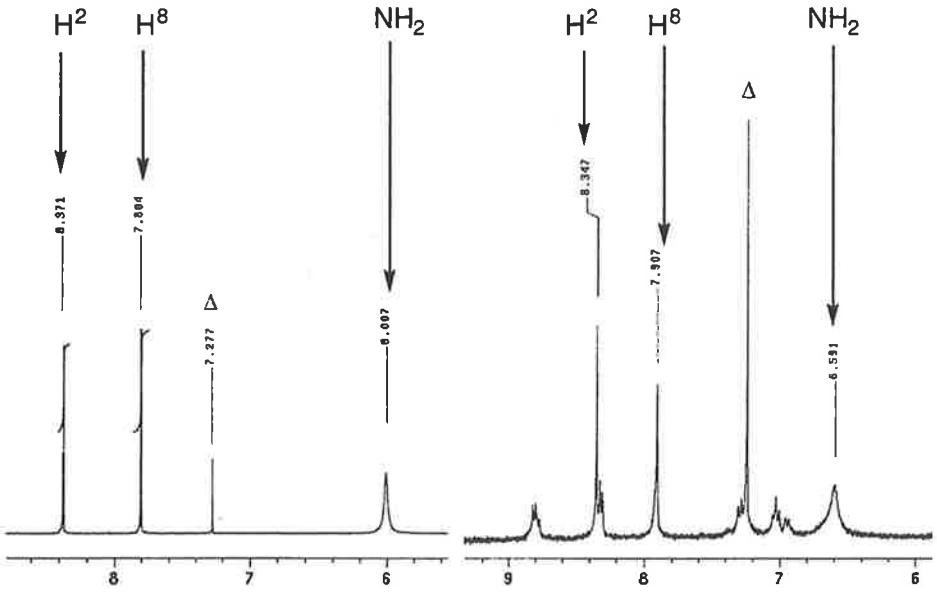

Figure 19. ^{1}H NMR spectra of (a) 9-sec-pentyladenine, and (b) 9-sec-pentyladenine + complex (47); Δ = residual $CHCl_3$.

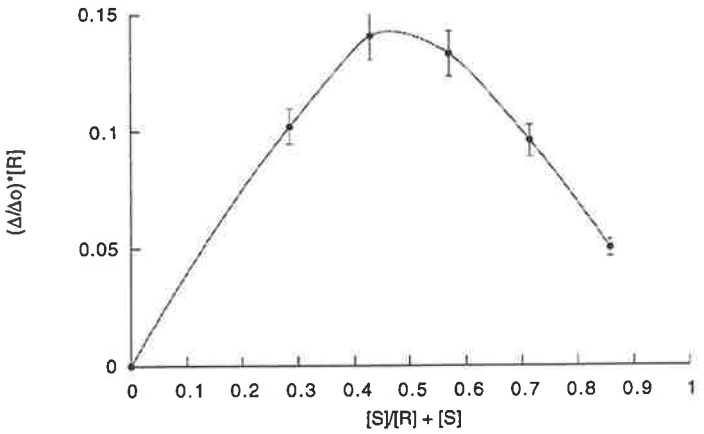

Figure 20. Job plot for complex (47) and 9-sec-pentyladenine.

Figure 20 shows the Job plot derived from the spectra of complex (**47**) with 9-sec-pentyladenine. The maximum appears over a mole fraction of 0.5 which indicates that the complex is binding to 9-sec-pentyladenine in a 1:1 binding mode. The shift of the H^8 signal is much more marked than that of H^2 so one can propose that the complex is binding at the H^8 (Hoogsteen) site. The dramatic shift of the NH_2 signal also supports this binding mode.

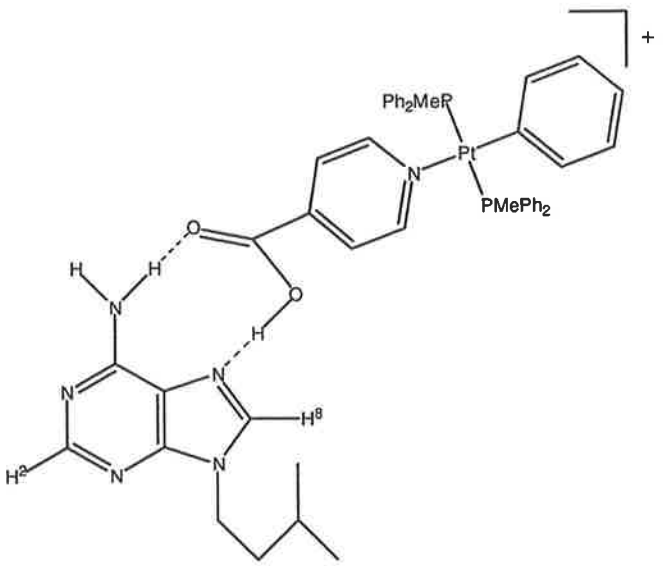

Figure 21. The proposed binding of (47) to 9-sec-pentyladenine

4.1 Association Studies of Mononuclear Platinum(II) Complexes with 9-sec-pentyladenine

Job plots for selected platinum(II) complexes (**42**), (**43**), (**46**) – (**50**) are shown in Figures 24 and 25. These plots provided a means of determining the binding modes of the selected platinum(II) complexes to 9-sec-pentyladenine. The plots that have maxima over a mole fraction of 0.5 are indicative of 1:1 association, while the plots that have a maxima over 0.66 are indicative of 2:1 association.

The Job plot for complex (**48**) showed us that at a concentration of 12 mM a 2:1 complex association was observed. This was clearly evident as the maximum of the plot appeared at 0.66. A 2:1 association in this case is indicative of complex (**48**) binding simultaneously to both the Watson-Crick and Hoogsteen sites of 9-sec-pentyladenine, (Figure 19). Literature studies with simple carboxylic acids have shown that one can obtain 1:1 complexes at low concentrations, while for the same carboxylic acid compound at higher concentrations, a 2:1 association occurs. The experiment was also repeated for (**48**) at 6 mM. This again resulted in a 2:1 association with 9-sec-pentyladenine. This showed that this complex had a tendency to bind to both Watson-Crick sites and Hoogsteen sites on 9-sec-pentyladenine simultaneously, and the binding also occurs at low concentrations.

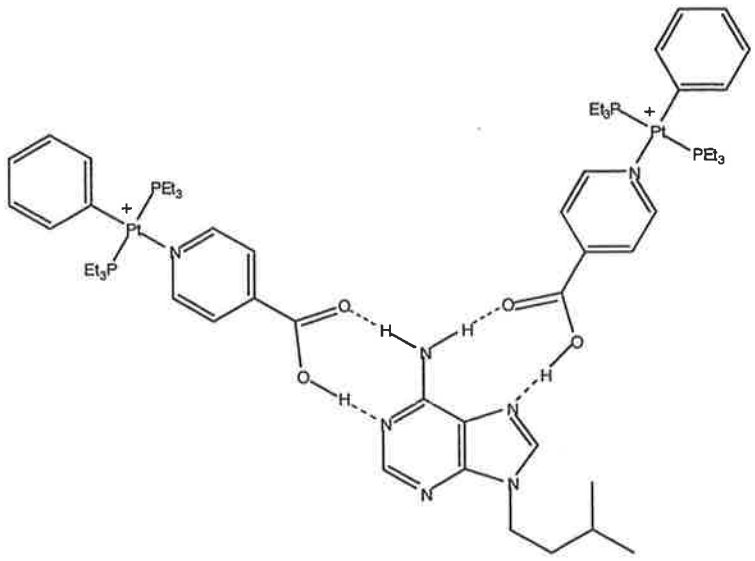

Figure 22. Suggested mode of binding for complex (48) with 9-sec-pentyladenine

Table 14 presents the various binding modes attributed to the mononuclear complexes (**42**) - (**50**). Complexes (**42**), (**43**), (**47**), (**49**) showed a 1:1 binding interaction with 9-sec-pentyladenine. To determine which side of the 9-sec-pentyladenine the platinum(II) complex was binding to, one must look at the NMR shifts of the H^2 and H^8 protons. If a significant proton signal shift occurs for the H^2 signal one can assume there is a preference for Watson-Crick association, while if the shift is more pronounced for the H^8 signal then there is a preference for the Hoogsteen mode of binding[44]. In this case, complexes (**42**), (**47**), and (**49**) showed preference for Hoogsteen binding, while (**43**) showed a preference for Watson-Crick binding. Complexes (**46**) and (**50**) had somewhat unexpected Job plots, with maxima appearing at approximate mole fraction equal to 0.75. This mole fraction is usually indicative of a 3:1 binding interaction. The only way that this can occur on adenine is if a third binding site is available. In this case there is the possibility for a third binding site, although it is not as common as Watson-Crick and Hoogsteen binding, and is shown in Figure 23. Complexes (**46**) and (**50**) appear to be associating at all three sites simultaneously. Maitra and co-workers report that aromatic carboxylic acids have preference for Hoogsteen binding, while aliphatic carboxylic acids prefer Watson-Crick binding[44]. Complexes (**42**), (**47**) and (**49**) showed a preference for Hoogsteen binding, and this is similar to the results reported by Maitra *et al*[44]. as they contain aromatic carboxylic acid functionalities. Complex (**43**) prefers Watson-Crick binding while (**46**), (**48**) and (**50**) appear to bind at more than one site. This somewhat unexpected and unusual results may be explained by the association of the triflate counterion with 9-sec-pentyladenine interfering with the association of the complex with 9-sec-pentyladenine.

The values for the equilibrium association constants were calculated graphically using a Scatchard plot for all complexes that showed a 1:1 association with 9-sec-pentyladenine. The Scatchard plot results in a straight line plot with a slope equal to the negative association constant (K). These plots are presented in Figure 26 for complexes (**42**), (**43**), (**47**), and (**49**).

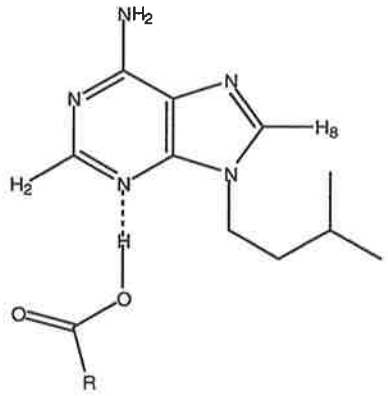

Figure 23. Third mode of binding of a carboxylic acid to 9-sec-pentyladenine

There appears to be no apparent trend in the nature of the platinum(II) complex investigated and the mode of adenine binding. The type of phosphine ligand coordinated to the platinum(II) metal centre does not appear to affect the association process. Factors such as steric bulk and basicity of the phosphine ligands do not appear to affect the association process. The position of the carboxylic acid group on the pyridine carboxylic acid does not appear to affect the association process either. Complex (**43**) bound quite strongly (2216 M^{-1}) to the Hoogsteen site compared to complex (**47**) which bound to the Watson-Crick site (25 M^{-1}). Also, the pKa value does not appear to correlate with the mode or degree of association. The low pKa values of our complexes may have interfered with the association, however this does not appear likely as Maitra reports acids of even lower pKa values associating with adenine[44].

We have shown that the complexes do indeed show some form of interaction with 9-sec-pentyladenine. These interactions vary from 1:1, 2:1, and possibly 3:1 interactions incorporating Watson-Crick and Hoogsteen binding sites. It would appear that the nature of the platinum(II) complex does not appear to affect the association, however there are most probably other factors at play, for example the association of the triflate counter ion with 9-sec-pentyladenine, which could complicate the binding of the metal complex to the substrate molecule.

It is possible for the triflate anion (OTf^-) to play a role in the aggregation process, as it can potentially bind to the NH_2 group of the adenine. ^{19}F NMR experiments were conducted for complexes (**42**), (**43**), (**47**) and (**48**) with and without 9-sec-pentyladenine. The chemical shift differences between the free platinum(II) complexes and the complexes with adenine were not significant (~ 0.1 ppm). Thus the triflate does not appear to play a large role in the aggregation of

the complexes with 9-sec-pentyladenine, although conclusions should be made with care as the hydrogen-bonding may not lead to large chemical shift differences.

Table 14. Stoichiometry of association and K_{eq} values for the interaction of (42), (43), (46) – (50) with 9-sec-pentyladenine in $CDCl_3$ solution

Complex	Concentration (mM)	Binding mode (site)	K (M^{-1})
42	3.30	1:1 (HG)	180 ± 27
43	4.40	1:1 (WC)	2200 ± 330
46	4.70	3:1	--
47	12.00	1:1 (HG)	25 ± 4
48	6.86	2:1	--
49	4.86	1:1 (HG)	180 ± 26
50	5.50	3:1	--

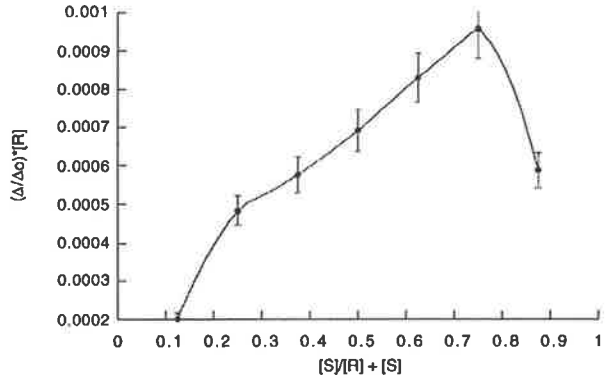

Complex (46)

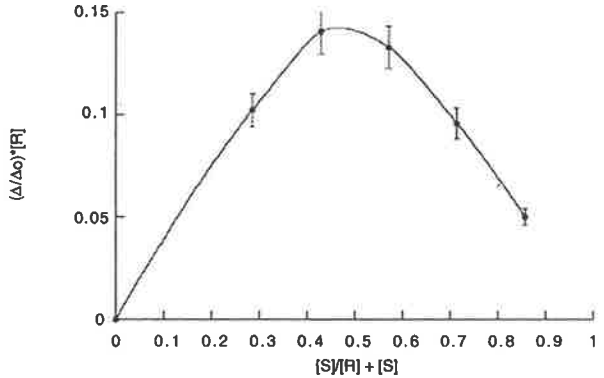

Complex (47)

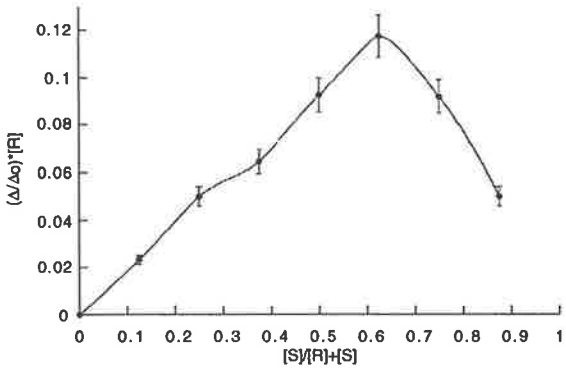

Complex (48)

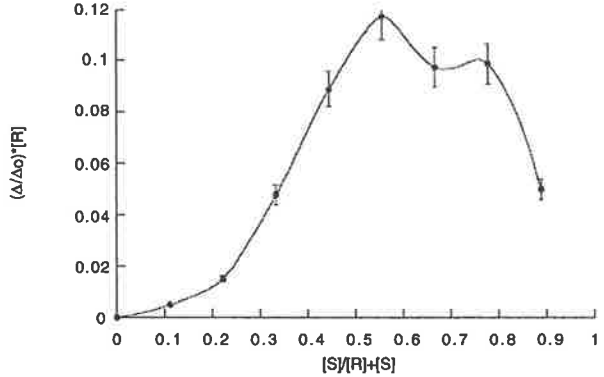

Complex (49)

Figure 24. Job Plots of isonicotinic acid complexes (46), (47), (48), and (49) and 9-sec-pentyladenine.

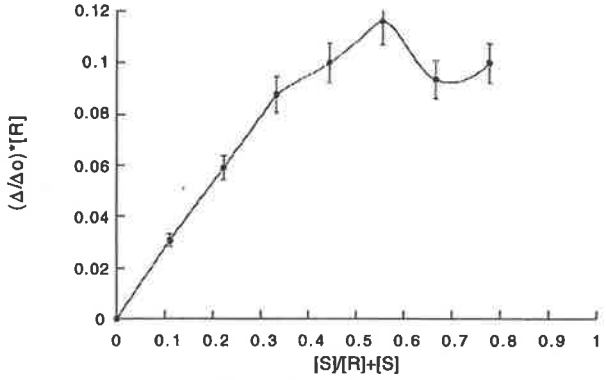

Complex (42)

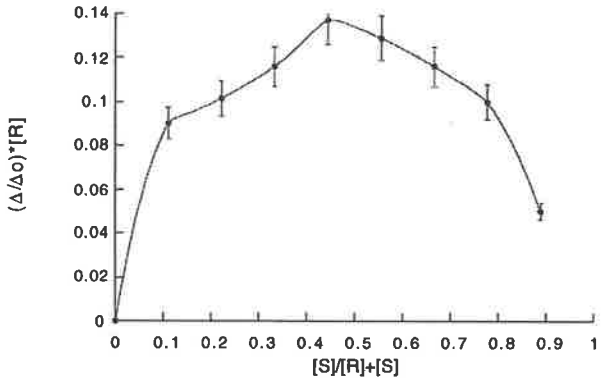

Complex (43)

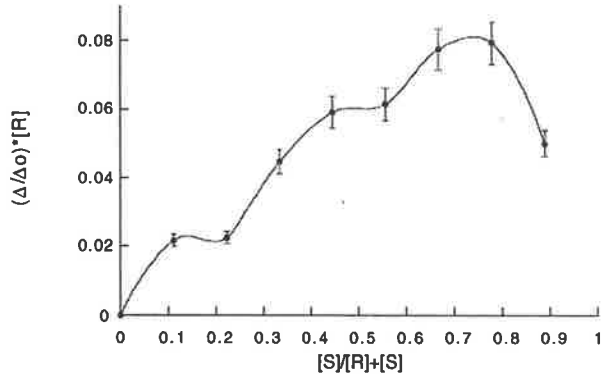

Complex (50)

Figure 25. Job Plots of nicotinic acid complexes (42), (43), and (50) and 9-sec-pentyladenine.

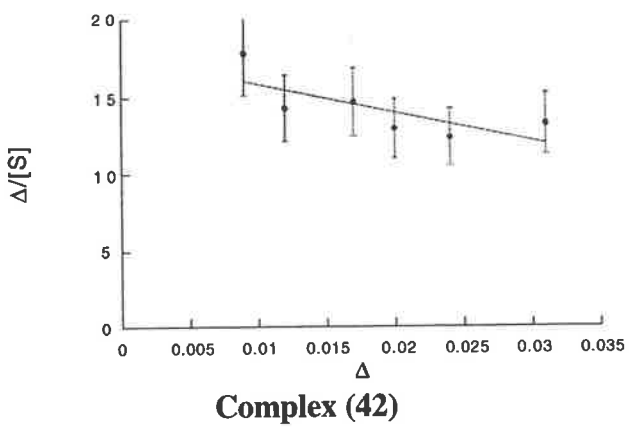

Complex (42)

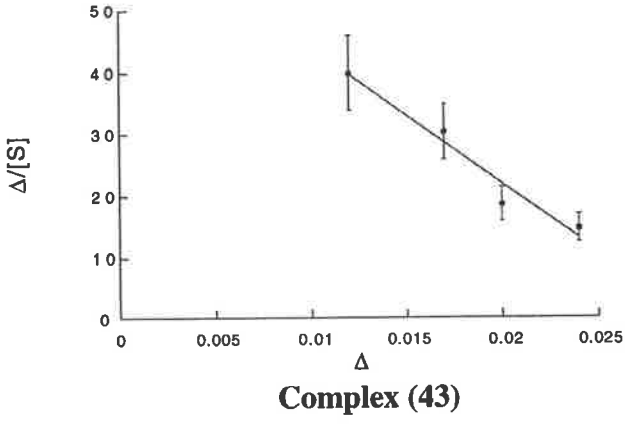

Complex (43)

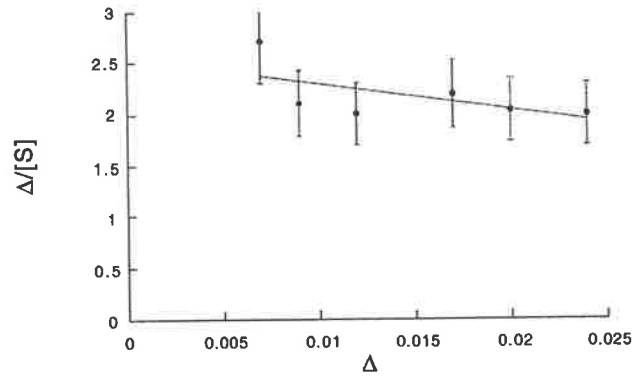

Complex (47)

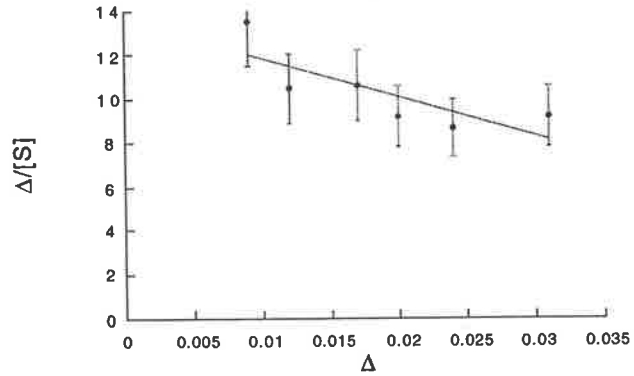

Complex (49)

Figure 26. Scatchard Plots for complexes (42), (43), (47), and (49).

4.2 Association Studies of Dinuclear Platinum(II) Complexes (**67**) and (**68**) with 9-sec-pentyladenine

Job's method of continuous variations was employed to investigate the interaction between the dinuclear organoplatinum(II) complexes (**67**) and (**68**) and 9-sec-pentyladenine. The plots for (**67**) are presented in Figure 29. It appeared from the Job plots of complex (**67**) that there was a 2:1 ratio of host to guest. This did not support our expectations of a 1:1 binding interaction expected for a molecular tweezer. The Job plot of (**68**) are incomplete due to the difficulty in interpreting the spectra after the concentration of the guest became too low. The guest signals were overlapped by the ^{1}H NMR signals from (**68**) and thus it was not able to be completed. The ^{1}H NMR titration data suggests that there was a 2:1 binding interaction for (**67**) and that the pyrazolyl N-H proton was possibly involved (Figure 27). This was determined by the fact that there was a marked shift in not only the 9-sec-pentyladenine proton signal but also a shift in the pyrazolyl N-H proton resonance. This is entirely possible as the pyrazolyl N-H proton provides complex (**67**) with an additional group that is capable of hydrogen-bonding interactions. It would appear, however, that by removing the pyrazolyl N-H proton, for example by replacing it with a phenyl group, as in complex (**68**) that there is still a 2:1 interaction between the platinum complex and 9-sec-pentyladenine (Figure 28). This scenario is also entirely possible as there are still two binding sites on the adenine and two binding sites on the platinum complex. While it appears that the platinum(II) complex is not acting as a molecular tweezer in the manner that was predicted, there is indeed evidence for an interaction between the platinum complexes (**67**) and (**68**) and 9-sec-pentyladenine.

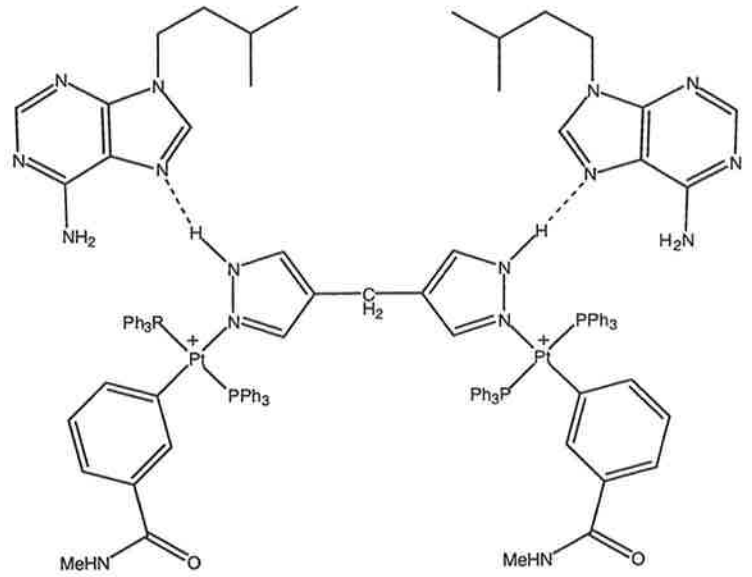

Figure 27. Possible mode of association between complex (67) and 9-sec-pentyladenine.

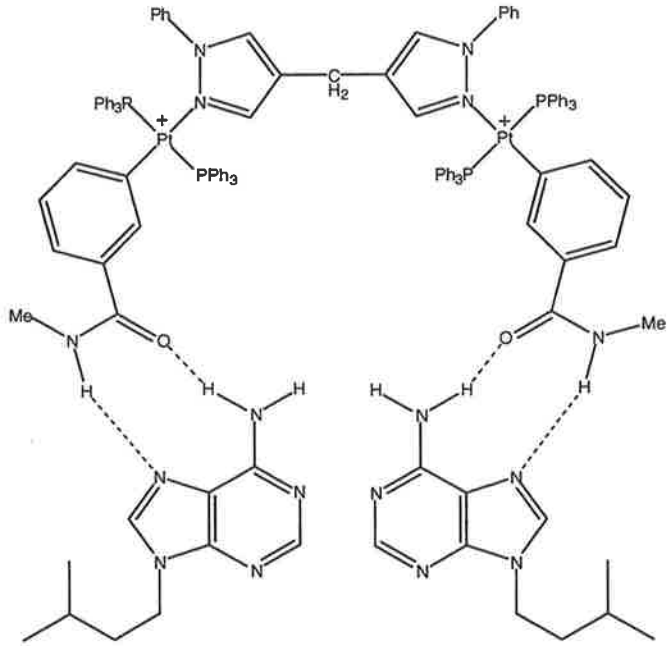

Figure 28. Possible mode of association between complex (68) and 9-sec-butyladenine.

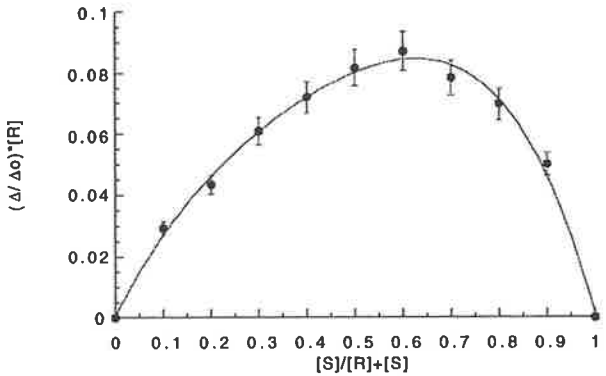

Complex (67)

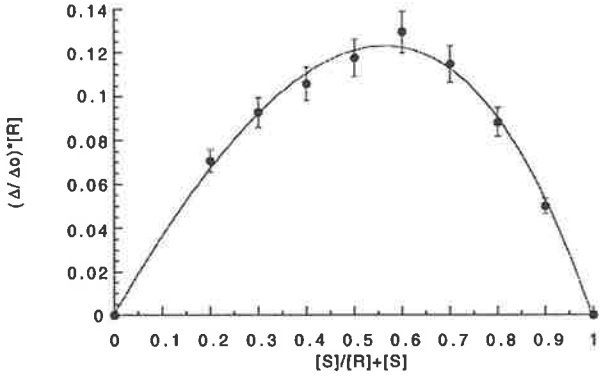

Complex (67)

Figure 29. Job Plots for complex (67) and 9-sec-pentyladenine, observing the H^8 (left) and the pyrazolyl N-H (right) ^1H NMR signals.

5. Conclusion

There were three main aims of this project. The first was to synthesise and characterise a series of mononuclear organoplatinum(II) complexes with hydrogen-bonding functionality. This thesis reports the successful synthesis of several novel mononuclear organoplatinum(II) complexes with hydrogen-bonding functionality. These were successfully characterised by a combination of $^{31}P\{^{1}H\}$ NMR spectroscopy, ^{1}H NMR spectroscopy, microanalysis and, in some cases, X-ray crystallography. The main interesting features of these complexes in the cationic square-planar platinum(II) metal centre and the hydrogen-bonding functionality of the attached ligand. These complexes have the ability to associate in the solid state, as was shown by the x-ray structure of complex (**47**). Not only did the complexes posses the ability to self-associate in the solid state, they were also showed potential for molecular recognition of guest molecules such as adenine.

The second aim of the work was to synthesise a number of dinuclear organoplatinum(II) complexes with hydrogen-bonding functionality. These complexes were successfully characterised by a combination of $^{31}P\{^{1}H\}$ NMR spectroscopy, ^{1}H NMR spectroscopy (1-D and 2-D), and microanalysis. The main interesting features of these complexes were the two cationic square-planar platinum(II) metal centres and the two hydrogen-bonding functionalities present within the one molecule. These complexes were symmetrical and had the potential to act as molecular tweezers in interactions with large guest molecules such as adenine.

The third aim was to test whether any of these complexes were suitable host molecules for adenine. ^{1}H NMR spectroscopy provided us with a powerful tool for the investigation of our complexes interacting with an adenine derivative. By utilising Job's method of continuous variation we were able to determine whether the complexes associated with 9-sec-pentyladenine and the type of association that was occurring. Various modes of binding were encountered for these complexes including a mixture of 1:1, 2:1, and 3:1 ratios as well as a mixture of Watson-Crick and Hoogsteen binding modes. These are the first examples of cationic organoplatinum(II) receptors for nucleobases.

6. Experimental

All complexes were synthesised under an inert atmosphere of high purity N_2, using standard Schlenk equipment and techniques. All solvents, except acetone, were specially dried and purified in the following manner: CH_2Cl_2 was distilled from CaH_2 and toluene was pre-dried over $CaSO_4$ followed by distillation from sodium. Dry CH_2Cl_2 and toluene were stored under N_2 over 4Å molecular sieves.

All 1D- and 2D-NMR spectra were recorded on a Varian Gemini 2000 NMR spectrometer, with an Oxford 300 MHz magnet, at room temperature. ^1H chemical shifts were reported in ppm relative to tetramethylsilane (TMS). $^{31}P\{^1H\}$ NMR spectra were referenced to sealed external standard of 85% phosphoric acid. ^{19}F NMR spectra were referenced to an external standard of $C_6H_5CF_3$. Coupling constants ($^nJ_{ij}$) were reported in Hz, and all multiplicities are abbreviated: s = singlet, d = doublet, dd = doublet of doublets, t = triplet, m = multiplet. IR spectra were recorded as nujol mulls on a Perkins-Elmer FT-IR spectrophotometer in the range 4000 – 400 cm^{-1}.

Compounds, $Pt(PPh_3)_4$[96], [PtIPh(cod)][55], 3-iodo-N-methylbenzamide[68] were prepared and purified according to literature procedures.

Elemental analysis was performed by CMAS (Chemical and MicroAnalytical Services Pty. Ltd.). Belmont, Victoria. The agreement between the found and calculated C and N analyses for complexes (**52**) and (**53**) is beyond the normal limits of acceptability. The reasons are unknown, and attempts at purification by recrystallisation in most cases were unsuccessful.

Trans-iodophenylbis(triphenylphosphine)platinum(II) (37)

PPh_3 (0.445 g, 1.695 mmol) was added to a solution of [PtIPh(cod)] (0.286 g, 0.565 mmol) in toluene. The mixture was stirred overnight at 80 °C. The volume of toluene was reduced *in vacuo* and hexane (30 mL) was added to the flask to precipitate (**37**) as a white solid that was collected by filtration (0.407 g, 78%). ^{1}H NMR ($CDCl_3$) δ 6.65 (d, 2H, $^3J_{HH}$ = 7.8 Hz, $^3J_{PtH}$ = 29 Hz, H_o), 6.10 (m, 2H, H_m), 6.24 (m, 1H, H_p), 7.57 - 7.20 (m, 30H, PPh_3). $^{31}P\{^1H\}$ NMR δ 22.0 (s, $^1J_{PtP}$ = 3087 Hz).

Trans-iodobis(methyldiphenylphosphine)phenylplatinum(II) (38)

Following a procedure similar to that described for (**37**) $PMePh_2$ (0.592 g, 0.556 mmol) was treated with [PtIPh(cod)] (0.500 g, 0.986 mmol) in toluene solution to give (**38**) as a white solid (0.500 g, 63%). ^{1}H NMR ($CDCl_3$) δ 6.81 (d, 2H, $^3J_{HH}$ = 7.8 Hz, $^3J_{PtH}$ = 30 Hz, H_o), 6.46 (m, 3H, $H_{m/p}$), 7.56 - 7.13 (m, 20H, $PMePh_2$). $^{31}P\{^1H\}$ NMR δ 4.7 (s, $^1J_{PtP}$ = 2935 Hz). *Anal.* Calcd for $C_{32}H_{31}IP_2Pt$: C, 48.07; H, 3.91. Found: C, 48.09; H, 3.96.

Trans-iodophenylbis(triethylphosphine)platinum(II) (39)

Following a procedure similar to that described for (**37**) PEt_3 (0.274 g, 2.319 mmol) was treated with [PtIPh(cod)] (0.294 g, 0.580 mmol) in toluene solution. The crude solid was left under high vacuum to remove excess PEt_3, and (**39**) was obtained as a white solid (0.300 g, 82%). ^{1}H NMR ($CDCl_3$) δ 7.28 (d, 2H, $^3J_{HH}$ = 7.2 Hz, $^3J_{PtH}$ = 36 Hz, H_o), 6.92 (m, 2H, H_m), 6.81 (m, 1H, H_p), 1.86 - 1.00 (m, 30H, PEt_3). $^{31}P\{^1H\}$ NMR δ 9.4 (s, $^1J_{PtP}$ = 2739 Hz).

Trans-iodophenylbis(tricyclohexylphosphine)platinum(II) (40)

Following a procedure similar to that described for (**37**) PCy_3 (1.106 g, 3.945 mmol) was treated with [PtIPh(cod)] (0.500 g, 0.986 mmol) in toluene solution. The mixture was stirred at 80 °C for three days. The volume of toluene was reduced *in vacuo* and hexane was added to the flask to precipitate (**40**) as a white solid that was collected by filtration (0.703 g, 74%). ^{1}H NMR ($CDCl_3$) δ 6.52 (d, 2H, $^3J_{HH}$ = 6.6 Hz, $^3J_{PtH}$ = 32 Hz, H_o), 6.84 (m, 2H, $H_{m/p}$), 1.91 - 0.98 (m, 60H, PCy_3).

$^{31}P\{^1H\}$ NMR δ 13.0 (s, $^1J_{PtP}$ = 2745 Hz). *Anal.* Calcd for $C_{42}H_{65}IP_2Pt$: C, 52.88; H, 6.87. Found: C, 52.81; H, 6.86.

Trans-(nicotinic acid)phenylbis(triphenylphosphine)platinum(II) triflate (42)

To a stirred solution of (**37**) (0.300 g, 0.325 mmol) in CH_2Cl_2 was added AgOTf (0.079 g, 0.309 mmol). The mixture was stirred in the absence of light for 16 h. AgI was removed by filtration through Celite filter aid. To the clear filtrate was added nicotinic acid (0.040 g, 0.325 mmol), and the mixture was stirred for 16 h at room temperature. The solvent was removed *in vacuo* to yield (**42**) as a white solid (0.312 g, 90%). IR (nujol) 1720 ν(C=O), 2800-3200 ν(O-H) cm^{-1}. ^1H NMR ($CDCl_3$) δ 6.74 (d, 2H, $^3J_{HH}$ = 7.5 Hz, H_o), 6.37 (m, 2H, H_m), 6.53 (m, 1H, H_p), 8.57 (s, 1H, H_2), 8.20 (d, 1H, $^3J_{HH}$ = 5.7 Hz, H^6), 6.82 (m, 1H, H^5), 7.84 (d, 1H, $^3J_{HH}$ = 7.8 Hz, H^4), 7.57 - 7.14 (m, 30H, PPh_3). $^{31}P\{^1H\}$ NMR δ 20.8 (s, $^1J_{PtP}$ = 3045 Hz). ^{19}F NMR δ 48.4. *Anal.* Calcd for $C_{49}H_{40}F_3NO_5P_2PtS$: C, 55.06; H, 3.77; N, 1.31. Found: C, 55.09; H, 3.78 ; N, 1.40.

Trans-(nicotinic acid)phenylbis(methyldiphenylphosphine)platinum(II) triflate (43)

Following a similar procedure to that described for (**42**), complex (**38**) (0.348 g, 0.436 mmol) was treated with AgOTf (0.106 g, 0.414 mmol), followed by nicotinic acid (0.537 g, 0.436 mmol) to afford (**43**) as a white solid (0.312 g, 88%). IR (nujol) 1720 ν(C=O) , 2800-3200 ν(O-H) cm^{-1}. ^1H NMR ($CDCl_3$) δ 8.37 (s, 1H, H^2), 8.19 (d, 1H, $^3J_{HH}$ = 4.8 Hz, H^6), 6.89 (m, 1H, H^5), 7.88 (d, 1H, $^3J_{HH}$ = 8.1 Hz, H^4), 7.52 - 7.16 (m, 20H, $PMePh_2$). $^{31}P\{^1H\}$ NMR δ 9.4 (s, $^1J_{PtP}$ = 2870 Hz). ^{19}F NMR δ 48.5. *Anal.* Calcd for $C_{39}H_{36}F_3NO_5P_2PtS$: C, 49.58; H, 3.84; N, 1.48. Found: C, 49.60 ; H, 3.74 ; N, 1.53.

Trans-(nicotinic acid)phenylbis(triethylphosphine)platinum(II) triflate (44)

Following a similar procedure to that described for (**42**), complex (**39**) (0.100 g, 0.157 mmol) was treated with AgOTf (0.040 g, 0.157 mmol) followed by nicotinic acid (0.020 g, 0.157 mmol), to afford (**44**) as a white solid (0.100 g, 82%). IR (nujol) 1725 ν(C=O), 2800-3200 ν (O-H) cm^{-1}. ^1H NMR ($CDCl_3$) δ 9.19 (s, 1H, H^2), 8.88 (d, 1H, $^3J_{HH}$ = 5.4 Hz, H^6), 8.54 (d, 1H, $^3J_{HH}$ = 7.8 Hz H_4), 8.00 (m, 1H, H^5), 7.28 (m, 2H, H_o), 7.03 (m, 2H, H_m), 6.93 (m, 1H, H_p), 1.23 - 0.96 (m, 30H,

PEt_3). $^{31}P\{^1H\}$ NMR δ 13.9 (s, $^1J_{PtP}$ = 2698 Hz). *Anal.* Calcd for $C_{25}H_{40}F_3NO_5P_2PtS$: C, 38.46; H, 5.16; N, 1.79. Found: C, 38.29; H, 5.21; N, 1.91.

Trans-(nicotinic acid)phenylbis(tricyclohexylphosphine)platinum(II) triflate (45)

Following a similar procedure to that described for (**42**), complex (**40**) (0.300 g, 0.313 mmol) was treated with AgOTf (0.764 g, 0.297 mmol) followed by nicotinic acid (0.076 g, 0.297 mmol), to afford (**45**) as a white solid (0.242 g, 70%). IR (nujol) 1732 ν(C=O) , 2800-3100 ν(O-H) cm^{-1}. ^1H NMR ($CDCl_3$) δ 7.40 (m, 2H, H_o), 6.83 (m, 2H, H_m), 7.01 (m, 1H, H_p), 9.30 (s, 1H, H_2), 8.94 (d, 1H, $^3J_{HH}$ = 6.9 Hz, H^6), 7.77 (m, 1H, H^5), 8.68 (d, 1H, $^3J_{HH}$ = 7.8 Hz, H^4), 1.91 - 0.86 (m, 60H, PCy_3). $^{31}P\{^1H\}$ NMR δ 13.4 (s, $^1J_{PtP}$ = 2724 Hz). *Anal.* Calcd for $C_{49}H_{70}F_3NO_5P_2PtS$: C, 53.54; H, 6.42; N, 1.27. Found: C, 53.21; H, 6.39; N, 1.20.

Trans-(isonicotinic acid)phenylbis(triphenylphosphine)platinum(II) triflate (46)

Following a similar procedure to that described for (**42**), complex (**37**) (0.075 g, 0.081 mmol) was treated with AgOTf (0.019 g, 0.077 mmol), followed by isonicotinic acid (0.010 g, 0.081 mmol), to afford (**46**) as a white solid (0.078 g, 90%). IR (nujol) 1726 ν(C=O), 2800-3100 ν(O-H) cm^{-1}. ^1H NMR ($CDCl_3$) δ 6.75 (d, 2H, $^3J_{HH}$ = 6.9 Hz, $^3J_{PtH}$ = 24 Hz, H_o), 6.31 (m, 2H, H_m), 6.51 (m, 1H, H_p), 8.35 (d, 2H, $^3J_{HH}$ = 8.1 Hz, $H^{2/6}$), 7.20 (m, 2H, $H^{3/5}$), 7.43 - 7.27 (m, 30H, PPh_3). $^{31}P\{^1H\}$ NMR δ 22.1 (s, $^1J_{PtP}$ = 3054 Hz). *Anal.* Calcd for $C_{49}H_{40}F_3NO_5P_2PtS$: C, 55.06; H, 3.77; N, 1.31. Found: C, 54.91 ; H, 3.73 ; N, 1.37.

Trans-(isonicotinic acid)phenylbis(methyldiphenylphosphine)platinum(II) triflate (47)

Following a similar procedure to that described for (**42**), complex (**38**) (0.132 g, 0.165 mmol) was treated with AgOTf (0.040 g, 0.157 mmol), followed by isonicotinic acid (0.020 g, 0.165 mmol), to afford (**47**) as a white solid (0.132 g, 85%). IR (nujol) 1712 ν(C=O), 2500-3000 ν(O-H) cm^{-1}. ^1H NMR ($CDCl_3$) δ 8.17 (d, 2H, $^3J_{HH}$ = 6.6 Hz, $H^{2/6}$), 6.78 (m, 2H, $H^{3/5}$), 1.64 (m, 3H, CH_3), 7.45 - 7.23 (m, 20H, $PMePh_2$). $^{31}P\{^1H\}$ NMR δ 9.4 (s, $^1J_{PtP}$ = 2914 Hz). ^{19}F NMR δ 48.5. *Anal.* Calcd for $C_{39}H_{36}F_3NO_5P_2PtS$: C, 49.58; H, 3.84; N, 1.48. Found: C, 49.44 ; H, 3.88 ; N, 1.42.

Trans-(isonicotinic acid)phenylbis(triethylphosphine)platinum(II) triflate (48)

Following a similar procedure to that described for (**42**), complex (**39**) (0.255 g, 0.402 mmol) was treated with AgOTf (0.098 g, 0.381 mmol), followed by isonicotinic acid (0.049 g, 0.402 mmol) to afford (**48**) as a white solid (0.298 g, 95%). IR (nujol) 1731 ν(C=O), 2700-3100 ν(O-H) cm^{-1}. ^1H NMR ($CDCl_3$) δ 7.32 (d, 2H, $^3J_{HH}$ = 8.1 Hz, $^3J_{PtH}$ = 29 Hz, H_o), 6.87 (m, 2H, H_m), 7.05 (m, 1H, H_p), 8.89 (d, 2H, $^3J_{HH}$ = 6.3 Hz, $H^{2/6}$), 8.27 (m, 2H, $^3J_{HH}$ = 6.6 Hz, $H^{3/5}$), 1.73 - 1.02 (m, 30H, PEt_3). $^{31}P\{^1H\}$ NMR δ 13.4 (s, $^1J_{PtP}$ = 2697 Hz). ^{19}F NMR δ 48.2. *Anal.* Calcd for $C_{25}H_{40}F_3NO_5P_2PtS$: C, 38.46; H, 5.16; N, 1.79. Found: C, 38.46 ; H, 5.15 ; N, 1.72.

Trans-(isonicotinic acid)phenylbis(tricyclohexylphosphine)platinum(II) triflate (49)

Following a similar procedure to that described for (**42**), complex (**40**) (0.300 g, 0.313 mmol) was treated with AgOTf (0.076 g, 0.297 mmol) followed by isonicotinic acid (0.038 g, 0.313 mmol) to afford (**49**) as a white solid (0.249 g, 72%). IR (nujol) 1736 ν(C=O), 2700-3100 ν(O-H) cm^{-1}. ^1H NMR ($CDCl_3$) δ 8.83 (d, 2H, $^3J_{HH}$ = 6.3 Hz, $H^{2/6}$), 8.42 (m, 2H, $^3J_{HH}$ = 6.6 Hz, $H^{3/5}$), 1.87 - 0.83 (m, 60H, PCy_3). $^{31}P\{^1H\}$ NMR δ 17.5 (s, $^1J_{PtP}$ = 2792 Hz). *Anal.* Calcd for $C_{49}H_{70}F_3NO_5P_2PtS$: C, 53.54; H, 6.42; N, 1.27. Found: C, 53.39; H, 6.41; N, 1.27.

Trans-(picolinic acid)phenylbis(triphenylphosphine)platinum(II) triflate (50)

Following a similar procedure to that described for complex (**42**), complex (**37**) (0.400 g, 0.433 mmol) was treated with AgOTf (0.106 g, 0.433 mmol) followed by picolinic acid (0.533 g, 0.4333 mmol) to afford (**50**) as a white solid (0.270 g, 68%). IR (nujol) 1720 ν(C=O), 2800-3100 ν(O-H) cm^{-1}. ^1H NMR ($CDCl_3$) δ 6.63 (d, 2H, $^3J_{HH}$ = 7.5 Hz, H_o), 6.33 (m, 2H, H_m), 6.33 (m, 1H, H_p), 8.69 (m, 1H, H^3), 8.03 (d, 1H, $^3J_{HH}$ = 7.8 Hz, H^6), 8.28 (td, 1H, $^4J_{HH}$ = 1.8 Hz, $^3J_{HH}$ = 7.4 Hz, H^5), 7.75 (m, 1H, H^4), 7.52 - 7.14 (m, 30H, PPh_3). $^{31}P\{^1H\}$ NMR δ 23.0 (s, $^1J_{PtP}$ = 3212 Hz). *Anal.* Calcd for $C_{25}H_{40}F_3NO_5P_2PtS.CH_2Cl_2$: C, 52.05; H, 3.67; N, 1.21. Found: C, 52.27 ; H, 3.86 ; N, 1.40.

Trans-(picolinic acid)phenylbis(methyldiphenylphosphine)platinum(II) triflate (51)

Following a similar procedure to that described for complex (**42**), complex (**38**) (0.400 g, 0.501 mmol) was treated with AgOTf (0.122 g, 0.501 mmol) followed by picolinic acid (0.062 g, 0.501 mmol), to afford (**51**) as a white solid (0.200 g, 58%). IR (nujol) 1725 ν(C=O), 2700-3200 ν(O-H) cm^{-1}. ^1H NMR ($CDCl_3$) δ 6.55 (m, 2H, H_o), 6.87 (m, 2H, H_m), 6.87 (m, 1H, H_p), 7.60 (m, 1H, H^3), 8.68 (d, 1H, $^3J_{HH}$ = 4.5 Hz, H^6), 7.99 (td, 1H, $^3J_{HH}$ = 7.4 Hz, $^4J_{HH}$ = 1.8 Hz, H^5), 8.25 (dt, 1H, $^3J_{HH}$ = 7.50 Hz, $^4J_{HH}$ = 1.2 Hz, H^4), 7.42 - 7.18 (m, 20H, $PMePh_2$). $^{31}P\{^1H\}$ NMR δ 6.5 (s, $^1J_{PtP}$ = 3089 Hz). *Anal.* Calcd for $C_{25}H_{40}F_3NO_5P_2PtS$: C, 49.58; H, 3.84; N, 1.48. Found: C, 49.53; H, 3.63; N, 1.59.

Trans-(picolinic acid)phenylbis(triethylphosphine)platinum(II) triflate (52)

Following a similar procedure to that described for complex (**42**), complex (**39**) (0.400 g, 0.630 mmol) was treated with AgOTf (0.154 g, 0.630 mmol) followed by picolinic acid (0.077 g, 0.630 mmol), to afford (**52**) as a white solid (0.112 g, 23%). IR (nujol) 1725 ν(C=O), 2750-3000 ν(O-H) cm^{-1}. ^1H NMR ($CDCl_3$) δ 6.63 (d, 2H, $^3J_{HH}$ = 7.5 Hz, H_o), 6.97, (m, 2H, H_m), 6.91 (m, 1H, H_p), 6.33 (m, 1H, H^3), 8.79 (d, 1H, $^3J_{HH}$ = 4.5 Hz, H^6), 8.04 (td, 1H, $^3J_{HH}$ = 7.2 Hz, $^4J_{HH}$ = 1.5 Hz, H^5), 7.64 (m, 1H, H^4). $^{31}P\{^1H\}$ NMR δ 11.1 (s, $^1J_{PtP}$ = 2840 Hz).

Trans-(picolinic acid)phenylbis(tricyclohexylphosphine)platinum(II) triflate (53)

Following a similar procedure to that described for complex (**42**), complex (**40**) (0.400 g, 0.417 mmol) was treated with AgOTf (0.101 g, 0.417 mmol) followed by picolinic acid (0.051 g, 0.417 mmol), to afford (**53**) as a white solid (0.083 g, 18 %). IR (nujol) 1726 ν(C=O), 2750-3000 ν(O-H) cm^{-1}. ^1H NMR ($CDCl_3$) δ (d, 2H, $^3J_{HH}$ = 7.5 Hz, H_o), 7.01, (m, 2H, H_m), 6.96 (m, 1H, H_p), 6.33 (m, 1H, H^3), 8.25 (d, 1H, $^3J_{HH}$ = 7.8 Hz, H^6), 7.98 (td, 1H, $^3J_{HH}$ = 8.1 Hz, $^4J_{HH}$ = 1.8 Hz, H^5), 7.61 (m, 1H, H^4). $^{31}P\{^1H\}$ NMR δ 17.2 (s, $^1J_{PtP}$ = 3067 Hz).

Trans-(isonicotinamide)phenylbis(methyldiphenylphosphine)platinum(II) triflate (54)

Following a similar procedure to that described for complex (**42**), complex (**38**) (0.296 g, 0.298 mmol), was treated with AgOTf (0.076 g, 0.298 mmol) followed by isonicotinamide (0.036 g,

0.296 mmol) to afford (**54**) as a white crystalline solid (0.202 g, 60%). IR (nujol) 1671 ν(C=O) cm^{-1}. ^1H NMR ($CDCl_3$) δ 7.16 (d, 2H, $^3J_{HH}$ = 7.8 Hz, H_o), 6.83 (m, 3H, $H_{m/p}$), 7.94 (d, 2H, $^3J_{HH}$ = 6.3 Hz, H^2), 5.66 (s, 1H, NH_2), 7.57 – 7.34 (m, 20H, $PMePh_2$), 1.56 (m, 6H, PCH_3). $^{31}P\{^1H\}$ NMR δ 9.1 ($^1J_{PtP}$ = 2888 Hz). *Anal.* Calcd for $C_{39}H_{37}F_3N_2O_4P_2PtS$: C, 49.63; H, 3.95; N, 2.97. Found: C, 49.33; H, 4.06; N, 2.74.

Trans-(nicotinamide)phenylbis(methyldiphenylphosphine)platinum(II) triflate (55)

Following a similar procedure to that described for complex (**42**), complex (**38**) (0.296 g, 0.298 mmol), was treated with AgOTf (0.076 g, 0.298 mmol) followed by nicotinamide (36.1 g, 0.298 mmol) to afford (**55**) as a white crystalline solid (0.175 g, 52%). IR (nujol) 1697 ν(C=O) cm^{-1}. ^1H NMR ($CDCl_3$) δ 6.98 (m, 2H, H_o), 6.82 (m, 2H, H_m), 6.67 (m, 1H, H_p), 8.62 (s, 1H, H_2), 7.99 – 7.96 (m, 3H, $H^{4/5/6}$), 1.69 (m, 6H, PCH_3). $^{31}P\{^1H\}$ NMR δ 10.1 ($^1J_{PtP}$ = 2927 Hz). *Anal.* Calcd for $C_{39}H_{37}F_3N_2O_4P_2PtS$: C, 49.63; H, 3.95; N, 2.97. Found: C, 48.66; H, 3.46; N, 3.03.

Trans-iodo(*N*-methylbenzamide)bis(triphenylphosphine)platinum(II) (59)

3-iodo-*N*-methylbenzamide (0.11 g, 0.402 mmol) was placed in a Schlenk flask with $Pt(PPh_3)_4$ (0.500 g, 0.402 mmol). Toluene (20 mL) was added to the flask and the reaction was stirred for 16 h at 80 °C. Hexane was added to the solution to precipitate the product, which was collected by filtration to afford (**59**) as a white crystalline solid (0.344 g, 88%). IR (nujol) 1632 ν(C=O) cm^{-1}. ^1H NMR ($CDCl_3$) δ 7.56 – 7.22 (m, 30H, PPh_3), 6.96 (d, 1H, $^3J_{HH}$ = 7.5 Hz, $^1J_{PtH}$ = 29.3 Hz, H^6), 6.72 (d, 1H, $^3J_{HH}$ = 8.4 Hz, H^4), 6.67 (s, 1H, $^1J_{PtH}$ = 28.8 Hz, H^2), 6.24 (t, 1H, $^3J_{HH}$ = 7.8 Hz, H^5), 2.76 (d, 3H, $^3J_{HH}$ = 4.8 Hz, NCH_3), 4.98 (br.m, 1H, NH). δ $^{31}P\{^1H\}$ NMR δ 22.0 ($^1J_{PtP}$ = 3029 Hz). *Anal.* Calcd for $C_{44}H_{38}INOP_2Pt$: C, 53.89; H, 3.91; N, 1.43. Found: C, 53.37; H, 3.85; N, 1.45.

Trans-μ-4,4'-bipyridinebis[(*N*-methylbenzamide)bis(triphenylphosphine)platinum(II)] bis(triflate) (65)

Following a procedure similar that described for (**42**), complex (**59**) (0.400 g, 0.401 mmol) was treated with AgOTf (0.103 g, 0.401mmol) The reaction mixture was stirred for 3 h in the absence of light. After the reaction AgI was removed through Celite filter aid, and 4,4'-dipyridine (0.031

g, 0.201 mmol) was added to the solution and it was stirred over-night. Solvent was removed to afford (**65**) as a white crystalline solid (0.260 g, 60%). IR (nujol) 1655 ν(C=O) cm^{-1}. ^1H NMR ($CDCl_3$) δ 7.34 – 7.19 (m, 60H, PPh_3), 7.03 (d, 2H, $^3J_{HH}$ = 7.5 Hz, H^6), 6.81 (d, 2H, $^3J_{HH}$ = 7.5 Hz, H^4), 6.83 (s, 2H, H^2), 6.39 (t, 2H, $^3J_{HH}$ = 7.8 Hz, H^5), 6.83 (s, 4H, H_m). $^{31}P\{^1H\}$ NMR δ 20.9 ($^1J_{PtP}$ = 3008 Hz). *Anal.* Calcd for $C_{44}H_{38}INOP_2Pt$: C, 55.56; H, 3.92; N, 2.59. Found: C, 54.62; H, 3.51; N, 2.64.

Trans-μ-4,7-phenanthrolinebis[*N*-methylbenzamide)bis(triphenylphosphine)platinum(II)] bis(triflate) (66)

Following a procedure similar to that described for complex (**65**), complex (**59**) (0.400 g, 0.401 mmol) was treated with AgOTf (0.103 g, 0.401 mmol) followed by 4,7-phenathroline (0.036 g, 0.201 mmol) to afford (**66**) as a white crystalline solid (0.360 g, 55%). IR (nujol) 1641 ν(C=O) cm^{-1}. ^1H NMR (CD_2Cl_2) δ 7.41 – 7.11 (m, 20H, $PMePh_2$), 9.40 (d, 2H, $^3J_{HH}$ = 9.3 Hz, $H^{1,10}$), 9.07 (d, 1H, $^3J_{HH}$ = 4.2 Hz, $H^{3,8}$), 6.38 (t, 2H, $^3J_{HH}$ = 8.1 Hz, H^{15}), 5.96 (br. s, 2H, NH), 2.84 (d, 6H, $^3J_{HH}$ = 4.8 Hz, NMe), 9.05 (s, 2H, $H^{5,6}$), 6.88 (d, 2H, $^3J_{HH}$ = 7.8 Hz, H^{14}). δ $^{31}P\{^1H\}$ NMR δ 19.5 ($^1J_{PtP}$ = 3003 Hz). *Anal.* Calcd for $C_{102}H_{84}F_6N_4O_8P_4Pt_2S_2$: C, 56.04; H, 3.87; N, 2.56. Found: C, 55.94; H, 3.45; N, 3.18.

Trans-μ-4,4'-dipyrazolylmethanebis[(*N*-methylbenzamide)bis(triphenylphosphine)platinum(II)] bis(triflate) (67)

Following a procedure similar to that described for (**65**), complex (**59**) (0.400 g, 0.401 mmol) was treated with AgOTf (0.103 g, 0.401 mmol) followed by 4,4'-dipyrazolylmethane (0.029 g, 0.201 mmol) to afford (**67**) as a white crystalline solid (0.369 g, 81%). IR (nujol) 1643 ν(C=O), 3400 ν(N-H) cm^{-1}. ^1H NMR ($CDCl_3$) δ 6.40 (s, 2H, H^2), 6.77 (t, 2H, $^3J_{HH}$ = 7.2 Hz), 6.35 (t, 2H, $^3J_{HH}$ = 7.2 Hz, H^5), 7.00 (d, 2H, $^3J_{HH}$ = 7.8 Hz, H^6), 12.45 (s, 2H, pyr-NH), 7.04 (s, 2H, H^9), 6.10 (s, 2H, H^{10}), 2.53 (s, 2H, $-CH_2-$), 6.01 (m, 2H, NH), 2.83 (d, 6H, $^3J_{HH}$ = 4.8 Hz, NHMe), 7.45 – 7.25 (m, 60H, PPh_3). $^{31}P\{^1H\}$ NMR δ 20.8 ($^1J_{PtP}$ = 3022 Hz). *Anal.* Calcd for $C_{97}H_{84}F_6N_6O_8P_4Pt_2S_2$: C, 54.09; H, 3.93; N, 3.90. Found: C, 53.98; H, 4.09; N, 3.71.

Trans-μ-1,1'-phenyl-4,4'-dipyrazolylmethanebis[(*N*-methylbenzamide)bis(triphenylphosphine)platinum(II)] bis(triflate) (68)

Following a procedure similar to that described for (**65**), complex (**59**) (0.400 g, 0.401 mmol) was treated with AgOTf (0.103 g, 0.401 mmol) followed by 1,1'-phenyl-4,4'-dipyrazolylmethane (0.060 g, 0.201 mmol) to afford (**68**) as a white crystalline solid (0.129 g, 54%). ^{1}H NMR ($CDCl_3$) δ 6.69 (br.s, 2H, H^2), 6.58 (br.s, 2H), 6.25 (br.s, 2H, H^5), 6.94 (br.s, 2H, H^6), 3.11 (s, 2H, -CH_2-), 5.70 (m, 2H, NH), 2.84 (d, 6H, $^3J_{HH}$ = 4.5 Hz, NHMe), 7.64 – 7.28 (m, 60H, PPh_3). δ $^{31}P\{^1H\}$ NMR δ 25.0 ($^1J_{PtP}$ = 3084 Hz). *Anal.* Calcd for $C_{109}H_{92}F_6N_6O_8P_4Pt_2S_2$: C, 56.77; H, 4.02; N, 3.64. Found: C, 56.57; H, 4.09; N, 3.49.

Preparation of Samples for Job Plots

Job's method was carried out by mixing aliquots of two equimolar stock solutions of the two species to be observed. This was done to keep the total concentration of the two components constant, while the ratio of the two components varies in each NMR tube[91]. Stock solutions of the desired concentrations of the complexes and of 9-sec-pentyladenine were made in volumetric flasks in $CDCl_3$. In NMR tubes, aliquots of each solution were added such that the stoichiometry of each component varied, but the total volume of solution remained at 500 μL. For example, the first tube may contain 450 μL of the Pt(II) complex solution and 50 μL of 9-sec-butylbutyladenine solution at the same concentration. The ^{1}H NMR spectrum was obtained for each tube, and the chemical shift of the H^2, H^8, or NH_2 signals were used to calculate the concentration. This value was then plotted against the mole fraction of the platinum(II) complex using KaleidaGraph™ v3.08c, on a Power Macintosh 7220/200.

Determination of pKa values

pKa determinations were carried out by making up a stock solution of the complex to be investigated in 50% ethanol solution. The complex solution was then titrated with KOH in 50% ethanol solution. The pH was measured using a glass electrode with 0.1 M silver-silver chloride electrode at 25 °C. The electrode was calibrated with buffer solution (pH 4.0)[83].

7. References

(1) Braga, D.; Grepioni, F.; Desiraju, G. R. *Chem. Rev.* **1998**, *98*, 1375-1405.

(2) Burrows, A. D.; Chan, C.-W.; Chowdry, M. M.; McGrady, J. E.; Mingos, D. M. P. *Chem. Soc. Rev.* **1995**, *24*, 329-339.

(3) Fraser, S. A.; Jenkins, H. A.; Jennings, M. C.; Puddephatt, R. J. *Organometallics* **2000**, *19*, 1635-1642.

(4) Sherrington, D. C.; Taskinen, K. A. *Chem. Soc. Rev.* **2001**, *30*, 83-93.

(5) James, S. L.; Mingos, D. M. P.; Xu, X.; White, A. J. P.; Williams, D. J. *J. Chem. Soc., Dalton Trans.* **1998**, 1335-1340.

(6) Gianneschi, N. C.; Tiekink, E. R. T.; Rendina, L. M. *J. Am. Chem. Soc.* **2000**, *122*, 8474-8479.

(7) Brammer, L.; Rivas, J. C. M.; Atencio, R.; Fang, S.; Pigge, F. C. *J. Chem. Soc., Dalton Trans.* **2000**, 3855-3867.

(8) Stang, P. J.; Persky, N. E.; Manna, J. *J. Am. Chem. Soc.* **1997**, *119*, 4777-4778.

(9) Stang, P. J.; Olenyuk, B. *Acc. Chem. Res.* **1997**, *30*, 502-518.

(10) Stang, P. J. *Chem. Eur. J.* **1998**, *4*, 19-27.

(11) Kuehl, C. J.; Mayne, C. L.; Arif, A. M.; Stang, P. J. *Organic Lett.* **2000**, *2*, 3727-3729.

(12) Cao, D. H.; Chen, K.; Fan, J.; Manna, J.; Olenyuk, B.; Whiteford, J. A.; Stang, P. J. *Pure Appl. Chem.* **1997**, *69*, 1979-1986.

(13) Park, S. J.; Hong, J. I. *Chem. Commun.* **2001**, 1554-1555.

(14) Fujita, M. *Chem. Soc. Rev.* **1998**, *27*, 417-425.

(15) Olenyuk, B.; Fechtenkotter, A.; Stang, P. J. *J. Chem. Soc., Dalton Trans.* **1998**, 1707-1728.

(16) Stang, P. J.; Cao, D. H.; Chen, K.; Gray, G. M.; Muddiman, D. C.; Smith, R. D. *J. Am. Chem. Soc.* **1997**, *119*, 5163-5168.

(17) Stang, P. J.; Chen, K. *J. Am. Chem. Soc.* **1995**, *117*, 1667-1668.

(18) Fujita, M.; Kwon, Y. J.; Washizu, S.; Ogura, K. *J. Am. Chem. Soc.* **1994**, *116*, 1151-1152.

(19) Hunter, C. A. *Angew. Chem. Int. Ed. Engl.* **1995**, *34*, 1079-1081.

(20) Jones, C. J. *Chem. Soc. Rev.* **1998**, *27*, 289-299.

(21) Manna, J.; Whiteford, J. A.; Stang, P. J. *J. Am. Chem. Soc.* **1996**, *118*, 8731-8732.

(22) Manna, J.; Kuehl, C. J.; Whiteford, J. A.; Stang, P. J.; Muddiman, D. C.; Hofstadler, S. A.; Smith, R. D. *J. Am. Chem. Soc.* **1997**, *119*, 11611-11619.

(23) Stang, P. J.; Zhdankin, V. V. *J. Am. Chem. Soc.* **1993**, *115*, 9808-9809.

(24) Stang, P. J.; Whiteford, J. A. *Organometallics* **1994**, *13*, 3776-3777.

(25) Kuehl, C. J.; Huang, S. D.; Stang, P. J. *J. Am. Chem. Soc.* **2001**.

(26) Manna, J.; Kuehl, C. J.; Whiteford, J. A.; Stang, P. J. *Organometallics* **1997**, *16*, 1897-1905.

(27) Stang, P. J.; Cao, D. H.; Saito, S.; Arif, A. M. *J. Am. Chem. Soc.* **1995**, *117*, 6273-6283.

(28) Fujita, M.; Nagao, S.; Iida, M.; Ogata, K.; Ogura, K. *J. Am. Chem. Soc.* **1993**, *115*, 1574-1577.

(29) Crisp, M. G.; Pyke, S. M.; Rendina, L. M. *Journal of Organometallic Chemistry* **2000**, *607*, 222-226.

(30) Gallasch, D. P.; Tiekink, E. R. T.; Rendina, L. M. *Organometallics* **2001**, *20*, 3373-3382.

(31) Fraser, C. S. A.; Jennings, M. C.; Puddephatt, R. J. *Chem. Commun.* **2001**, 1310-1311.

(32) Kuehl, C. J.; Tabellion, F. M.; Arif, A. M.; Stang, P. J. *Organometallics* **2001**, *20*, 1956-1959.

(33) Burrows, A. D.; Mingos, D. M. P.; White, A. J. P.; Williams, D. J. *J. Chem. Soc., Dalton Trans.* **1996**, 3805-3812.

(34) Sigel, R. K. O.; Freisinger, E.; Metzger, S.; Lippert, B. *J. Am. Chem. Soc.* **1998**, *120*, 12000-12007.

(35) Metzger, S.; Lippert, B. *J. Am. Chem. Soc.* **1996**, *118*, 12467-12468.

(36) Mann, B. E.; Musco, A. *J. C. S. Dalton* **1980**, 776-785.

(37) Ladipo, F. T.; Kooti, M.; Merola, J. S. *Inorg. Chem.* **1993**, *32*, 1681.

(38) Van Doorn, J. A.; Masters, S.; Van der Woude, C. *J. Chem. Soc., Dalton Trans.* **1978**, 1213.

(39) Marder, T. B.; Cham, D. M.-T.; Fultz, W. C.; Callabrese, J. C.; Milstein, D. *J. Chem. Soc., Chem. Commun.* **1987**, 1885.

(40) Askew, B.; Ballester, P.; Buhr, C.; Jeong, K. S.; Jones, S.; Parris, K.; Williams, K.; Rebek Jr., J. *J. Am. Chem. Soc.* **1989**, *111*, 1082-1090.

(41) Tsukube, H.; Furuta, H.; Odani, A.; Takeda, Y.; Kudo, Y.; Inoue, Y.; Liu, Y.; Sakamoto, H.; Kimura, K. *Supramolecular Chemistry,* 8, Pergaon Press, (1996), 425-482.

(42) Searle, M. S. *Progress in NMR Spectroscopy* **1993**, *25*, 403-463.

(43) Goswami, S.; Hamilton, A. D.; Van Engen, D. *J. Am. Chem. Soc.* **1989**, *111*, 3425-3426.

(44) Rao, P.; Ghosh, S.; Maitra, U. *J. Phys. Chem. B* **1999**, *103*, 4528-4533.

(45) Lancelot, G. *J. Am. Chem. Soc.* **1977**, *99*, 7037-7042.

(46) Nemoto, H.; Kawano, T.; Ueji, N.; Bando, M.; Kido, M.; Suzuki, I.; Shibuya, M. *Organic Lett.* **2000**, *2*, 1015-1017.

(47) Zimmerman, S. C.; Wu, W. *J. Am. Chem. Soc.* **1989**, *111*, 8054-8055.

(48) Adrian, J. C.; Wilcox, C. S. *J. Am. Chem. Soc.* **1989**, *111*, 8055-8057.

(49) Yu, L.; Schneider, H.-J. *Eur. J. Org. Chem.* **1999**, 1619 - 1625.

(50) Mann, B. E.; Musco, A. *J. Chem. Soc., Dalton* **1980**, 776-778.

(51) Tolman, C. A. *Chem. Rev.* **1975**, *77*, 313.

(52) Kickham, J. E.; Loeb, S. J.; Murphy, S. L. *Chem. Eur. J.* **1997**, *3*, 1203-1213.

(53) Kickham, J. E.; Loeb, S. J.; Murphy, S. L. *J. Am. Chem. Soc.* **1993**, *115*, 7031-7032.

(54) Clark, H. C.; Itoh, K. *Inorganic Chemistry* **1971**, *10*, 1707-1711.

(55) Clark, H. C.; Manzer, L. E. *J. Organomet. Chem.* **1973**, *59*, 411-428.

(56) Kistner, C. R.; Hutchinson, K. H.; Doyle, J. R.; Storlie, J. C. *Inorg. Chem.* **1963**, *2*, 1255-1261.

(57) Green, M.; Howard, J. A.; Spencer, J. L.; Stone, F. G. A. *J.C.S. Chem. Comm.* **1975**, *1*, 3-4.

(58) Crisp, M. G.; Rendina, L. M.; Tiekink, E. R. T. *Z. Kristallogr. NCS* **2001**, *216*, 243-244.

(59) Pregosin, P. S.; Kunz, R. W. *^{31}P and ^{13}C-NMR of Tranistion Metal Complexes*; Springer: Berlin, 1979.

(60) Anderson, G. K.; Clark, H. C.; Davies, J. A. *Organometallics* **1982**, *1*, 64.

(61) Harris, R. K. *Can. J. Chem.* **1964**, *42*, 2275-2281.

(62) Yoshida, T.; Ueda, Y.; Otsuka, S. *J. Am. Chem. Soc.* **1978**, *100*, 3941-3942.

(63) Kingston, D. G. I.; Kolpak, M. X. *J. Am. Chem. Soc.* **1980**, *102*, 5966-5967.

(64) Yoshida, T.; Okano, T.; Ueda, Y.; Otsuka, S. *J. Am. Chem. Soc.* **1981**, *103*, 3411-3422.

(65) Milstein, D.; Callabrese, J. C.; Williams, D. J. *J. Am. Chem. Soc.* **1986**, *108*, 6387-6389.

(66) Yoshida, T.; Okano, T.; Saito, K.; Otsuka, S. *Inorg. Chim. Acta* **1980**, *44*, L135-L136.

(67) Seligson, A. L.; Cowan, R. L.; Trogler, W. C. *Inorg. Chem.* **1991**, *30*, 3371-3381.

(68) Brunner, H.; Nuber, B.; Prommesberger, M. *J. Organomet. Chem.* **1996**, 179-185.

(69) Baggaley, S. H.; English, P. D.; Jennings, J. A.; Morgan, B.; Nunn, B.; Tyrrell, W. R. *J. Med. Chem.* **1985**, *28*, 1661-1667.

(70) Boykin, D. W.; Kumar, A. *J. Heterocyclic Chem.* **1992**, *29*, 1-4.

(71) Kamigata, N.; Hashimoto, S.; Kobayashi, M.; Nakanishi, H. *Bull. Chem. Soc. Jpn.* **1985**, *58*, 3131-3136.

(72) Munoz Mena, E.; Jimenez Nunez, E. *Ciencia* **1954**, *14*, 156-162.

(73) Nacci, v.; Garofalo, A.; Campiani, G. *J. Heterocyclic Chem.* **1988**, *25*, 1007-1013.

(74) Pizey, S. S. *Synthetic Reagents* **1974**, *1*, 321-357.

(75) Villani, F. J.; King, M. S. *Org. Synth. Coll. Vol. 4* **1963**, *4*, 88.

(76) Yevich, J. P.; New, J. S.; Smith, D. W.; Lobeck, W. G.; Catt, J. D.; Minielli, J. L.; Eison, M. S.; Taylor, D. P.; Riblet, L. A.; Temple, D. L. *J. Med. Chem.* **1986**, *29*, 359-369.

(77) Williams, D. H.; Fleming, I. *Spectroscopic Methods in Organic Chemistry*; 5 ed.; McGraw-Hill: London, 1995.

(78) Benet, L. Z.; Goyan, J. E. *J. Pharm. Sci.* **1967**, *56*, 665-680.

(79) Perrin, D. D.; Dempsey, B.; Serjeant, E. P. *pKa Prediction for Organic Acids and Bases*; 1 ed.; Chapman and Hall: Cambridge, 1981.

(80) Frassineti, C.; Ghelli, S.; Gans, P.; Sabatini, A.; Moruzzi, M. S.; Vacca, A. *Analytical Biochemistry* **1995**, *231*, 374-382.

(81) Grunwald, E.; Berkowitz, B. J. **1951**, *73*, 4939-4944.

(82) Niazi, M. S. K.; Mollin, J. *Bull. Chem. Soc. Jpn.* **1987**, *60*, 2605-2610.

(83) Albert, A.; Serjeant, E. P. *The Determination of Ionization Constants*; 3 ed.; Chapman and Hall: Cambridge, 1984.

(84) Julia, S.; Sala, P.; del Mazo, J.; Sancho, M. *J. Heterocyclic Chem.* **1982**, *19*, 1141-1145.

(85) Salomon, M. *J. Solution Chem.* **1986**, *15*, 237-241.

(86) Peral, F.; Gallego, E. *Journal of Molecular Structure* **1992**, *274*, 105-114.

(87) Madec, P. J.; Marechal, E. *Journal of Macromolecular Science - Chemistry* **1978**, 1091-1098.

(88) Macomber, R. S. *J. Chem. Ed.* **1992**, *69*, 375-378.

(89) Hynes, M. J. *J. Chem. Soc. Dalton Trans* **1993**, 311-312.

(90) Horman, I.; Dreux, B. *Anal. Chem.* **1983**, *55*, 1219-1221.

(91) Hill, Z. D.; MacCarthy, P. *J. Chem. Ed.* **1986**, *63*, 162-167.

(92) Job, P. *Ann. Chim. (Serie 10)* **1928**, *9*.

(93) Scatchard, G. *Ann. N. Y. Acad. Sci.* **1949**, *51*, 660.

(94) Inouye, M.; Hyodo, Y.; Nakazumi, H. *J. Org. Chem.* **1999**, *64*, 2704-2710.

(95) Xu, X.; James, S. L.; Mingos, M. P.; White, A. J. P.; Williams, D. J. *J. Chem. Soc., Dalton Trans.* **2000**, 3783-3790.

(96) Ugo, R.; Cariati, F.; La Monica, G. *Inorg. Synth.* **1968**, *11*, 105.